THREE ESSAYS ON OZONE POLLUTION, BIOFUEL PRODUCTION, AND CLIMATE CHANGE

A Dissertation

by

YABIN DA

Submitted to the Graduate and Professional School of
Texas A&M University
in partial fulfillment of the requirements for the degree of

DOCTOR OF PHILOSOPHY

Chair of Committee, Bruce A. McCarl
Committee Members, Yangyang Xu
Richard T. Woodward
Ximing Wu
Joshua Yuan
Head of Department, Rodolfo M. Nayga, Jr.

May 2022

Major Subject: Agricultural Economics

ABSTRACT

Climate change and surface ozone have been proven to impose significant threats on crop productions and the interactions between these two factors further make the issue more complicated. Although the quantification of damages has been well established in the literature, the consideration of ozone-climate interactions is mostly absent from such studies. On the other hand, mitigation is recognized as one of the most important strategies to address climate change challenges and cellulosic ethanol production from biomass is a promising solution. This dissertation covers the above climate change-related topics in three essays.

The first essay explores ozone impacts on corn, soybeans, spring wheat, winter wheat, barley, cotton, peanuts, rice, sorghum, and sunflowers in the United States. We also incorporate a variety of climatic variables to investigate potential ozone-climate interactions. The results shed light on future yield consequences of ozone and climate change individually and jointly under a projected climate scenario. Our results suggest that the damages caused by climate change-induced ozone elevation are much smaller than the damages caused by the direct effects of climate change itself.

The second essay focuses on climate change and winter wheat, a stable crop that plays a critical role in food security and nutrient balance. We examine potentially differential climatic impacts depending on winter wheat's growth stages, using data collected from China, the largest wheat producer in the world. We also address the concerns of short- and long-run climate effects and reveal the effects of long-run climate change adaptations. Our

findings suggest that reductions in the number of freezing days induced by global warming have strong implications for climate change impacts on winter wheat yields. We find substantial long-run adaptation effects that could reverse the sign of climate impacts on winter wheat.

The third essay consists of two parts. We build life cycle analysis models to measure the environmental performance of a proposed Multi-Stream Integrated Biorefinery (MIBR) platform. The goal of the MIBR is to enhance the profitability and sustainability of lignocellulosic biofuel by producing valuable byproducts (i.e., carbon fiber) from lignin-containing biorefinery wastes. We also perform market analysis on carbon fiber to understand the current market and prospective market in the foreseeable future. Market penetration analysis suggests minimal price impacts of MIBR carbon fiber. However, scaling up the platform to a capacity level comparable with a corn ethanol plant will reduce carbon fiber price by 28%, posing challenges to the profitability of lignin-based byproducts.

DEDICATION

To my dear family

ACKNOWLEDGEMENTS

I want to express my deepest gratitude to my dissertation committee chair, Dr. Bruce A. McCarl, for his support during my Ph.D. study at Texas A&M University. Dr. McCarl is one of the kindest advisors I have ever met. He gave me excellent guidance and shared his philosophy of doing research while I was lost in the fog (especially during the pandemic). Dr. McCarl was unexpectedly tolerant of my mistakes, continued to grant me his greatest support, and timely corrected me in the right direction. It is my fortune and honor to be one of his graduate students. I cannot imagine how hard my life would have been (both academically and financially) without his help.

I want to express my sincere thanks to my committee member, Dr. Yangyang Xu, who tirelessly guided and encouraged me. Without his encouragement, I would have already given up my first project in early 2020 and would not be able to publish it in a decent journal eventually. I also want to give special thanks to Dr. Joshua Yuan, my committee member and the PI for the DOE project in my last chapter. Dr. Yuan and his team members (Dr. Jinghao Li and Cheng Hu) kindly invited me to their lab and provided me with all the data needed to complete my dissertation. Lastly, I want to thank my committee members, Dr. Richard T. Woodward and Dr. Ximing Wu, for their excellent comments and (ongoing) support on my research.

I would also like to express my great appreciation to Melanie Magre. Melanie is a senior research specialist at the Blackland Research Center, Texas A&M University, and my co-worker for the USDA NRCS project on agricultural conservation. I had pleasant

and fruitful working experience with Melanie. Together we were able to realize great accomplishments for the Conservation Effects Assessment Project (CEAP-II). In addition, she generously helped me extend USDA funding from one semester to four semesters, which significantly relieved my financial burdens at the final stage of my Ph.D. study.

I also thank the department graduate office and other department faculties and staff for making my time at Texas A&M University a great experience. I thank my friends Ying Wang, Xingguo Wang, Ruixin Jia, Xiaoyang Deng, Hyung Ho Park, Phatchaya Piriyathanasak, Jorge Martinez, and many others for their help and encouragement.

Finally, thanks to my father, mother, younger brother, and younger sister for their countless supports, and to my girlfriend (soon will be fiancée) Zeya Li for her patience and love!

CONTRIBUTORS AND FUNDING SOURCES

Contributors

This work was supervised by a dissertation committee consisting of Professors Bruce A. McCarl, Richard T. Woodward, and Ximing Wu from the Department of Agricultural Economics, and Professor Yangyang Xu from the Department of Atmospheric Sciences, and Professor Joshua Yuan from the Department of Plant Pathology and Microbiology.

All work for the dissertation was completed by the student but benefitted from advice from others. Specifically, while doing the ozone-climate and climate-winter wheat studies (Chapter 2 and Chapter 3), the student had substantial interactions with Professors Bruce A. McCarl and Yangyang Xu and obtained valuable advice from Professors Richard T. Woodward and Ximing Wu. Chapter 4 on biofuel was done with substantial interactions with Professors Bruce A. McCarl, Joshua Yuan, and members of Professor Joshua Yuan's group.

Funding Sources

Chapter 3 was supported by the Intergovernmental Panel on Climate Change (IPCC) and the Cuomo Foundation through the Fifth IPCC Scholarship Program. Chapter 4 was supported by a research grant from the United States Department of Energy (DOE) entitled Multi-stream Integrated Biorefinery Enabled by Waste Processing which was DOE grant Number DE-EE-0008250.

The contents of this dissertation are solely the responsibility of the student (as well as his co-authors) and do not necessarily represent the official views of the organizations mentioned above.

NOMENCLATURE

ABA	Abscisic Acid
DOE	United States Department of Energy
EPA	United States Environmental Protection Agency
GREET	The Greenhouse Gases, Regulated Emissions, and Energy Use in Technologies Mode
FAO	Food and Agriculture Organization
IPCC	Intergovernmental Panel on Climate Change
MIBR	Multi-stream Integrated Biorefinery
NARR	The North American Regional Reanalysis
NASA	The National Aeronautics and Space Administration
NASS	National Agricultural Statistics Service
NOAA	National Oceanic and Atmospheric Administration
PAN	Polyacrylonitrile
PHA	Polyhydroxyalkanoates
RCP	Representative Concentration Pathway
SSP	Shared Socioeconomic Pathway
USDA	United States Department of Agriculture
USGCRP	The United States Global Change Research Program

TABLE OF CONTENTS

Page

ABSTRACT II

DEDICATION IV

ACKNOWLEDGEMENTS V

CONTRIBUTORS AND FUNDING SOURCES VII

NOMENCLATURE IX

TABLE OF CONTENTS X

LIST OF FIGURES XIII

LIST OF TABLES XV

CHAPTER I INTRODUCTION 1

Surface ozone pollution, climate change, and agricultural productivities 1
Biofuel production and climate change mitigation 3

CHAPTER II EFFECTS OF SURFACE OZONE AND CLIMATE ON HISTORICAL (1980-2015) CROP YIELDS IN THE UNITED STATES: IMPLICATION FOR MID-21ST CENTURY PROJECTION 5

Data Collection 8
Crop yield data 8
Climate data 8
Drought data 10
Ozone data 11
Methodology 14
Results 17
Examining the impacts of ozone on crop yields 17
Cross-validations and robustness checks 22
Exploring the impacts of climate and ozone-climate interactions 25
Historical crop production reductions and revenue losses 27
Future yield consequences of ozone and climate 28
Comparison of results with other climate and ozone studies 33

Conclusion 35

CHAPTER III ARE CLIMATE CHANGE DAMAGES ON WINTER WHEAT OVERSTATED? EVIDENCE FROM CHINA 37

Data collection 41
Yield data and the study region 41
Weather data 43
Empirically estimating temperature thresholds for deriving degree-day variables: What is considered too cold/hot? 45
The estimation model 47
Empirical results 50
Regression results from the baseline panel model 51
The examination of model performance and robustness checks 53
Short-run impacts, long-run impacts, and adaptations 56
What do we expect for climate change impacts on winter wheat? 59
How large are the adaptation potentials? 62
Conclusion 65

CHAPTER IV ENVIRONMENTAL ASSESSMENT OF THE PROPOSED MIBR PLATFORM AND MARKET IMPLICATIONS FOR CARBON FIBER 66

An introduction to the MIBR platform 69
LCA analysis on the MIBR platform 71
System boundary and the functional unit 72
Process and input data 73
Allocation method for byproducts 76
LCA analysis results 78
Environmental impacts of the MIBR with ethanol being the main product 78
Environmental impacts when carbon fiber is treated as the main product 81
Market analysis for carbon fiber 83
Demand projections for carbon fiber 85
The supply capacity of carbon fiber 87
The costs and prices of carbon fiber 88
Market responses to lignin-based carbon fiber 90
Conclusion 94

CHAPTER V CONCLUSIONS AND FUTURE RESEARCH 96

Conclusion 96
Limitations and future research 98

REFERENCES 101

APPENDIX A EFFECTS OF SURFACE OZONE AND CLIMATE ON HISTORICAL (1980-2015) CROP YIELDS IN THE UNITED STATES: IMPLICATION FOR MID-21ST CENTURY PROJECTION 121

Addressing multi-collinearity issues 121
Addressing the potential endogeneity of ozone 122
Climate change driven AOT40 projections 123
Supplementary figures 125
Supplementary tables 127

APPENDIX B ARE CLIMATE CHANGE DAMAGES ON WINTER WHEAT YIELDS OVERSTATED? EVIDENCE FROM CHINA 154

A suite of robustness checks 154
Future yield projection results with SSP scenarios 156
Supplementary tables 158
Supplementary figures 163

LIST OF FIGURES

Page

Figure 1. Incidence of observed M7 (left panel) and corrected model results on M7 (right panel) over winter wheat regions in the United States 11

Figure 2. Seasonal patterns of observed ozone and modeled ozone before and after correction 12

Figure 3. Frequency density of observed AOT40 for spring wheat and winter wheat over their ozone sensitive periods..... 20

Figure 4. The impacts of AOT40 for different crops 21

Figure 5. Changes in production (in percentage) as a function of time 29

Figure 6. Future changes in climate conditions and climate change-induced ozone changes for spring crops 31

Figure 7. Projected yield changes associated with future climate change alone and climate change plus ozone change..... 32

Figure 8. Spatial and temporal variation within the winter wheat yield data for the study region. 42

Figure 9. The trends in seasonal temperature and growing-period precipitation..... 44

Figure 10. Winter wheat's responses to temperatures across different seasons..... 52

Figure 11. Out-of-sample prediction comparison for multiple model specifications 55

Figure 12. Projected yield consequences under a range of uniform warming scenarios .61

Figure 13. Yield projections with short-run impacts, basic panel estimates, and long-run impacts, respectively 64

Figure 14. Main processes in the MIBR platform..... 70

Figure 15. CO2 emissions per gallon of produced ethanol 79

Figure 16. A general process for producing carbon fiber from lignin 82

Figure 17. Cost comparisons across different composite materials (2012) 84

Figure 18. The projections of global carbon fiber demand 86

Figure 19. Carbon fiber consumption by sectors 87
Figure 20. The theoretical supply capacity of carbon fiber in 2018 88
Figure 21. The distribution of carbon fiber production cost 90

LIST OF TABLES

Page

Table 1. Regression Results for the Crop Yield Sensitivity to Selected Variables.....18

Table 2. Estimations for Winter Wheat with Observed and Corrected Ozone 19

Table 3. The Average Annual Production Reductions and Revenue Losses Induced by Ozone from 1980 to 2015.....28

Table 4. The estimated temperature thresholds.....47

Table 5. The regression results with climate penalty terms 59

Table 6. The input and output information 74

Table 7. The displacement ratios between lignin-based products and their counterparts 78

Table 8. A comparison of emissions reported in GREET2021 and the literature.....81

Table 9. Emissions (in kg CO2) per kg of carbon fiber produced 83

CHAPTER I

INTRODUCTION

Climate and atmospheric characteristics coupled with possible mitigation actions all have the potential to impact agriculture and production prospects for agriculture as an energy supplier (McCarl and Schneider 2001). In this dissertation, three aspects of this massive issue are examined. First, we look at how ozone affects agricultural productivities with an eye toward how this might be altered by climate change focusing on a suite of crops in the United States. Second, we focus on the impacts of climate change on winter wheat, the empirical studies on which are still limited. Third, we turn to a mitigation effort and examine how biofuel production profitability and climate change-related greenhouse gas emissions can be affected by processes that make use of waste lignin to create high-value byproducts.

Surface ozone pollution, climate change, and agricultural productivities

Surface ozone is recognized as one of the most damaging air pollutants to human health and crop growth (Adams and McCarl 1985; Bell et al. 2007; Tai, Martin, and Heald 2014; West et al. 2013; L. Zhang et al. 2019). Globally, estimated yield losses due to elevated ozone in soybean, wheat, and maize in 2000 ranged from 8.5% to 14%, 3.9% to 15%, and 2.2 to 5.5% respectively, with associated economic losses estimated at $11 to 18 billion (Avnery et al. 2011a). This raises a major challenge to fulfill future food demands and closing the food security gap, particularly in developing countries.

On the other hand, future climate models indicate global ozone concentrations to raise due to the growth of ozone precursor emissions (Guarin et al. 2019). Under the IPCC highest emissions

scenario, RCP 8.5, the risk of ozone injury in global vegetation is projected to increase by 70% from 2000 to 2100 (Sicard et al. 2017).

While significant ozone damages and their interactions with climate change are reported (Jacob and Winner 2009; Tai, Martin, and Heald 2014; Pu et al. 2017; Ma et al. 2019), it is striking that few (empirical) assessments take into account those two factors jointly. In contrast, what is commonly seen in the literature is estimating the impacts of climate change in the absence of potential ozone effects. This raises omitted variable concerns as addressed by (Tai, Martin, and Heald 2014). On the ozone side, the quantification of damages (also known as dose-response functions) is largely derived from chamber-based experiments (Avnery et al. 2011a, 2011b; Amin 2013; Debaje 2014; Lal et al. 2017; Gina et al. 2018; Gina et al. 2018; Feng et al. 2019, 2020; Hu et al. 2019). Although those dose-response functions are widely used in practice, arguments have been postulated that experimental studies could be plagued by their limitations in spatial scale, timing, and geographic diversity (McGrath et al. 2015; Yi et al. 2016; Carter et al. 2017; Tai and Val Martin 2017). More importantly, the interaction of ozone and climate is also absent from experimental studies.

The first essay addresses the above issues by jointly examining the impacts of historic ozone and climate conditions on crop yields in the United States. The second essay is closely related to the topic but with a focus on climate change and winter wheat, which is one of the most extensively grown cereal crops worldwide and contributes to one-fifth of the calories people consume every day. The present study differs from previous examinations of climate change impacts on winter wheat in important ways. We build an econometric model that is consistent with winter wheat's growing stages as opposed to existing studies' simple aggregations of seasonal weather conditions

(Tack, Barkley, and Nalley 2015). We also move forward to differentiate the short- and long-run climate impacts to reveal the potential of adaptations (Mérel and Gammans 2021).

Biofuel production and climate change mitigation

While studies have shown that climate change poses real risks to agricultural production, many are considering ways that agriculture may participate in reducing the magnitude of future climate change. One promising avenue is through the production of bioenergy (biofuel). The IPCC special report on 1.5 °C warming indicates that in 2050, biofuel will still be as important as electromobility in the displacement of carbon-emitting fossil fuels (IPCC 2018).

First generation biofuel produced from food crops (i.e., corn) has been extensively developed and well commercialized. However, concerns arise due to its competition with food supplies as documented in (Chen and Khanna 2013; Boddiger 2007; Zilberman et al. 2013; Koizumi 2015), and its lower greenhouse gas emission efficiency (McCarl 2008). As a result, second generation biofuel productions from lignocellulosic biomass (i.e., crop and forest residuals) have drawn more and more attention (Falano, Jeswani, and Azapagic 2014).

Nevertheless, lignocellulosic biorefinery still faces challenges in terms of profitability because of high production costs. A promising solution is to develop valuable byproducts from the platform using lignin-containing biorefinery wastes. This leads to the proposed Multi-Stream Integrated Biorefinery (MIBR). The MIBR would utilize the lignin-containing biorefinery wastes as feedstock for high-value bioproducts (i.e., carbon fiber, asphalt binder modifiers, and bioplastics), which offers a significant opportunity to enhance operational efficiency, reduce cost, as well as minimize carbon emission, and maximize the sustainability of lignocellulosic biofuels.

In accordance with the MIBR, the first goal of the third essay is to build life cycle models to evaluate the platform's environmental performance. The evaluation results will be used to optimize

the production processes. The second goal is to conduct market analysis on the byproducts (particularly carbon fiber). The market analysis consists of two components. The first component examines the demand and supply of the current carbon fiber markets and projects future demand potentials. The second component assesses market reactions to the introduction of lignin-based carbon fiber based on estimated elasticities. The market analysis provides insights for scaling up and commercializing the MIBR platform.

CHAPTER II

EFFECTS OF SURFACE OZONE AND CLIMATE ON HISTORICAL (1980-2015) CROP YIELDS IN THE UNITED STATES: IMPLICATION FOR MID-21ST CENTURY PROJECTION[1]

While many have found that climate change poses threats to crop production (Deschênes and Greenstone 2007; Lobell, Schlenker, and Costa-Roberts 2011; Schlenker and Roberts 2009), the damages induced by surface ozone pollution are also important but somehow less addressed. Agronomically, ozone pollution reduces photosynthesis activities, accelerates senescence, and consequently decreases crop yields. For instance, dose-response functions derived from chamber experiments indicate that an AOT40 (i.e., hourly ozone concentration accumulated over a threshold of 40 ppb during daylight hours) of 3.3 ppm·hour[2] tends to reduce wheat yield by 5.0%. This can cause large losses. For example, Avnery et al. (2011a) estimate that globally ozone-induced crop production reductions (soybean, maize, and wheat) reached 79-121 million metric tons in 2000, translating to economic losses of $11-18 billion (in 2000 U.S. dollars). There are also indications that climate change may increase ozone incidence and in turn damages (Jacob and Winner 2009; Tai, Martin, and Heald 2014; Pu et al. 2017; Ma et al. 2019). In particular, estimates indicate that climate change would increase ozone concentration by 1-10 ppb in many regions by the 2050s (Jacob and Winner 2009; Fiore et al. 2012).

[1]Reprinted with permission from "Effects of Surface Ozone and Climate on Historical (1980–2015) Crop Yields in the United States: Implication for Mid-21st Century Projection" by Yabin Da, Yangyang Xu, and Bruce McCarl, 2021. *Environmental and Resource Economics* 1-24, Copyright [2021] by Springer Nature.

[2]To clarify, ppm and ppb are ozone concentration units and stand for parts per million and parts per billion, respectively. 1 ppm = 1000 ppb.

Given the large magnitude of ozone damages (both physically and economically) on crops and the likelihood that climate change will exacerbate this, it is surprising that few empirical assessments of climate change's effects on crop production take ozone pollution into account.[3] The omission of ozone could lead to omitted variable bias (Tai, Martin, and Heald 2014) due to its interactions with climate conditions, especially extreme heat (Pu et al. 2017). Important questions arise such as: How much of the estimated climate change damage on crop yields is attributable to climate change-induced ozone concentration elevation? How the ozone damages compare to the direct effects stemming from climate change itself? And more broadly: Could a significant amount of climate change damages be offset by ozone control?

On the ozone damage side, existing evidence is largely derived from chamber-based experiments (Avnery et al. 2011a, 2011b; Amin 2013; Debaje 2014; Lal et al. 2017; Mills et al. 2018; Mills et al. 2018; Feng et al. 2019, 2020; Hu et al. 2019). Arguments have been postulated that those experimental studies could be plagued by their limitations in spatial scale, timing, and geographic diversity (McGrath et al. 2015; Yi et al. 2016; Carter et al. 2017; Tai and Val Martin 2017). More importantly, the interaction of ozone and climate is also absent from experimental studies,[4] which has important implications for the evaluation of ozone effects on yields.[5]

[3]See for example studies in the United States (Deschênes and Greenstone 2007; Schlenker and Roberts 2009; Burke and Emerick 2016), studies in China (Chen, Chen, and Xu 2016; Zhang, Zhang, and Chen 2017; Chen and Gong 2020), and studies from a global perspective (Lobell, Schlenker, and Costa-Roberts 2011; Deryng et al. 2014; Wing, De Cian, and Mistry 2021).

[4]For instance, the dose-response functions derived from experiments are usually expressed with simple linear functional forms (nonlinear functional forms also exist but are much less widely used). The most widely used linear function takes the form: $y = a * Ozone + b$. Where y is the relative yield (RY); *Ozone* indicates ozone measurement; a is a negative coefficient indicating ozone damages; b normally takes a value around 1 so that in scenarios with no ozone, the relative yield will be 1 (i.e., no ozone damages).

[5]Agronomically, ozone enters plants via stomata and damages both the internal structure and physiological function (Fuhrer, Skärby, and Ashmore 1997; Mills et al. 2007; Pleijel et al. 2007; Ainsworth 2008; Ainsworth et al. 2012). Additionally, temperature and water availability also impact stomatal conductance, and thus impact ozone uptake (Tai and Val Martin 2017).

This paper addresses these issues by jointly examining the impacts of historic ozone and climate conditions on observed crop yields. To do this we collected the United States county-level agricultural data, weather data, and fine-scale hourly ozone concentration data from 1980 to 2015. We then employed it in estimating a panel data model with fixed effects (as has been widely used in the literature, i.e., Chen, Chen, and Xu 2016; Trinh 2018; Xie et al. 2019). Besides a variety of ozone variables in our model, we included two sets of climatic variables. Specifically, we added seasonal degree-days and precipitation variables calculated over the *entirety* of the growing season. We also included maximum temperatures and drought indicators calculated over the *ozone sensitive period* (a time interval during which crops are particularly sensitive to ozone exposure - Amundson et al. 1987; Lee et al. 1988; Mills et al. 2007; Avnery et al. 2011b; McGrath et al. 2015; Yi et al. 2016) to disentangle possible interaction effects with ozone exposure on crop yields.

Our work contributes to the existing literature in several ways. First, we provide *empirical* evidence of the historical observed relationship between ozone exposure and county-level crop yields. Our estimates arise from historical data with large spatial and long temporal dimensions, in contrast to chamber experiments' narrow coverage. Second, the simultaneous inclusion of a rich set of climatic variables along with ozone variables allows us to examine the potential ozone-climate interactions which are not generally treated in experimental studies, or empirical climate change assessments. It also allows us to remove bias in the estimated effects of temperature and other climate variables that are caused by not separating out the effects of ozone. Third, we cover a broader set of crops than has been examined in previous studies (McGrath et al. 2015; Yi et al. 2016; Yi et al. 2020; Carter et al. 2017; Lobell and Burney 2021). Namely, we cover corn, soybeans, spring wheat, winter wheat, barley, cotton, peanuts, rice, sorghum, and sunflowers that jointly account for 80% of total 2018 United States crop production value (USDA NASS 2020).

Finally, based on our estimates, we project future yield consequences and decompose the ozone and climate change effects with the consideration of both independent and complementary ozone control and climate change mitigation policies.

The rest of this paper is organized as follows. The next section describes the collection of data. Following that, we introduce our empirical strategy. In the fourth and fifth sections, we summarize our key findings and compare them with existing evidence. Finally, the sixth section contains concluding remarks.

Data Collection

We compiled a data set consisting of the United States county-level agricultural data, weather (temperature and precipitation) data, and fine-scaled hourly ozone pollution data from 1980 to 2015. Each of these components is described below.

Crop yield data

County-level crop yield data were obtained from USDA (United States Department of Agriculture) Quick Stats (USDA NASS 2019). We only used dryland yields[6] to avoid issues with irrigation following arguments in Schlenker, Hanemann, and Fisher (2005). Harvested acres data were also collected from the same source.

Climate data

County-level daily average temperature, monthly average maximum temperature,[7] and monthly total precipitation were downloaded from NOAA (National Oceanic and Atmospheric

[6]We did this by excluding counties that were labelled "irrigated" in USDA NASS.

[7]It is the monthly average of daily maximum temperature. It measures extreme temperatures, however, not as extreme as the hottest daily temperature in a certain month.

Administration -- NOAA 2019). In turn, we calculated crop-specific freezing and growing degree days as discussed below.

Freezing degree days (FDD, in degrees Celsius·days) are the accumulation of days during the growing season times the amount the daily average temperature falls below a crop-specific base temperature. The base temperature used on spring crops (corn, soybeans, spring wheat, barley, cotton, peanuts, rice, sorghum, and sunflower) is 10 ℃ while 0 ℃ is used for winter wheat following Kukal and Irmak (2018). Note that while freezing degree days might not be so relevant for summer crops, it is critical for winter wheat which is particularly vulnerable to early spring freezing (Xiao et al. 2018).

Growing degree days (GDD, in degrees Celsius·days) are an accumulation of daily average temperature above the base temperature during the growing season where we used the same base as for FDD. Following Schlenker and Roberts (2009) we use a March to August growing season for corn and soybeans for all regions. For the other spring crops, we use April to August following USDA NASS (2010). For winter wheat, we generally use September to June and allow the growing season to vary regionally (see Table A1 in Appendix A).

It is worth noting that a variety of climate variables have been employed to examine climate change impacts on crop yields such as a) dividing the temperatures into bins and calculating the effects of temperature exposure by bins allowing non-linear relationships (see Schlenker and Roberts (2009) and Zhang et al. (2017)), b) including degree-day variables to portray cumulative exposure effects (Chen, Chen, and Xu 2016), and c) average temperatures (Lobell, Schlenker, and Costa-Roberts 2011). In this paper, we primarily use degree-day variables and their square for several reasons. First, existing studies on the US agricultural response to climate suggest that the degree-day framework indicates similar results to those estimated with much more complicated

functional forms (i.e., temperature bins, high-order polynomial, etc.) (see (Schlenker and Roberts 2009; Burke and Emerick 2016)). Second, the complicated models typically feature flexible functional forms and higher-order terms, which in a panel setting means that unit-specific means re-enter the estimation. This not only raises omitted variables concerns (McIntosh and Schlenker 2006; Burke and Emerick 2016) but also exacerbates measurement error problems (Griliches 1979). Third, a more flexible function form normally includes more variables and thus requires more observations to obtain reliable estimates. In our case, the number of observations for certain crops is very limited so we restricted our climatic variable complexity.

Drought data

Given prior ozone findings on water sensitivity (Khan and Soja 2003; Biswas and Jiang 2011; McGrath et al. 2015), we felt it was important to include data on drought incidence. We used the Standardized Precipitation-Evapotranspiration Index (SPEI) measure based on arguments in Vicente-Serrano, Beguería, and López-Moreno (2010). SPEI has positive and negative ranges where values greater than 2 are considered extremely wet, 1.5 to 2 is very wet, 1 to 1.5 moderately wet, -1 to 1 normal, -1.5 to -1 moderately dry, -2 to -1.5 severely dry, and values below -2 extremely dry (Vicente-Serrano, Beguería, and López-Moreno 2010; Li et al. 2015; Zarei and Moghimi 2019; Yao et al. 2019).

Monthly SPEI data for 1980 to 2015 were obtained from the Global SPEI database (SPEI 2019) and as downloaded were gridded at a 0.5° x 0.5° spatial resolution. We calculated county-level data by weighted averaging over grid cells that overlap each county.

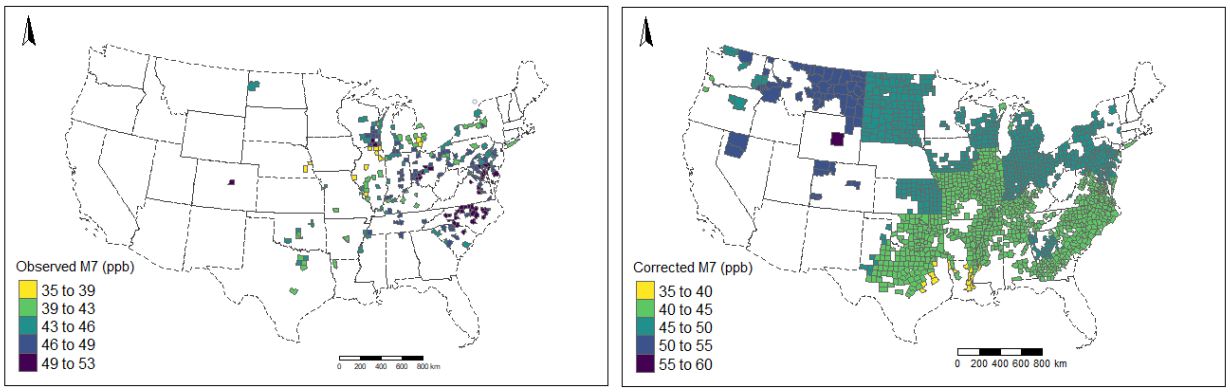

Figure 1. Incidence of observed M7 (left panel) and corrected model results on M7 (right panel) over winter wheat regions in the United States

Ozone data

Two ozone data sources were used. Ground-level hourly observations were drawn from the United States Environmental Protection Agency Air Quality System (EPA AQS) (US EPA 2019) but these data had limitations in spatial coverage particularly in winter wheat production areas, as shown in the left panel of Figure 1. Modeled hourly ozone data were also gathered to permit more complete spatial coverage and were drawn from the NASA MERRA-2 database (Modern-Era Retrospective Analysis for Research and Applications, Version 2, National Aeronautics and Space Administration- NASA, 2019).

The seasonal patterns for the observed and modeled data sets were consistent in shape, but inconsistent in magnitude (see the green and blue lines in Figure 2). To correct for that bias while maintaining the seasonal pattern, we performed the following calibration process. First, we averaged hourly concentrations on a daily basis. We then calculated differences between the EPA observed and NOAA modeled daily series and corrected the modeled ozone by adding and

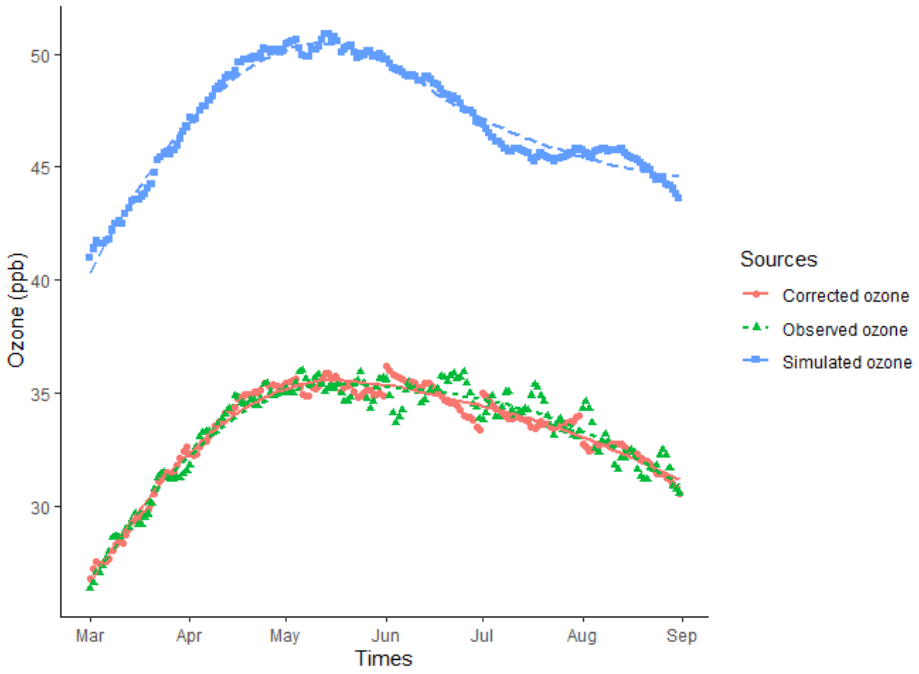

Figure 2. Seasonal patterns of observed ozone and modeled ozone before and after correction

subtracting the differences. This corrects the bias in magnitudes but maintains the seasonal pattern. We call this data set the *corrected* ozone. Note Figure 2 shows the corrected ozone closely matches the EPA observational data. More importantly, this endeavor allows us to extend the ozone coverage in the winter wheat production areas, as shown in the right panel of Figure 1.

Multiple ozone indices were considered for use. We computed all during what the literature identifies as the ozone sensitive period, which is three months before the harvest date (Amundson et al. 1987; Lee et al. 1988; Mills et al. 2007; Avnery et al. 2011b; McGrath et al. 2015; Yi et al. 2016, see Table A1 in Appendix A for examples). The first index we considered is the widely adopted M7, one that indicates 7-hour (local 09:00 to 16:00) average ozone concentration (Mills et al. 2007). Three additional metrics were also considered: 1) **AOT40** (in units ppm·hour) is the sum of daylight (local 08:00 to 20:00) hourly ozone concentrations that are greater than 40 ppb during the ozone sensitive period computed in much the same way as degree days (McGrath et al.

2015); 2) **SUM60** (in ppm·hour) is the sum of daylight hourly concentrations that are greater than 60 ppb (McGrath et al. 2015); and 3) **W126** (in ppm·hour) is the sum of daylight hourly concentrations *weighted* by a sigmoidal function, which assigns larger weights to higher ozone concentrations (McGrath et al. 2015).

The calculations of the last three metrics are shown as follows.

- AOT40 (ppm•hour) $= \sum_h^n OZ_h$, where $OZ_h = \begin{cases} ozone_h - 0.04, & ozone_h > 0.04 \\ 0, & ozone_h \le 0.04 \end{cases}$
- SUM60 (ppm•hour) $= \sum_h^n OZ_h$, where $OZ_h = \begin{cases} ozone_h, & ozone_h > 0.06 \\ 0, & ozone_h \le 0.06 \end{cases}$
- W126 (ppm•hour) $= \sum_h^n w_h \times ozone_h$, where $w_h = 1/(1+(4403 \times \exp[-126 \times ozone_h]))$

Here h is the index for hours and n is the total number of daylight hours during the ozone sensitive period. $ozone_h$ is the ozone concentration level (in ppm). w_h is the sigmoidal function that assigns weights. The SUM60 and W126 indices have been widely used in the US, and AOT40 has been extensively used in Europe.

Agronomic chamber studies have found the accumulative indices are more relevant measures for explaining yield impact (EPA 1996; Fuhrer et al. 1997; Mauzerall and Wang 2001; Emberson et al. 2009). While we ran regressions using each of these indices, we will only show results from the AOT40 measure in the main text to make our results comparable with the bulk of previous studies.

Table A2 in Appendix A reports summary statistics on key variables for all ten crops. Additionally, we also provided correlation tables across the yield, climate, and ozone variables in Table A3 to show interrelationships. In line with expectations, we observed strong positive

correlations (i.e., ranging from 0.91 to 0.99) among the four ozone indices. We also observed a statistically significant positive correlation between monthly average maximum temperature and the ozone indices (i.e., ranging from 0.24 to 0.65) which supports the argument that ozone is correlated with temperatures, especially extreme heat.[8]

Methodology

The literature reveals two basic approaches for empirically estimating climate impacts on the agricultural sector (crop yields, land values, etc.): use of a cross-sectional model (multiple counties each with one observation) and use of a panel data model with fixed effects (multiple counties with multiple years of observations in each). The advantages of the former are that it implicitly takes account of long-run climate change adaptations (such as crop mix, crop calendar, large agricultural facilities, etc.) because it directly compares outcomes across different regions (i.e., the cross-sectional variation) in which farm practices have been optimized for long-run local climate (Deschênes and Greenstone 2007; Fezzi and Bateman 2015; Hsiang 2016). However, it is plagued by endogeneity issues such as omitted variable bias (i.e., ignoring differences in soil quality and other location-specific characteristics).

On the other hand, recent studies have favored the use of panel data models with fixed effects (partially due to the availability of data). These models are able to alleviate the omitted variable bias to some extent by introducing location-specific fixed effects (Schlenker and Roberts 2009; Dell, Jones, and Olken 2012; Zhang, Zhang, and Chen 2017; Chen and Gong

[8]To address potential multi-collinearity issues among climatic variables (FDD, GDD, precipitation, monthly maximum temperature, and SPEI), we report the variance inflation factor (VIFs) for corn, soybeans, spring wheat, and winter wheat in Table A4 in Appendix A. VIFs for precipitation, FDD, and SPEI are well below 10 (Wooldridge 2013). VIFs for GDD and monthly maximum temperature are higher but mostly remain below the cutoff, except for the GDD of soybean which has a VIF of 11.3. Nevertheless, we do not feel that VIF with such a margin would be a major threat to our estimation. See more discussion in Appendix A.

2020), which control for time-invariant characteristics that would otherwise confound the estimates if omitted. However, panel regressions rely on time-series variations, i.e., comparing yield changes and weather conditions across each year for each location. In this respect, fixed effect panel models tend to reflect the effects of weather shocks (year-to-year weather variation) on the outcomes. As a result, they do not fully take into account the long-run adaptations as in the cross-sectional models (see detailed reviews in Hsiang (2016), Blanc and Schlenker (2017), and Kolstad and Moore (2020)).

To address this concern in panel models, several hybrid approaches have been developed, such as the long-difference model (Burke and Emerick 2016) and the multistage model (Butler and Huybers 2013; Carleton et al. 2020; Heutel, Miller, and Molitor 2020). Additionally, Mérel and Gammans (2021) recently proposed a novel method to estimate the short-run and long-run impacts by adding "climate penalty" terms to the traditional panel model. Also Wing, De Cian, and Mistry (2021) employed a panel error-correction model (ECM) to distinguish short-run and long-run impacts.

In the present study, we primarily use the panel data model with fixed effects following (Chen, McCarl, and Schimmelpfennig 2004; Chen, Chen, and Xu 2016; Deschênes and Greenstone 2007; Schlenker and Roberts 2009) as the existing literature finds limited evidence of adaptations in the US agricultural sector either using a long-difference approach (Burke and Emerick 2016; Miller, Tack, and Bergtold 2021) or the "climate penalty" method (Mérel and Gammans 2021).

Our final model takes the following form:

$$\begin{aligned} yield_{it} = {} & \alpha_i + \gamma_1 tt_{it} + \gamma_2 tt_{it}^2 + \rho Harv_{it} + \beta_1 FDD_{it} + \beta_2 GDD_{it} + \beta_3 GDD_{it}^2 \\ & + \beta_4 Prec_{it} + \beta_5 Prec_{it}^2 + \beta_6 Ozone_{it} + \beta_7 Tmax_{it} + \beta_8 Ozone_{it} \times Tmax_{it} \\ & + \beta_9 SPEI_{it} + \beta_{10} Ozone_{it} \times SPEI_{it} + e_{it} \end{aligned} \quad (1)$$

Here i and t indicate county and year. $yield_{it}$ denotes crop yield in that county and year. Estimations were done for each crop independently. α_i denotes a county-specific fixed effect to control for time-invariant characteristics. The model explicitly includes climatic variables giving county and year specific freezing degree days FDD_{it}, growing degree days GDD_{it} and its square GDD_{it}^2, growing season accumulated precipitation $Prec_{it}$, and its square $Prec_{it}^2$. These five variables are designated to capture the general impacts of climate (weather conditions) on crop yields.

It is worth noting that a few studies also include a number of other climatic variables in their models, such as wind speed, humidity, solar duration, etc. (Chen and Gong 2020). While introducing more variables is likely to improve the model fit (in terms of r square), the tradeoff is that these climatic variables are highly correlated and it may lead to new bias, i.e., bad controls, though this is unlikely to happen if we consider the climate variables are strongly exogenous. On the other hand, the improvement in model fit from including these variables is often small. For instance, in Zhang, Zhang, and Chen (2017) the model fit improvement for rice and wheat was significant, whereas the improvement for corn was neglectable. In this paper, while we mainly focused on primary climatic variables (temperatures and precipitations), we provided robustness checks with the inclusion of a number of secondary variables.

To examine the ozone-related damages, we included the AOT40 measure $Ozone_{it}$ in linear form following the previous literature (Yi et al. 2016).[9] A potential caveat that arises here is that ozone concentration could be endogenous because its formation is closely related

[9]While a linear relationship between ozone exposure and crop yields is recommended, we are not aware any evidence in the literature indicating a nonlinear relationship (i.e., a quadratic term of ozone).

to economic activities such as power generation, transportation, etc., which is critical for studies that examine the impacts of air pollution on human health.[10] However, we feel this is not a great concern herein as we are estimating crop yields that are largely determined by weather conditions and farm management practices, and thus socioeconomic factors may play minor roles.[11]

We included maximum temperature $Tmax_{it}$ and the drought indicator $SPEI_{it}$ (averaged over the ozone sensitive period to be consistent with the ozone measure) as well as their interactions with ozone to explore potential interaction effects. Time trends (tt_{it} and tt_{it}^2) are also included to reflect technical progress following (Schlenker and Roberts 2009; Tack, Barkley, and Nalley 2015; Miller, Tack, and Bergtold 2021). Harvested acres ($Harv_{it}$) are included to reflect scale effects. e_{it} is the error term and is clustered at the county level to account for arbitrary serial correlation within counties.

Results

As mentioned above only regression results using the AOT40 ozone measure are reported in the main text. Results for other measures are shown in Table A5-A14 in Appendix A.

Examining the impacts of ozone on crop yields

Table 1 presents the key estimation results by crop. Several major results emerge. First, we observed significant negative impacts of ozone on all crops, excepting winter wheat and barley where the estimate for barley is statistically insignificant. Second, we found that soybean yields

[10]For instance, Deryugina et al. (2019) instrumented for air pollution using changes in local wind direction. Godzinski and Castillo (2021) collected a novel and large set of altitude-weather data as candidates and then filtered optimal instrument variables (IVs) for air pollutants (i.e., 10 IVs for ozone, 14 IVs for NO_2, and 15 IVs for PM2.5).

[11]Nevertheless, we performed two sets of robustness checks with potential factors (i.e., nitrogen fertilizer application and electricity consumption) that could impact yields and ozone formation simultaneously. The estimations on ozone variables barely changed after the inclusion of those factors. See Appendix A for details.

Table 1. Regression Results for the Crop Yield Sensitivity to Selected Variables

	Yield				
	Corn	**Soybeans**	**Spring wheat**	**Winter wheat**	**Barley**
Ozone	-0.008***	-0.004***	-0.012***	0.003***	0.001
	(0.001)	(0.001)	(0.004)	(0.001)	(0.001)
Ozone*Tmax	-0.001**	-0.002***	-0.005***	-0.000	0.000
	(0.000)	(0.000)	(0.001)	(0.000)	(0.000)
Ozone*SPEI	0.009***	0.006***	-0.001	0.009***	0.001
	(0.001)	(0.001)	(0.004)	(0.001)	(0.001)
Observations	11801	8868	812	5504	3173
Adjusted R^2	0.489	0.460	0.230	0.300	0.087
	Cotton	**Peanuts**	**Rice**	**Sorghum**	**Sunflower**
Ozone	-0.008***	-0.005**	-0.003**	-0.003*	-0.008**
	(0.002)	(0.003)	(0.001)	(0.001)	(0.004)
Ozone*Tmax	-0.002	-0.001	0.001	-0.001	0.004
	(0.001)	(0.002)	(0.001)	(0.001)	(0.005)
Ozone*SPEI	0.009***	-0.002	-0.001	0.006***	0.032***
	(0.002)	(0.002)	(0.002)	(0.001)	(0.011)
Observations	1446	472	294	1955	189
Adjusted R^2	0.241	0.189	0.423	0.208	0.199

Note: This table only presents regression results for Ozone, Tmax, SPEI, and the interaction terms. See Table A5-A14 in Appendix A for the full results. In the regression, yield, Harv, and GDD are in log format. Note that crops have different units for yield. See Table A2 for details. All regressions include linear and quadratic time trends as indicated in equation (1). This is the case for all the regression result tables unless otherwise indicated. One should be noted that the log transformation barely changes the estimation of the interested variable of ozone. Numbers in parenthesis are standard errors clustered at the county level. *p<0.1; **p<0.05; ***p<0.01.

are less sensitive to ozone than are corn yields, as was also found by another statistical analysis in the United States (McGrath et al. 2015). This differs from chamber results that indicate the opposite. Specifically, we found that a 1 ppm·hour increase in AOT40 tends to reduce corn yields by 0.8%, whereas the reduction in soybean yields is 0.4%[12]. On the other hand, the review of

[12]The fixed effect panel data model used in this dissertation is a *within* estimator because the estimation of the model usually involves the de-mean process (see detailed discussion in the textbook by (Wooldridge 2010)). However, it should be noted that within estimators only reflect the correlation between the dependent variable and changes for panel subjects (in this case counties) relative to their means. In other words, the effects of differences in means across counties (i.e., cross-sectional variation) are not

Table 2. Estimations for Winter Wheat with Observed and Corrected Ozone

	Yield	
	EPA AOT40	Corrected AOT40
Ozone	0.003***	0.013***
	(0.001)	(0.001)
Tmax	-0.025***	-0.026***
	(0.003)	(0.001)
SPEI	-0.010**	-0.009***
	(0.004)	(0.002)
Ozone*Tmax	-0.000	-0.002***
	(0.000)	(0.000)
Ozone*SPEI	0.009***	0.012***
	(0.001)	(0.001)
Observations	5504	43852
Adjusted R^2	0.300	0.298

Note: Column "EPA AOT40" denotes regression results based on observed ozone data from EPA. "Corrected AOT40" refers to regression results with corrected NASA ozone data. Numbers in parenthesis are standard errors clustered at the county level. *p<0.1; **p<0.05; ***p<0.01.

chamber results in Mills et al. (2007) indicate corn sensitivity is a 0.36% yield reduction per ppm·hour ozone increase and a soybean yield reduction of 1.16% - more than 3 times that of corn.[13]

Third, our winter wheat yield results show weak positive effects which differs from the chamber and crop simulator findings of strong negative ozone impact (Biswas and Jiang 2011; Mills et al. 2018). For instance, Mills et al. (2007) labeled winter wheat as one of the most ozone sensitive crops with summary results that a one ppm·hour AOT40 increase leads to a 1.16% reduction in yield.[14] To see if our results were influenced by the sparse regional ozone observations, we re-estimated using the *corrected* ozone data (Table 2).

identified. In most applications, such *between* effects can be important, such as the long-run climate change impacts, which we will discuss in detail in the next chapter.

[13]These dose-response functions are $y = -0.0036x + 1.02$ for corn and $y = -0.0116x + 1.02$ for soybean. Here y is the relative yield and x indicates the AOT40 ozone measure.

[14]This is based on the dose response function: $y=-0.0161x+0.99$ in Mills et al. (2007).

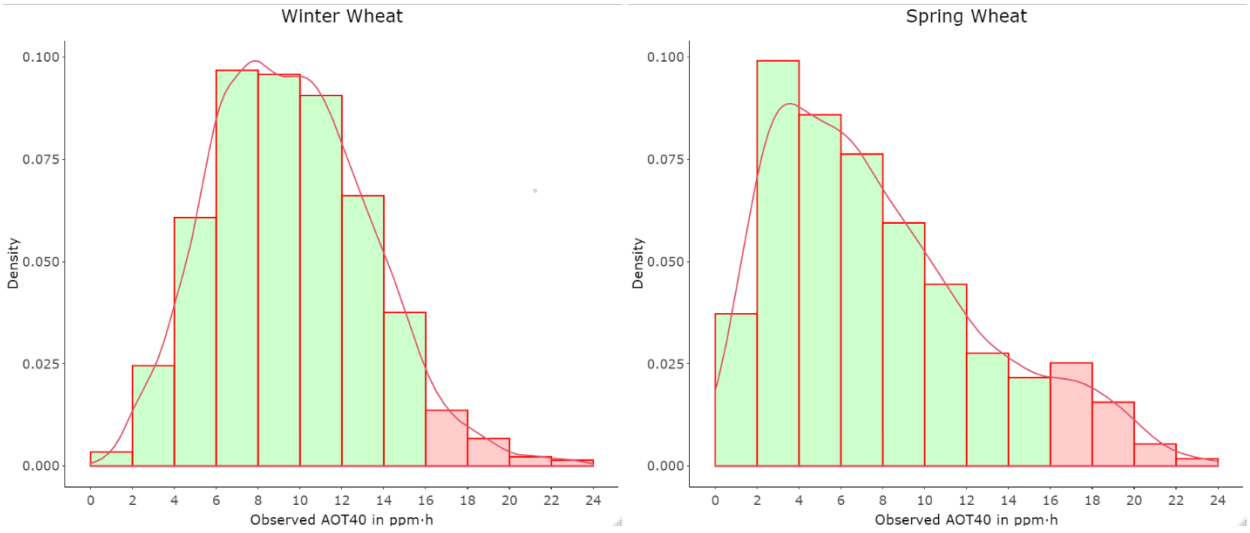

Figure 3. Frequency density of observed AOT40 for spring wheat and winter wheat over their ozone sensitive periods

Note: Bins in red represent higher AOT40 observations – those that are greater than 16 ppm·hour. For winter wheat, 5% of the observations have AOT40 greater than 16 ppm·hour, which is significantly less than that in spring wheat (10.7%).

There we continued to find positive ozone impacts. The finding may in part result from the relatively low ozone exposure levels in most of the winter wheat-producing areas in the United States. Typically, winter wheat is harvested before the extreme ozone summertime period and also is planted in geographic areas that exhibit lower ozone. In particular, AOT40 in the winter wheat areas clusters between 6-12 ppm·hour with observations above 16 ppm·hour appearing in only about 5% of the observations, which is significantly less than the higher ozone observations in the spring wheat areas (see Figure 3).

Fourth, for the rest of the crops, spring wheat exhibits the largest yield sensitivity followed by cotton, sunflower, peanuts, rice, and sorghum (Figure 4). It is also worth noting that the confidence intervals for spring wheat, cotton, peanuts, and sunflower are relatively large due to limited observations. Nevertheless, given the significance of ozone damages on crops, it is desirable to

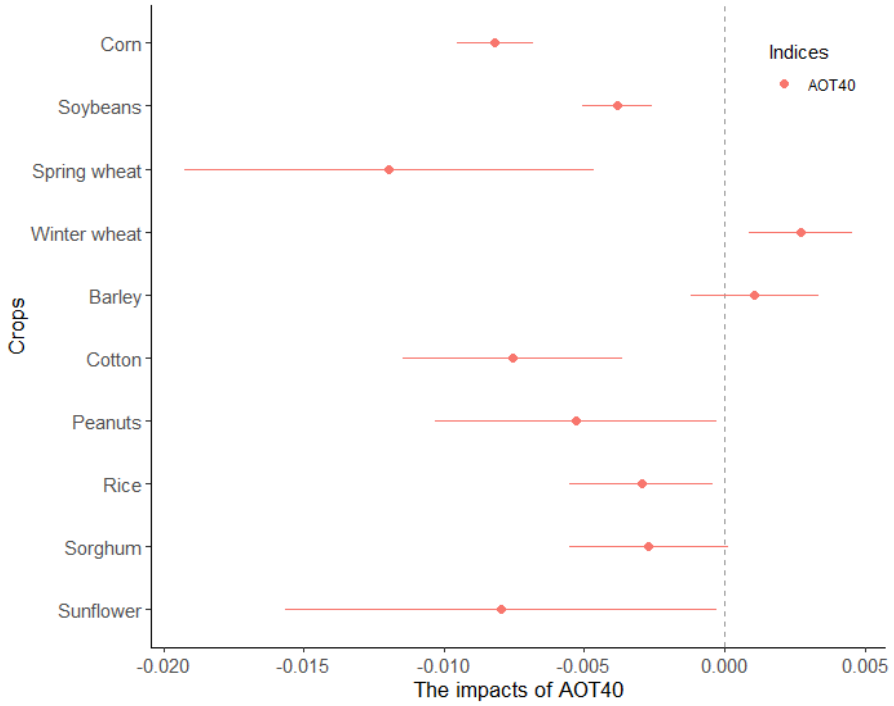

Figure 4. The impacts of AOT40 for different crops

Note: Dots represent the point estimates of AOT40 from the model in Table 1. Intuitively, the point estimates multiplying by 100 tell the marginal effects of AOT40 on crop yields, i.e., how much yields would change in percentage in response to one ppm·hour increase in AOT40. Bars are 95% confidence intervals.

compare our findings with those derived from chamber experiments as well as other empirical evidence (McGrath et al. 2015; Yi et al. 2016, 2020; Carter et al. 2017).

For experiment-based results, we mainly compared with the literature review results of Mills et al. (2007) which summarized 700 published papers and conference proceedings covering ozone dose-response functions from projects such as the US National Crop Loss Assessment Network (NCLAN) in the late 1980s, the European Open Top Chamber Programme (EOTCP) in 1980-1990, and more recent open-top chamber experiments in Europe.

In general, our empirical findings are largely consistent in sensitivity directions with those in Mills et al. (2007) but differ in magnitudes. Mills et al. (2007) categorized crops as 1) ozone

sensitive- wheat with a 1.61% yield reduction per 1 ppm·hour AOT40 increase,[15] cotton at 1.60%, and soybeans at 1.16%; 2) moderately sensitive - rice (0.39%) and corn (0.36%); and 3) ozone resistant - barley. Our results suggest: 1) the ozone sensitive group consists of spring wheat (1.2%), corn (0.8%), cotton (0.8%), and sunflowers (0.8%); 2) moderate sensitivity crops being peanuts (0.5%), soybeans (0.4%), rice (0.3%), and sorghum (0.3%); and 3) resistant groups with barley and winter wheat. Overall, ozone damages estimated from chamber experiments tend to be greater than that identified in our study.

On the empirical side, our results are pretty consistent with other United States study results. For instance, McGrath et al. (2015) estimated sensitivity to AOT40 at 0.62% for corn and 0.49% for soybeans. Liu and Desai (2021) reported AOT40 sensitivity levels of 0.83% for corn and 0.43% for soybeans - almost identical to ours, even though they included much more complicated interaction terms of ozone, atmospheric aerosols, and climatic variables. All these findings lead to the conclusion that corn tends to be more sensitive to ozone exposure than soybeans. In other countries such as China, Yi et al. (2020) detected a corn yield ozone sensitivity level of 0.62% after controlling the impact of climatic variables and related economic variables, which is again comparable with ours.

Cross-validations and robustness checks

We performed two sets of tests to validate our baseline results: out-of-sample cross-validation and several robustness checks. The former essentially compare the performance across different

[15]It should be noted that Mills et al. (2007) was not clear about which type of wheat they considered (i.e., spring wheat or winter wheat). They adopted the wheat-ozone relationship from Fuhrer, Skärby, and Ashmore (1997) where the authors pooled spring wheat and winter wheat data to estimate the dose-response function.

models in the lens of predicting power and serves as an extension to the traditional robustness checks.

Specifically, we conducted cross-validations with an alternative model specification, in which growing degree days were replaced with mean temperatures over the growing season (the freezing degree days were omitted) with other variables unchanged. In addition to that, we also set up a model with only fixed effects and time trend variables (i.e., no climatic and ozone variables included). This model serves as a reference model. The cross-validation exercise was performed in the following steps (Schlenker and Roberts 2009; Fan et al. 2020).

First, we randomly chose 85% of our full sample as training data for model estimation then used the remaining 15% of the sample to test model performance using root mean squared errors (RMSEs) calculated as follows.

$$\text{RMSE} = \sqrt{\frac{\sum_{1}^{n} (yield_{it} - yield_{it}) \wedge 2}{n}} \tag{2}$$

Where *i* and *t* are counties and years. *n* indicates the number of observations in the test data. $yield_{it}$ and $yield_{it}$ represent the actual yields and predicted yields, respectively. Smaller RMSEs indicate better model performance. We moved further by calculating the reduction of RMSEs relative to the reference model.

$$\text{Reduction in percentage} = \frac{RMSE_{ref} - RMSE_{j}}{RMSE_{ref}} \times 100 \tag{3}$$

Where *j* indicates either the baseline model or the alternative model. *ref* refers to the reference model that only has fixed effects and time trend variables. A greater reduction in RMSEs entails more variance is explained by the model and thus indicates a superior model performance.

The results can be found in Figure A1 in Appendix A. Our preferred model significantly outperforms the alternative model that drops the degree days variables in favor of average temperature in terms of the percent reduction in RMSEs (75.6% vs 35.2%) for seven out of the ten crops (corn, spring wheat, winter wheat, barley, peanut, rice, and sorghum). Soybeans, cotton, and sunflower results slightly improve when using the model with average temperature. However, across this exercise, the estimates for the ozone variable largely remained consistent.

In addition to the cross-validations, we also performed a suite of robustness checks.[16] To examine whether our results are sensitive to the inclusion of secondary climatic variables, we added relative humidity (in %), wind speed (in m/s), solar radiation (in W/m^2), and potential evaporation (in kg/m^2)[17] one at a time and jointly to our baseline model, respectively. The regression results can be found in Table A15-A18 in Appendix A. Here we found the inclusion of the secondary variables did not greatly improve the overall model fit nor did it significantly alter the estimates on the primary climatic variables and the ozone variable (AOT40). The significance and direction of signs for these variables varied by crop. For instance, in the corn regression, relative humidity and evaporation showed negative yield effects, whereas wind speed and solar radiation indicated positive effects. For soybeans, the coefficient signs were the same as for corn, but only the estimates of solar radiation and evaporation were statistically significant.

[16]It should be noted that while we performed robustness checks independently for each of the ten crops, we only report the results for corn, soybean, spring wheat, and winter wheat in Appendix A.

[17]The data were obtained from the North American Regional Reanalysis (NARR, https://psl.noaa.gov/data/gridded/data.narr.html) with a spatial resolution of 32km * 32km (0.3 degree) and a monthly temporal resolution. We converted the data to county level by weighted averaging over grid cells that overlap each county. The county level monthly variables were averaged across crop-specific growing seasons.

In our baseline model, we used linear and quadratic time trends to represent technological development, following (Schlenker and Roberts 2009; Tack, Barkley, and Nalley 2015; Miller, Tack, and Bergtold 2021). We ran additional regressions with year-fixed effects to see whether our results are robust to different time effect characterizations. The results are shown in Table A19 in Appendix A and are consistent with the baseline estimates. Taking corn as an example, the inflection points for the quadratic relationships between GDD and Prec and yields occurred at 7.9 (in the log) and 25 inches, respectively, compared with our baseline estimates of 7.6 and 27.5. Also, the coefficients of ozone variables remained largely unchanged.

Exploring the impacts of climate and ozone-climate interactions

In terms of climate, as reported in Table A5-A14 in Appendix A, we observed an inverse U-shaped nonlinear relationship between yields and growing degree days (GDD) for most crops (results for peanuts and rice are statistically insignificant), and a similar precipitation response (excepting for rice which is almost exclusively grown under irrigation and exhibits statistically insignificant results). These findings are consistent with findings in Schlenker and Roberts (2009) and Tack, Barkley, and Nalley (2015). In the climate change projection section below, we further compared our estimates with existing evidence.

We do find increases in maximum temperature during the ozone sensitive period impose negative impacts on yields for eight of the ten crops (with insignificant results for peanuts and positive results for sunflowers, see Table 1). A 1 ºC increase in Tmax triggers a yield reduction spanning from 2.0% to 13.2%. These impacts are larger than those for ozone exposure. On the

other hand, a 0.1 increase[18] in the SPEI drought measure improves yields by 0.6%, 0.9%, and 2.0% for corn, soybeans, and sunflower, respectively.

Estimation of the interaction term between ozone and Tmax indicates that ozone interactions significantly damage yields for corn, soybeans, and spring wheat. Holding AOT40 fixed at current levels, a unit increase in Tmax drops corn yield by 0.1%, soybeans by 0.2%, and 0.5% for spring wheat. This raises the concern that climate change will not only pose direct effects on agricultural productivity but possibly lead to indirect effects via increased ozone pollution in the future. An interesting question to ask is which effects will dominate? This matters because climate change mitigation and adaptation are costly, so is pollution regulation. A good understanding of the relative effects of ozone and climate change is required for developing cost-effective strategies to combat food security problems.

On the other hand, an increase in the SPEI drought measure (reflecting wetter conditions) mitigates ozone damages for corn, soybeans, cotton, sorghum, and sunflowers. A 0.1 unit increase alleviates ozone exposure effects for these crops by 0.09%, 0.06%, 0.09%, 0.06%, and 0.32%, respectively. These findings also differ from the chamber experiment results (Khan and Soja 2003; Biswas and Jiang 2011; Guarin et al. 2019). Nevertheless, our results are consistent with McGrath et al. (2015)'s results for corn and soybeans who argued elevated ozone level impairs abscisic acid (ABA) signaling, which reduces stomatal conductance, water loss, and resultant water stress. Ainsworth et al. (2012) presented similar findings. For summer crops that frequently suffer from drought, irrigation might not only relieve the challenges of extreme heat but also mitigate the damage caused by ozone.

[18]One should be noted that SPEI is an index variable. A unit increase in SPEI could indicate a significant change in water conditions from dry to wet. Therefore, we adopted an increase in 0.1.

Historical crop production reductions and revenue losses

To develop information on the economic implication of ozone effects, we estimated US level production and gross revenue losses by averaging summed acreage-weighted results on county crop losses from 1980 to 2015. We did this for the ozone-sensitive crops. The production loss is reflected by the yield difference between estimates under historical AOT40 measures and a scenario where AOT40 was set at zero following the assumption in McGrath et al. (2015).

To estimate revenue loss, we reduced USDA reported national crop revenues in 2015 U.S. dollars (USDA NASS 2020) by the percentage loss in production. It bears noting that the revenue evaluations here do not account for changes in prices triggered by changes in supply. The results are shown in Table 3.

Production reductions range from 1.7% to 9.5%, with the reduction of sunflower at the lower end and corn at the higher end. For revenue loss, corn and soybeans are the largest due to both their high sensitivity to ozone exposure and large production level.[19] Though revenue losses for the other crops seem negligible compared to corn and soybeans, the production reductions are still alarming (i.e., for spring wheat, cotton, and peanuts). The combined economic losses averaged just over 6 billion dollars per year, accounting for 5.8% of 2018 total revenue to these crops (USDA NASS 2020).

Another interesting finding is that, in line with McGrath et al. (2015), our estimated production reductions become smaller since 1980 due to decreasing ozone concentration levels, as shown in Figure 5 below. For instance, production reductions for corn decreased from 12.1% in 1980 to 3.9% in 2015. According to EPA, ozone concentrations have decreased by 31% from

[19]These two crops are the most widely planted crops in the United States with a total of 179.2 million planted acres in 2018 (USDA NASS 2019).

Table 3. The Average Annual Production Reductions and Revenue Losses Induced by Ozone from 1980 to 2015

Crops	Average annual production reduction (in %)	Average annual revenue losses (in billion 2015 U.S. dollars)
Corn	9.5	3.9
Soybeans	4.5	1.2
Spring wheat	5.6	0.2
Cotton	7.8	0.5
Peanuts	5.9	0.1
Rice	3.7	0.09
Sorghum	1.8	0.04
Sunflower	1.7	0.01

Note: The production reductions and revenue losses were derived by comparing the differences between estimates under historical AOT40 measures and a scenario where AOT40 was set at zero following McGrath et al. (2015). The national results stemmed from weighted county-level losses with harvested acres being the weights.

1980 to 2018 (21% from 1990 to 2018 and 16% from 2000 to 2018), benefiting both human health and agricultural productions (US EPA 2020).

Future yield consequences of ozone and climate

As addressed above, climate change is expected to increase ozone formation due to increased heat (USGCRP 2018). This currently happens when we have heat waves where Zhang et al. (2018) reported a 22% increase in US maximum 8-hour average ozone concentrations. On the other hand, climate change itself has been found to impose negative effects on yields (Schlenker and Roberts 2009). To see which effects dominate, we will and decompose future yield consequences into those induced by climate change and those induced by ozone exposure increases driven by climate change as we describe below.

To examine the climate impacts we used projection output from IPSL-CM6A-LR (Boucher et al. 2019) under the SSP4-6.0 (Shared Socioeconomic Pathways) (Riahi et al. 2017). Using those projections, we calculated changes in our climatic variables, i.e., FDD, GDD, Prec, and Tmax in

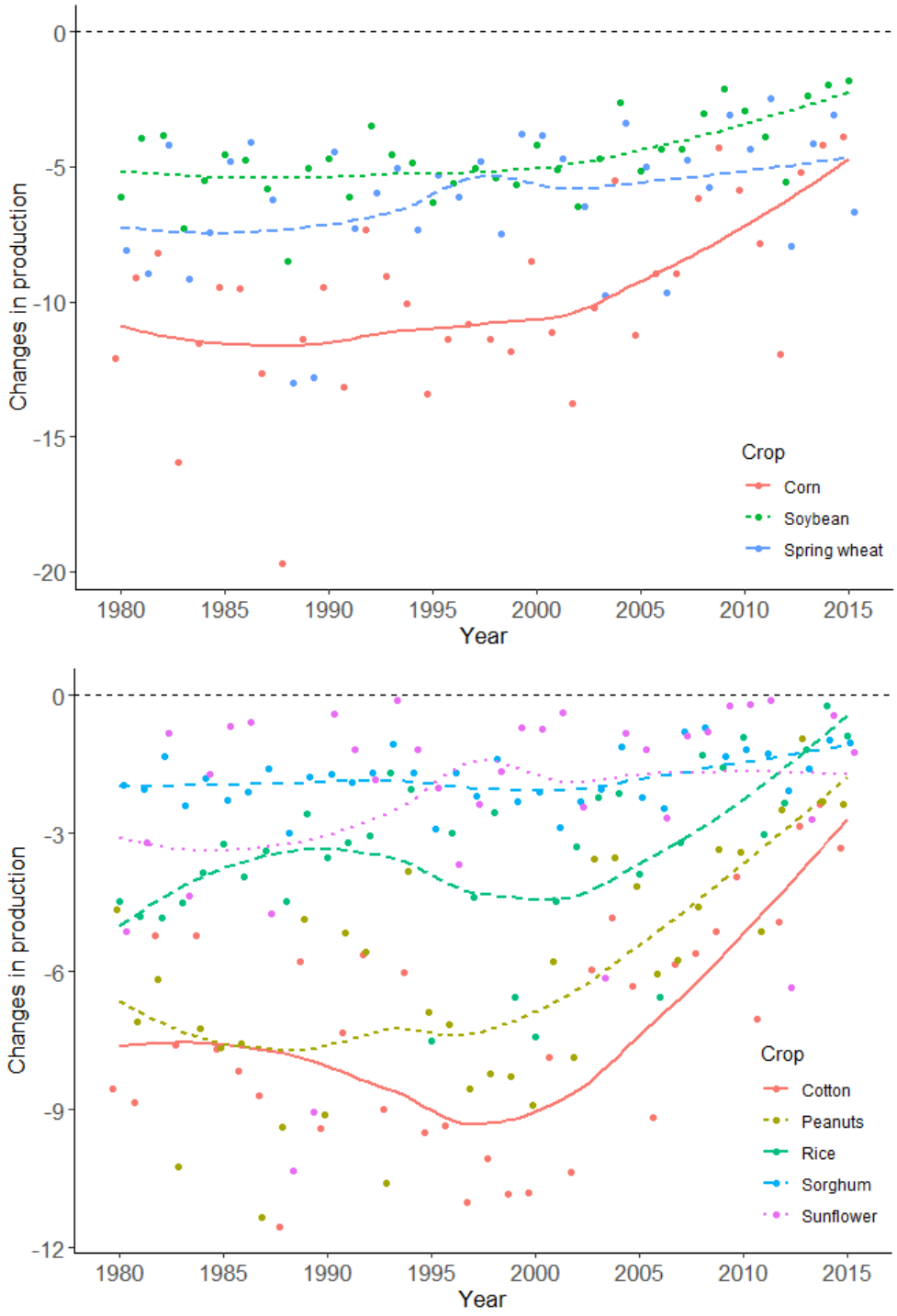

Figure 5. Changes in production (in percentage) as a function of time

Note: We report the production reductions in two charts for a better presentation. In the figure, each dot is a weighted mean for all counties with harvested acres as weights. The lines are LOESS fits to the points.

2048-2052, relative to 2015-2019. Due to large uncertainty in their future projection, we held the Harv and SPEI variables at their respective 2015 levels.

Climate change-driven ozone projections were constructed based on a regression of historical ozone on observed climate. Specifically, we estimated a panel data regression with historical AOT40 as the dependent variable as a function of observed US climate data. We then applied the IPSL-CM6A-LR climate change projections to project associated AOT40 (see Appendix A for details). Figure 6 shows the resultant climate change projections for spring crops as well as the estimated ozone changes (see Figure A2 in Appendix A for results on winter wheat). Our resultant projection shows climate change, alone, leads on average to 36% increases in AOT40.

Following that, we evaluated our baseline model under the projected climate and ozone results to obtain future yield estimates for 2048-2052. Note our projections do not account for any additional adaptation beyond what is inherent in the yield estimations.

As can be seen from Figure 7, climate change-induced increases in AOT40 decrease yields for all crops except winter wheat and barley. Spring wheat exhibited the largest reduction in yields (1.8%), followed by corn (1.2%), sunflower (1.0%), soybeans (0.6%), cotton (0.5%), peanuts (0.3%), and sorghum (0.2%), with rice as the least affected (0.1%). On the other hand, changes in climatic variables impose larger impacts. The resultant yield reductions span from 5.2% for winter wheat to 25.5% for sorghum with a 4.3% gain for rice (note these results for rice are less reliable because the baseline estimates are statistically insignificant). The rising maximum temperature is the largest contributor to the damages where five of the ten crops benefit from the moderate increases in growing degree days. In conclusion, our results suggest that ozone impacts induced by climate change are less damaging than the direct effects of climate change itself.

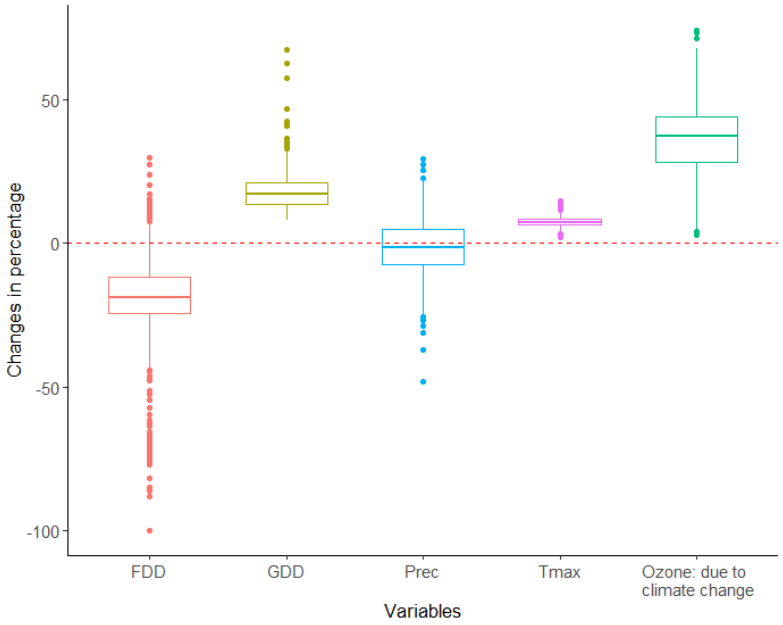

Figure 6. Future changes in climate conditions and climate change-induced ozone changes for spring crops

Note: This boxplot also reflects the distribution of changes across counties. Each box is defined by the upper and lower quartile, and the horizontal line within the box depicts the median. The endpoints for the whiskers are the upper and lower adjacent values, which are defined as the relevant quartile +/- three-halves of the interquartile range, and the dots refer to changes outside of the adjacent values.

This finding is pretty consistent with recent work by Liu and Desai (2021) which jointly considered the impacts of future climate change, ozone exposure, and atmospheric aerosols on corn and soybean yields. Their results suggested that more than 95% of yield reductions are contributed by future warming. This confirms that climate change is a critical threat to crop yields and tends to impose damages larger than that induced by ozone pollution. From this point of view, climate change mitigation and adaptation strategies are likely to have a larger impact than air pollution regulations. However, it bears noting that the potential health benefits stemming from pollution controls should not be ignored, which are usually significant (Sarofim, Waldhoff, and Anenberg 2017; Deryugina et al. 2019). Moreover, environmental regulations (i.e., renewable

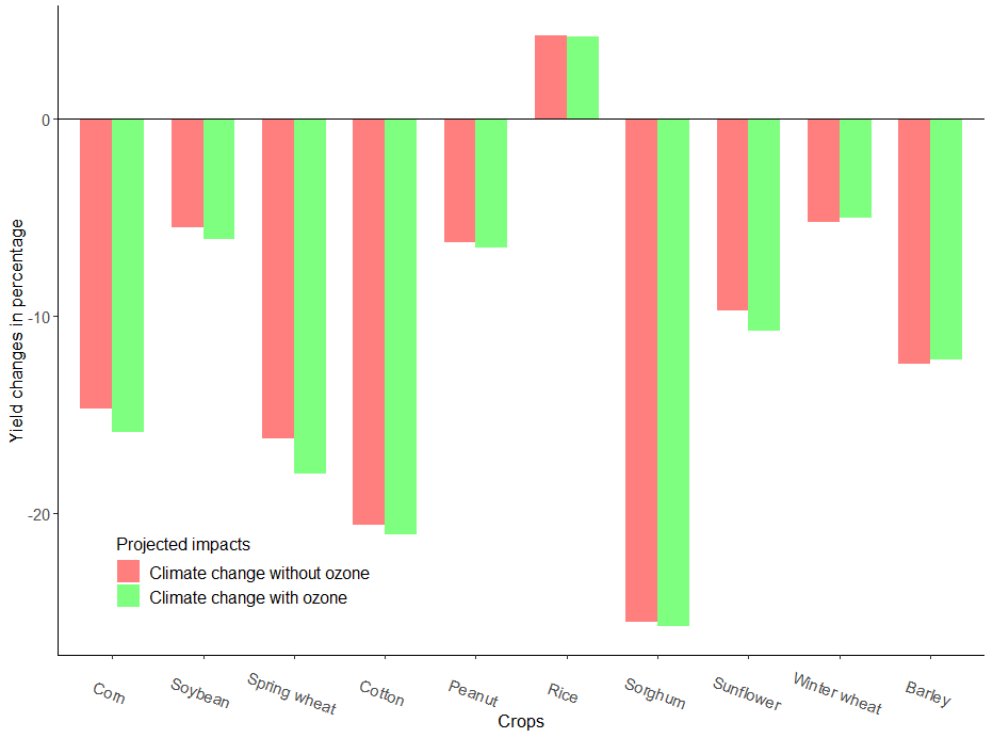

Figure 7. Projected yield changes associated with future climate change alone and climate change plus ozone change

energy standards) usually have dual effects on climate change and air pollution.

A potential caveat of our yield projection is that we did not project Harv and SPEI rather held them constant. Such projections are not readily available from the literature and performing projections for them are difficult (especially for Harv). Additionally, the drought indicator SPEI is determined by precipitation and potential evapotranspiration (Vicente-Serrano, Beguería, and López-Moreno 2010), and its projection is inherently uncertain due to high variability in both factors. Nevertheless, taking corn as an example, we projected SPEI in a similar fashion to what we did for AOT40. This results in a climate change induced decrease of 0.3 in SPEI (indicating drier conditions). The resultant projections indicate a corn yield reduction of 1.8%, which is much smaller than the effects stemming from changes in temperatures (i.e., yield reduction of 14.4%).

We recommend dedicated future studies focusing particularly on hydroclimate variables beyond precipitation, especially since extreme events such as long-duration drought could be deadly for vegetation growth and food production (Cook, Ault, and Smerdon 2015; Xu et al. 2019; Verschuur et al. 2021).

Comparison of results with other climate and ozone studies

Given the importance of climate change to future crop productivity as suggested by our results, it is desirable to compare our findings (both climate change impacts and ozone impacts) with existing evidence in the literature.

We compared our climate change estimations with two key papers - Schlenker and Roberts (2009) and Burke and Emerick (2016). Under a "business as usual" scenario (A1B) and using output from the same climate model as ours, Burke and Emerick (2016) concluded a yield reduction of 20% for corn in the middle of the century relative to the 1980s. With a comparable scenario (SSP4-6.0), our results suggest a yield reduction of 14.7%. The difference is primarily due to the differing base period, i.e., the 1980s in Burke and Emerick (2016) and 2015-2019 in our study. This argument is supported by examining the temperature changes. According to our calculation, on average, temperatures are expected to increase by 3.2 °C from the 1980s to 2050s compared to 2.0 °C increases between the 2010s and 2050s.

Although Schlenker and Roberts (2009) did not provide a comparable climate change scenario, we can still compare under uniform warming schemes. Schlenker and Roberts (2009) reported a yield reduction of 14.9%, 8.9%, and 8.3% for corn, soybeans, and cotton, respectively, under a uniform temperature increase of 2 °C. Our results are consistent with theirs except that we find a cotton yield reduction of 20.6%. This is mainly because we focused on dryland cotton

whereas Schlenker and Roberts (2009) did not have such restriction and over 58% of cotton is irrigated in the United States.

In terms of precipitation, both (Schlenker and Roberts 2009; Burke and Emerick 2016) and our study confirmed that precipitations play minor roles in climate change impact projections. Similar findings were observed in studies that examine climate change impacts on economic growth (Dell, Jones, and Olken 2012). Nevertheless, we directly compared the nonlinear precipitation-yield relationship across studies. The yield-maximizing precipitation level identified from our model was 26.7 inches and 22.6 inches for corn and soybeans, respectively, which are comparable with estimates (25.0 and 27.2 inches) from the more complicated temperature-exposure models in Schlenker and Roberts (2009) (note that they did not report the results from the degree-day model). Meanwhile, Burke and Emerick (2016), which used a degree-day model (though slightly different from ours), reported yield-maximization precipitations of 19.7 inches both for corn and soybeans.

There are also a few studies in the literature that investigated climate impacts and ozone impacts jointly such as (Tai, Martin, and Heald 2014; Liu and Desai 2021). As discussed in the previous section, our results are pretty consistent with those in (Liu and Desai 2021), however are quite different from findings in (Tai, Martin, and Heald 2014) regarding the magnitude of ozone and climate change effects on future yields. Specifically, Tai, Martin, and Heald (2014) presented an analysis of the combined effects of 2050 climate change and ozone trends on the production of four major crops (wheat, rice, corn, and soybean) under the scenario of RCP4.5 and RCP8.5. They concluded that ozone regulation as represented in RCP4.5 has the potential to completely reverse the warming impacts and lead to substantial yield gains for certain crops (i.e., wheat and rice) in the US. The differences between our findings and theirs could be possibly attributable to two

aspects. First, while we jointly included ozone variables and a suite of climatic variables in our panel data regression, Tai, Martin, and Heald (2014) estimated the climate change effects via a constrained linear regression model, and their ozone effects were estimated using dose-response functions. Another contributor could be the different sources of future ozone projections. Tai, Martin, and Heald (2014) simulated ozone projections using climate models, which allows them to not only include the effects of climate and land-use changes but also take account of the trends in anthropogenic precursor gas emissions, whereas our ozone projections were estimated via historical relationships between ozone and climate.

Conclusion

We investigate crop yield impacts of ozone exposure, as well as climate effects both independently and in interaction with ozone. This was done for US yields of corn, soybeans, spring wheat, winter wheat, barley, cotton, peanuts, rice, sorghum, and sunflower.

We find significant negative impacts of ozone exposure on all crops except for winter wheat and barley. We find that per one ppm·hour increase in AOT40 decreases annual yields by 0.3% to 1.2%, for the crops damaged by ozone. This translates to annual revenue losses of $6.03 billion (in 2015 U.S dollars) or 5.8% of 2018 total revenue for these damaged crops. We also find that winter wheat is not sensitive to ozone exposure, which differs from results found in chamber experiments. We speculate the discrepancy may arise due to the low ozone levels in major winter wheat-growing regions (e.g., the Great Plains), as well as the cooler production seasons (i.e., early spring). We also confirm the existing empirical evidence that corn tends to be more sensitive than soybeans, which also contradicts chamber experiments.

We examine historical climate change impacts on yield, both independently of ozone and in conjunction with ozone changes. Our results show that climate change exacerbates ozone damages

for ozone-sensitive crops, particularly for soybeans and spring wheat. We find a 1 ºC increase in maximum temperature averaged during the ozone sensitive period further drops yields by 0.2% for soybeans and 0.5% for spring wheat. On the other hand, drought mitigation alleviates ozone damages. For instance, a moderate move in the SPEI drought index by 0.1 toward wetter conditions mitigates ozone damages by 0.06% to 0.32%.

We also find mid-21st century projected climate change under an SSP4-6.0 warming scenario would increase ozone concentrations in the agricultural regions by 36% for spring crops, which would further decrease yields by 0.1% to 1.8%. Though small in magnitude, this implies that US climate change may increase demand for more stringent ozone reduction policies. This can be particularly important for countries with high ambient ozone concentrations over agricultural lands such as China.

We contrast ozone-induced future crop damages with damages due to future climate change. Our results showed that under the SSP4-6.0 scenario, the yield loss directly from climate change would range from 5.2% to 25.5% (mainly due to extreme heat), which is more than an order of magnitude greater than that from the climate-driven ozone increase.

Future research can be extended by expanding possible ozone impacts such as considering other variables, i.e., aerosols. The inclusion of aerosols in the assessment is important because there are projections of more frequent heatwaves and higher aerosol episodes (Xu et al. 2020).

CHAPTER III

ARE CLIMATE CHANGE DAMAGES ON WINTER WHEAT OVERSTATED? EVIDENCE FROM CHINA[20]

Climate change has been shown to have broad implications across the economy (Burke, Hsiang, and Miguel 2015; Dell, Jones, and Olken 2014; Stern 2007), and the agricultural sector is expected to experience evident challenges (Deschênes and Greenstone 2007; McCarl, Villavicencio, and Wu 2008; Schlenker and Roberts 2009). A better understanding of climate effects on crops and the consequences of climate change on production are important in determining the extent of needed reactive actions and the development of higher-yielding varieties and strategies that will be ready as climate change proceeds (Liu et al. 2016).

As one of the first domesticated food crops (Tack, Barkley, and Nalley 2015) and the most extensively grown cereal crop worldwide,[21] wheat makes up 20% of the calories people consume every day, among which over 70% come from winter wheat (FAOSTAT 2021). However, despite its importance in food and nutrient balances, *empirical* studies of the climate change impacts on winter wheat are surprisingly rare (compared with the other staple crops such as corn and soybeans - Burke and Emerick, 2016; Chen, Chen, and Xu 2016; Schlenker and Roberts, 2009). In contrast, most of the existing impact assessments are derived from crop simulation models (Asseng et al. 2015, 2013; Liu et al. 2016). Indeed, these models are built to reflect key biological processes governing crop growth and yield, but they are plagued by uncertainties associated with the

[20]This chapter is currently under revision per requests from *Journal of Environmental Economics and Management*. The contents of the chapter may (or may not) be published in the future. The student acknowledges potential copyright issues.

[21]According to the Food and Agriculture Organization of the United Nations (FAO), the harvested acres of wheat reached over 724 million hectares (roughly 1788 million acres) worldwide in 2019, accounting for 29.8% of total harvested land for cereal crops.

complicated model parameters (Lobell and Asseng 2017),[22] and impact assessments from an individual crop model are unlikely to represent the real crop responses to climate change.[23]

On the other hand, existing empirical examinations on winter wheat (though limited) rely on climatic variables (i.e., mean temperatures, degree days, etc.) that are calculated over the *entirety* of its growing period (Asseng et al. 2015; Lobell, Schlenker, and Costa-Roberts 2011; Xiong et al. 2014; Yi et al. 2016; Zhang and Huang 2013). However, winter wheat, generally planted in September/October and harvested in May/June next year, has a long growing period that covers three distinct growing stages corresponding to three seasons (Fall, Winter, and Spring).[24] Various growing stages require different climatic conditions (Tack, Barkley, and Nalley 2015). Thus simple aggregates of climatic variables over the entirety of the growing period may not only overlook the variation of climatic impacts across growing stages but also misrepresent the *real* climate-winter wheat relationships.

This paper addresses these issues by performing a rigorous empirical investigation of the climate change impacts on winter wheat using Chinese county-level data from 1981-2015. China is the largest wheat producer in the world, accounting for 17% of total wheat production (FAOSTAT, 2021), and over 90% of that production comes from winter wheat (National Bureau of Statistics 2019). Our empirical analysis proceeds as follows. First, we divide the long growing

[22]In fact, most of those climate change assessments were conducted at a few agricultural sites. In this regard, their external validities are also questioned. The exceptions are Lv et al. (2013) and Rosenzweig et al. (2014), in which the authors applied the crop simulation models to high-resolution raster data.

[23]Recent studies recommend considering the median of an ensemble of simulation models as an accurate estimate, rather than relying on the results of an individual model. See examples in (Asseng et al. 2015, 2013; Liu et al. 2016; Schauberger et al. 2017).

[24]For instance, the fall season covers the vegetative growth stage including the emergence and tillering of winter wheat. Growth has been found to be sensitive to high temperatures during this season (Porter and Gawith 1999). In the winter season, the wheat is dormant and largely insensitive to weather although during this period it transforms from vegetative growth to reproductive growth (Liu et al. 2016). Additionally, high winter temperatures could awake the wheat from dormancy and make it susceptible to early spring frost (Holman et al. 2011). Finally, in spring, wheat resumes growth and performs jointing, booting, and flowering and those processes are regarded as temperature-sensitive (Dreccer et al. 2018; Liu et al. 2016; Šebela et al. 2020; Tan et al. 2018; Zampieri et al. 2017).

period into three seasons (Fall, Winter, and Spring). We then run piece-wise regressions to empirically identify the lower and upper temperature thresholds separately for each season, based on which we construct a suite of degree-day variables. Second, we employ a panel data model with fixed effects to estimate the various climatic impacts across seasons (growing stages). Third, concerns have been raised that panel models are unable to take account of long-run climate change adaptations, thus tend to reflect short-run impacts (i.e., impacts induced by year-to-year weather shocks). To address this concern, we add "climate penalty" terms to the conventional panel data model following (Mérel and Gammans 2021), which allows us to differentiate the short-run and long-run impacts. Finally, based on our estimates, we project future yield consequences with a variety of climate change scenarios and compare our results with existing evidence from both crop simulation models and empirical studies.

Our work contributes to the literature in three important ways. First, our analysis is based on statistical models and adds new evidence to the current climate change assessments on wheat which are largely derived from crop simulation models (Asseng et al. 2013; Lobell and Asseng 2017). A comparison of future yield projections between our estimates and those from crop simulation models indicates that the latter may have overstated the climate change damages on winter wheat (i.e., 3%-6% yield reduction with 1 ºC increase in temperature in contrast to a weak yield gain of 0.4% in our analysis). Splitting the long growing period into three seasons allows us to reveal that the overestimation of damages in crop simulation models is mainly due to their omission of the potential benefits stemming from the (global warming-induced) reduction in the number of freezing days (i.e., temperatures below 0 ºC). This argument is supported by our empirical evidence. For instance, after we exclude the freezing day variables in our projection (i.e.,

we exclude the potential benefits of warming), we obtain a yield reduction of 4%, which closely converges to those found in crop simulation models.

Second, our work contributes to a broad range of literature that empirically examine the impacts of climate change on our economy, including agricultural productivities (Chen, Chen, and Xu 2016; Deschênes and Greenstone 2007; Lobell, Schlenker, and Costa-Roberts 2011; Schlenker and Roberts 2009), energy demand and supply (Auffhammer, Baylis, and Hausman 2017; Davis and Gertler 2015; Li, Pizer, and Wu 2019; Zhang et al. 2021), human health (Barreca et al. 2016, 2015; Barreca 2012; Deschênes and Greenstone 2011), and economic growth (Burke, Hsiang, and Miguel 2015; Dell, Jones, and Olken 2012; Newell, Prest, and Sexton 2021). As one of the most important food crops, our analysis of winter wheat provides insightful guidelines for agricultural activities in response to climate change, which seems to be inevitable (IPCC 2018). In terms of the crop we examine, our work is closely related to (Tack, Barkley, and Nalley 2015) where the authors performed a similar empirical examination on winter wheat in Kansas. But we construct the model slightly different from theirs in a way that we believe is more relevant to winter wheat growth. Out-of-sample cross-validations show that our model significantly outperforms four alternative models that are commonly seen in the literature.

Third, our work also contributes to a rapidly growing body of literature that discusses panel data models' inability of taking account of long-run adaptations in the estimation,[25] which is critical for climate change impact assessments (imagine a world where adaptations are large and rapid, then the resulting economic damages associated with climate change could be minimal). In this paper, we adopt a novel method recently proposed by (Mérel and Gammans 2021), which

[25]See examples in Burke and Emerick (2016), Chen and Gong (2020), Dell et al., (2012), and Miller et al., (2021), and also see reviews in Hsiang (2016) and Kolstad and Moore (2020).

allows us to recover the long-run adaptation effects. Our results suggest that such effects are substantial and could even reverse the sign of climate change impacts on winter wheat. For instance, projections using short-run estimates indicate a yield reduction of 4.9%, relative to a yield gain of 2.2% when projected using long-run estimates under a uniform warming scenario of 3 C°. This finding is different from those conducted in the United States using the long difference model where limited evidence of adaptation was found, but it is consistent with (Chen and Gong 2020) which concluded that long-run adaptation has offset 37% of the short-run effects of extreme heat exposure on agricultural total factor productivity in China.

The remainder of this paper is organized as follows. The next section illustrates the collection of data. The third section introduces the estimation of temperature thresholds for each season. Following that, we introduce the empirical model. The fifth section reports the main results and examines the future yield consequences. Lastly, the sixth section concludes the work.

Data collection

We assemble a data set unifying county-level winter wheat yield data and fine-scale weather data in China spanning from 1981 to 2015. Sources of each are discussed below.

Yield data and the study region

Herein we primarily focus on a sub-region within the North China Plain (NCP),[26] which produces over 70% of winter wheat in China (Zhao 2010). It covers the southern part of Hebei, most of Henan, the entirety of Shandong, and the northern part of Anhui and Jiangsu (see the map in Figure B1 in Appendix B). Additionally, we choose this region based on several considerations. First, this region has an arguably uniform growing period (October to May for winter wheat) and cropping

[26]This sub-region is also known as the "Huang-Huai-Hai" plain.

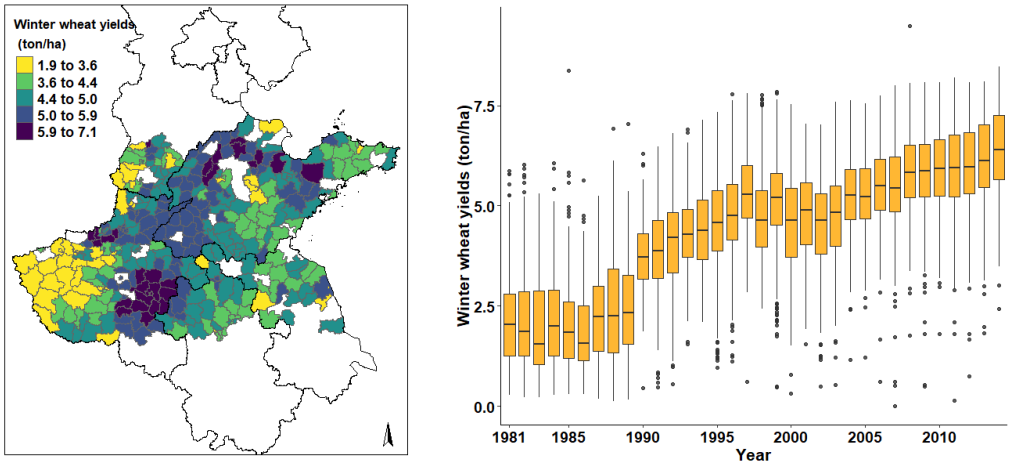

Figure 8. Spatial and temporal variation within the winter wheat yield data for the study region.

Note: The figure displays the county-level yield averages across 1981-2015 (left) and the changes in yield over time (right). The box shows the upper and lower quartiles for each year, and the mean is depicted as the horizontal bar. The endpoints for the whiskers represent the respective quartile +/- 1.5 times the interquartile range, and dots indicate yields outside of that range.

pattern (winter wheat plus summer corn). Second, rainfall in this region is greater than in the northern part of the NCP and we can assume that winter wheat is rain-fed (Zhang and Huang 2013; Zhao 2010). This allows us to focus on rain-fed winter wheat and overcomes the fact that we do not have high-quality data on irrigation, an approach similarly taken by (Schlenker, Hanemann, and Fisher 2005; Tack, Barkley, and Hendricks 2017).

County-level yield data (in tons/hectare) were obtained from the database of the Institute of Agricultural Information at the Chinese Academy of Agricultural Science (Yi et al. 2016). In using those data, we drop counties that have less than 10 years of yield observations. This leaves us with observations for 352 counties and 8867 annual data points in total.

The spatial and temporal variations of yield are shown in Figure 8. Yields are higher in the middle part of the study region (largely the eastern part of Henan and the northern part of Anhui and Jiangsu), whereas the yields in the western part (largely western Henan) are lower, presumably due to lower rainfall. Over time the average yield in the study region has steadily increased from 2.2 tons/ha in 1981 to 6.3 tons/ha in 2015.

Weather data

Temperature and precipitation data were assembled from two sources. Daily minimum and maximum temperatures were downloaded from the China Meteorological Data Service Center (CMDC) (Chen and Gong 2020). The initial data were gridded at a resolution of 0.5°×0.5°. We converted it to county-level by weighted-averaging over grid cells falling within each county with the size of the areas acting as weights following (Auffhammer et al. 2013; Burke et al. 2018).

We move further by constructing *hourly* temperatures from the daily data using a sine function Luedeling (2020).[27] We then use hourly temperatures to establish degree-hour measures then later degree-day variables. For instance, if we use a threshold of 20 ºC, then one hour of 30 ºC contributes to 10 degree-hours, which we convert to degree-days by dividing it by 24 following (Tack, Barkley, and Nalley 2015). We will get back to this in detail in the next section.

For precipitation, we downloaded monthly data from the China Meteorological Forcing Dataset, developed by (He et al. 2020). The initial data were gridded at 0.5°×0.5°, and we converted them to county-level following the same procedure above. In turn, the county-level

[27]The construction of hourly temperatures is done using the R package "chillR". The workhorse is the "stack_hourly_temps" function which employs a sine curve for daytime temperatures, with nighttime cooling represented by a logarithmic decay function. It should be noted that differences in day length between locations are also accounted for by computing sunrise and sunset times based on geographic latitudes and the day in a year. See technical details in (Luedeling 2020).

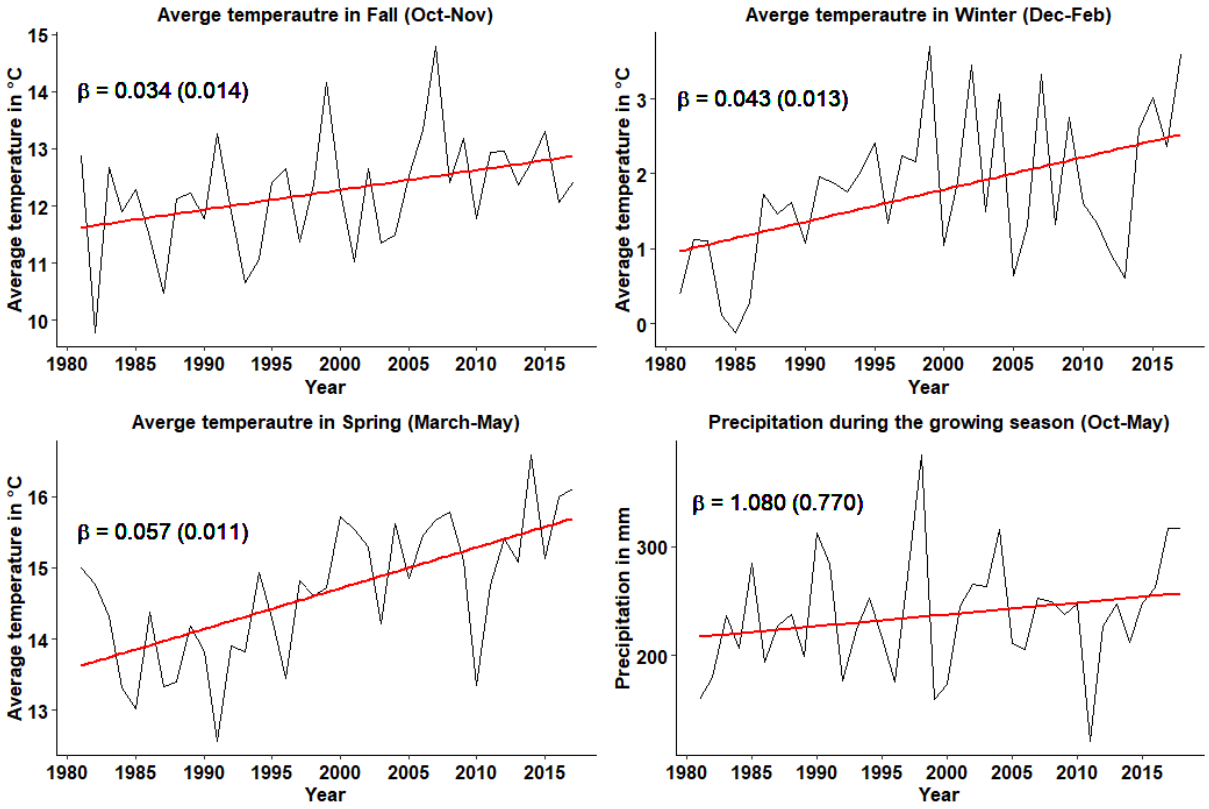

Figure 9. The trends in seasonal temperature and growing-period precipitation

Note that red lines in the figure indicate simple regressions of temperature/precipitation on years. β denotes the coefficients with the standard errors shown in the parentheses.

monthly precipitation data were aggregated over seasons, respectively (i.e., Fall, Winter, and Spring).

Figure 9 shows the general trends in seasonal temperature and precipitation from 1981 to 2015. Consistent with other climate change observations we see upward trends in all seasonal temperatures, particularly in the winter and spring. Precipitation exhibits more year-to-year variability and does not show significant trends.

Empirically estimating temperature thresholds for deriving degree-day variables: What is considered too cold/hot?

To calculate degree days there is a need for a base temperature and a time interval. A number of papers in the literature use a base temperature of 0 ºC for winter wheat (Dreccer et al. 2018; Yang et al. 2015; Yi et al. 2016). In terms of time interval, degree-day variables are usually calculated over the entirety of the growing period (Oct-May) (Dreccer et al. 2018; Yang et al. 2015; Yi et al. 2016). However, as discussed in the introduction, using such a simple base temperature and time interval ignores the possibility that different growing stages may have different temperature thresholds. Additionally, most existing studies omit the impacts of freezing days (temperatures below 0 ºC), which have been found to have important effects on winter wheat. For instance, agronomic studies show that freezing temperatures in spring could impose significant damages on winter wheat yields (Xiao et al., 2018), whereas mild freezing in the early winter could help winter wheat to prepare for the even lower temperatures during the winter season (Porter and Gawith, 1999).

Herein we divide the growing period (Oct-May) into three parts - fall (Oct-Nov), winter (Dec-Feb), and spring (March-May) following (Tan et al. 2018; Xiao et al. 2018; Zhou et al. 2018). We then employ piece-wise regressions to *empirically* identify temperature thresholds for each season (Tack, Barkley, and Nalley 2015).

Specifically, we set lower and upper non-freezing (above 0 ºC) temperature thresholds for each of the fall and spring seasons along with a freezing degree-day variable calculated independently (with 0 ºC as the threshold). That means we have four degree-day variables for each of the fall and spring seasons, namely, freezing degree-days (*Frez*), degree-days between zero and the lower threshold (*DDlow*), degree-days between the lower threshold and the upper threshold

(*DDmed*), and degree-days above the upper temperature threshold (*DDhigh*). We hypothesize that *DDmed* will be the key determinant of winter wheat growth, whereas *Frez*, *DDlow*, and *DDhigh* will reduce yields. Following (Tack, Barkley, and Nalley 2015), we loop over all possible threshold combinations doing a yield estimation for each season separately, and pick one which has the best fit (the highest r square). The number of candidate threshold combinations is determined by the maximum *hourly* temperatures in that season. For instance, if the maximum temperature in the fall is 40 ºC, the lower/upper threshold candidates can take the integer values from 1 to 40. Thus, in total there will be 800 (i.e., 40*40/2) threshold combinations (this number is 968 for the spring).[28]

The setup for the winter season is different. Specifically, we set the lower threshold slightly *below* zero and the upper threshold *above* zero. Because winter wheat is in dormancy during the winter season, this moderate temperature interval keeps it remaining in dormancy (i.e., not too cold to damage wheat or too hot to interrupt wheat from dormancy - Porter and Gawith, 1999). In this case, we only have three degree-day variables (i.e., we do not have an independent freezing degree-day variable as in fall and spring). We again loop over all possible threshold combinations (290 in total)[29] for the winter season and pick the pair which produces the best fit.

[28]It also should be noted that, in line with (Tack, Barkley, and Nalley 2015), when we are choosing the optimal thresholds, the lower threshold is restricted to be at least 5 ºC below the upper threshold to ensure that the temperature interval is not too narrow. (Tack, Barkley, and Nalley 2015) also impose additional restrictions such as the lower threshold to be at least 5 ºC above zero and 10 ºC below the maximum observed temperature and the upper threshold is restricted to be 5 ºC below the maximum. Our piece-wise regressions are insensitive to these additional restrictions.

[29]Here for the winter season, the lower threshold takes integer values from the minimum hour temperature (-20 ºC) to zero, while the upper threshold takes values from zero to the maximum hour temperature (29 ºC).

Table 4. The estimated temperature thresholds

Season	Lower and upper thresholds (in ºC)
Fall (Oct-Nov)	17 and 24
Winter (Dec-Feb)	-5 and 8
Spring (March-May)	25 and 30

The estimated temperature thresholds are shown in Table 4. We found that the thresholds chosen are robust to alternative growing period specifications, such as September-May and September-June (see the results in Table B1 in Appendix B).[30]

Our results are largely consistent with the thresholds estimated in (Tack, Barkley, and Nalley 2015) in a Kansas study. The difference is that Tack, Barkley, and Nalley (2015) adopt the same threshold setup for the winter season as for fall and spring and estimate winter temperature thresholds of 5 ºC and 10 ºC. Our thresholds are also in line with results from field experiments (Cao and Moss 1989; Narciso, Ragni, and Venturi 1992; Porter and Gawith 1999; Slafer and Rawson 1995).

Table B2 in Appendix B displays the summary statistics. In the table, we also computed degree-day variables using daily temperatures as opposed to hourly temperatures. The results show that hourly temperatures perform better in representing heat and freezing days than daily temperature (i.e., larger values of degree-day variables and more variations), as also suggested by (Schlenker and Roberts 2009).

The estimation model

The literature reveals two basic approaches for empirically estimating climate impacts on the agricultural sector: the use of a cross-sectional model and the use of a panel data model with fixed

[30]We also ran piece-wise regressions jointly with all three seasons and again the estimated thresholds were consistent with the results from separate regressions with individual seasons.

effects (Da, Xu, and McCarl 2021). The advantages of the former are that it implicitly takes account of long-run climate change adaptations (Deschênes and Greenstone 2007; Fezzi and Bateman 2015; Hsiang 2016). However, it is plagued by endogeneity issues such as omitted variable bias (Chen and Gong 2020).

On the other hand, panel data models with fixed effects seem to take the lead in empirical studies because they are able to alleviate the omitted variable bias to some extent by introducing location-specific fixed effects (Schlenker and Roberts 2009; Dell, Jones, and Olken 2012; Zhang, Zhang, and Chen 2017; Chen and Gong 2020). However, panel regressions rely on time-series variations and reflect the effects of weather shocks (year-to-year weather variation) on the outcomes. As a result, they do not fully take into account the long-run adaptations as in the cross-sectional models (see detailed reviews in Hsiang (2016), Blanc and Schlenker (2017), Kolstad and Moore (2020), and Da, Xu, and McCarl (2021)).

In this study, we use the panel data model with fixed effects as our baseline model following (Chen, McCarl, and Schimmelpfennig 2004; Chen, Chen, and Xu 2016; Deschênes and Greenstone 2007; Schlenker and Roberts 2009) and we address the concern of long-run adaptation effects by adding "climate penalty" terms to the baseline panel model, a novel approach recently proposed by (Mérel and Gammans 2021). In what follows, we introduce the baseline panel model and in the results section, we discuss the short-run and long-run climatic impacts in detail.

Our baseline panel data model takes the form below.

$$y_{it} = \delta_i + \alpha_1 t + \alpha_2 t^2 + \sum_s f_s(\mathbf{w}_{it}^s; \boldsymbol{\beta}^s) + \varepsilon_{it} \quad (4)$$

Where

i denotes the county.

t denotes the year.

s denotes the seasons of fall, winter, and spring.

y_{it} is the logarithm of winter wheat yields in county *i* and in year *t*.

δ_i indicates the fixed effects by county that absorb all time-invariant factors that only differ between counties, such as soil quality and other geographic features.

t and t^2 are the linear and quadratic terms of time trends representing the technology development over time following approaches in (Miller, Tack, and Bergtold 2021; Schlenker and Roberts 2009; Tack, Barkley, and Nalley 2015).

ε_{it} is the error term and we cluster it at the county level to take account of arbitrary serial correlations within the county.

The key term $\sum_s f_s(\mathbf{w}_{it}^s;\boldsymbol{\beta}^s)$ in equation (4) includes all the climatic variables for three seasons. Specifically, for the fall season (*s=fall*):

$$
\begin{aligned}
f_s(\mathbf{w}_{it}^s;\boldsymbol{\beta}^s) = {} & \beta_1^{fall} Frez\_fall_{it} + \beta_2^{fall} DDlow\_fall_{it} + \\
& \beta_3^{fall} DDmed\_fall_{it} + \beta_4^{fall} DDhigh\_fall_{it} + \\
& \beta_5^{fall} Prec\_fall_{it} + \beta_6^{fall} (Prec\_fall_{it})^2
\end{aligned} \tag{5}
$$

For the winter season (*s=winter*):

$$
\begin{aligned}
f_s(\mathbf{w}_{it}^s;\boldsymbol{\beta}^s) = {} & \beta_1^{winter} DDlow\_winter_{it} + \beta_2^{winter} DDmed\_winter_{it} + \\
& \beta_3^{winter} DDhigh\_winter_{it} + \beta_4^{winter} Prec\_winter_{it} + \\
& \beta_5^{winter} (Prec\_winter_{it})^2
\end{aligned} \tag{6}
$$

For the spring season (*s=spring*):

$$f_s(\mathbf{w}_{it}^s;\boldsymbol{\beta}^s) = \beta_1^{spring} Frez\_spring_{it} + \beta_2^{spring} DDlow\_spring_{it} + \beta_3^{spring} DDmed\_spring_{it} + \beta_4^{spring} DDhigh\_spring_{it} + \beta_5^{spring} Prec\_spring_{it} + \beta_6^{spring} (Prec\_spring_{it})^2 \quad (7)$$

Where for fall and spring:

$Frez\_fall_{it}$ and $Frez\_spring_{it}$	denote freezing degree-days (temperatures below 0 ºC).
$DDlow\_fall_{it}$ and $DDlow\_spring_{it}$	denote degree-days measuring temperatures falling between 0 ºC and the lower threshold.
$DDmed\_fall_{it}$ and $DDmed\_spring_{it}$	denote degree-days measuring temperatures falling between the lower threshold and the upper threshold (i.e., the optimal range).
$DDhigh\_fall_{it}$ and $DDhigh\_spring_{it}$	denote degree-days measuring temperatures above the upper threshold.

Degree-day variables for winter are slightly different as we do not have an independent freezing degree-day variable. Specifically,

$DDlow\_winter_{it}$	denotes degree-days below the lower threshold (-5 ºC).
$DDmed\_winter_{it}$	denotes degree-days between the lower threshold and the upper threshold (-5 ºC and 8 ºC).
$DDhigh\_winter_{it}$	denotes degree-days above the upper threshold (8 ºC).
$Prec_{it}$ and $(Prec_{it})^2$	denote linear and quadratic terms of seasonal precipitation.

Empirical results

In this section, we first report results from the baseline panel model. We then compare its performance with four alternative models that are commonly seen in the literature. Following that,

we discuss short- and long-run climatic impacts. Finally, we project future yield consequences of selected climate change scenarios plus examine the effect of adaptation actions.

Regression results from the baseline panel model

Figure 10 below portrays results from the baseline panel data model. Each bar presents coefficients from respective degree-day variables. The specific numerical results appear in Appendix B Table B3. The results are largely in line with our expectations. We consistently observe positive effects within the identified optimal temperature range. Also, we observe negative effects with temperatures outside of the optimal intervals, both under hot and freezing conditions.

We also find varying seasonal effects. Heat in the fall and freezing in the spring are the most significant drivers of yield losses. In the fall season, an additional 10 degree-days over 24 ºC is associated with an 11.4% yield reduction. Similarly, an additional 10 degree-days of freezing conditions in the spring reduces yields by 11.3%, as also found in (Xiao et al. 2018). Finally, for the winter season, cold temperatures below -5 ºC and hot temperatures above 8 ºC both have negative effects on yields, although the former is statistically insignificant.

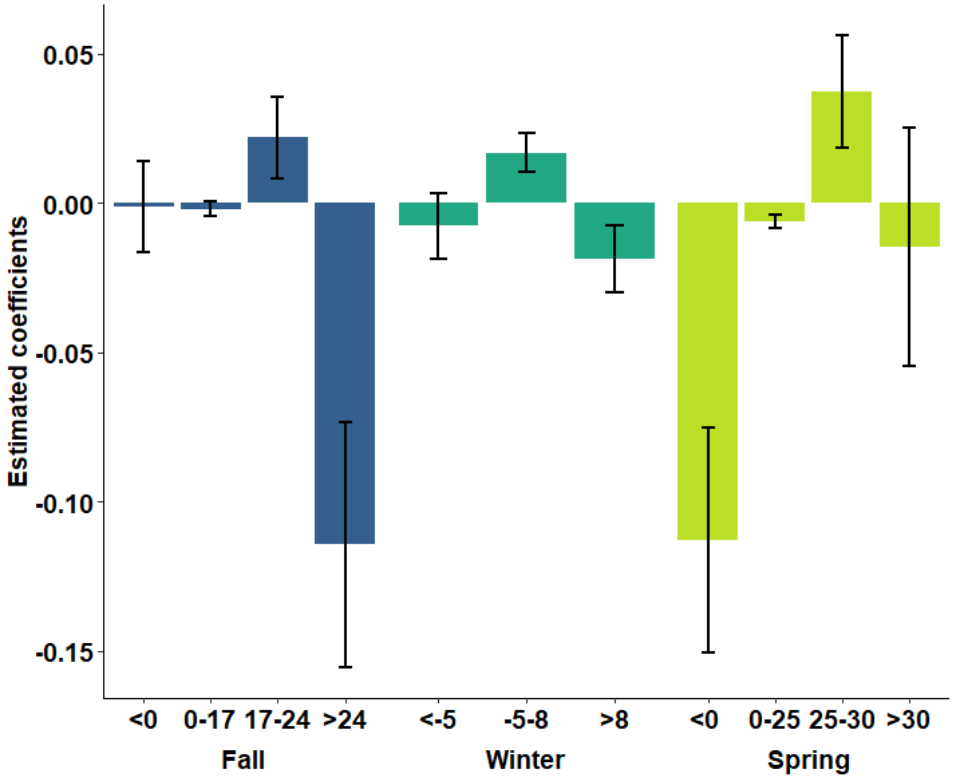

Figure 10. Winter wheat's responses to temperatures across different seasons

Note: The x-axis indicates the degree-day variables (expressed in the unit of 10 degree-days) constructed from the corresponding temperature thresholds. Bars show the estimated coefficients of the respective degree-day variables and the 95% confidence intervals using standard errors clustered at the county level.

Furthermore, we do not observe statistically significant heat damages in the spring contrary to findings in (Tack, Barkley, and Nalley 2015) who find springtime exposure above 34 ºC is associated with the largest yield reduction. This difference is probably attributable to several reasons. First, while Tack, Barkley, and Nalley (2015) focus on Kansas, we cover a larger geographic area and estimate an upper threshold of 30 ºC for spring, relative to 34 ºC in (Tack, Barkley, and Nalley 2015). Second, Tack, Barkley, and Nalley (2015) have more hot days in their sample. Namely, the degree-day variable above 34 ºC is non-zero in over 75% of their observations while this only occurs for 39% in our sample. Similar results to ours are found in (Schauberger et

al. 2017) in which they study country-wide US winter wheat yields but do not find observed or simulated heat effects in the spring.

Apart from the temperatures, precipitation exhibits an inverted U-shape effect on winter wheat yields (see Table B3 in Appendix B) with turning points at 134.6 mm for fall (accumulated in a season) and 188.3 mm for spring above which increasing precipitation leads to yield reductions. Note that the mean rainfall in these two seasons in our sample is respectively 62.0 mm and 159.1 mm, indicating a shortage of rainfall in both seasons (particularly the fall season) and demand for irrigation. We do not detect statistically significant effects of precipitation in the winter season. These findings are quite consistent with farm practices. Normally, irrigation is typically applied after sowing in the fall to meet the water demand for the emergence of winter wheat (Li et al. 2005).

The examination of model performance and robustness checks

Our baseline model has quite different degree-day variables from those used in previous winter wheat studies. In particular, we feel that it better reflects key climate influences that affect winter wheat growth stages and thus hypothesize that it will perform well in predicting yields. To examine this hypothesis, we conduct out-of-sample cross-validations versus a number of model specifications that are common in the literature.

The process is that we randomly choose 80% of data points from our full sample for model training. Then we use the trained models to predict yield outcomes within the remaining 20% of the sample (Fan et al. 2020; Schlenker and Roberts 2009). The root mean squared errors (RMSE) is used as a measure of fit. We repeat this process 1000 times for each of the models and compare average RMSEs. The alternative models we compare performance with are defined as follows:

- A model which includes linear and squared temperatures and precipitations that are averaged/accumulated over the entirety of the growing period and thus does not contain degree-day variables (i.e., “simple tavg” in Figure 11).
- A model which includes linear and squared temperatures and precipitations that are averaged/accumulated respectively for the three seasons (fall, winter, and spring) and again without degree-day variables (i.e., “seasonal tavg” in Figure 11).
- A model which includes linear and squared freezing and growing degree-day variables computed using a single threshold temperature of 0 ºC and over the entirety of the growing period (i.e., “simple dd” in Figure 11).
- A model which is similar to the third model above but includes linear and squared degree-day and precipitation variables defined respectively for each season (fall, winter, and spring) again based on a simple threshold temperature of 0 ºC (i.e., “seasonal dd” in Figure 11).
- The baseline model (i.e., “baseline” in Figure 11).

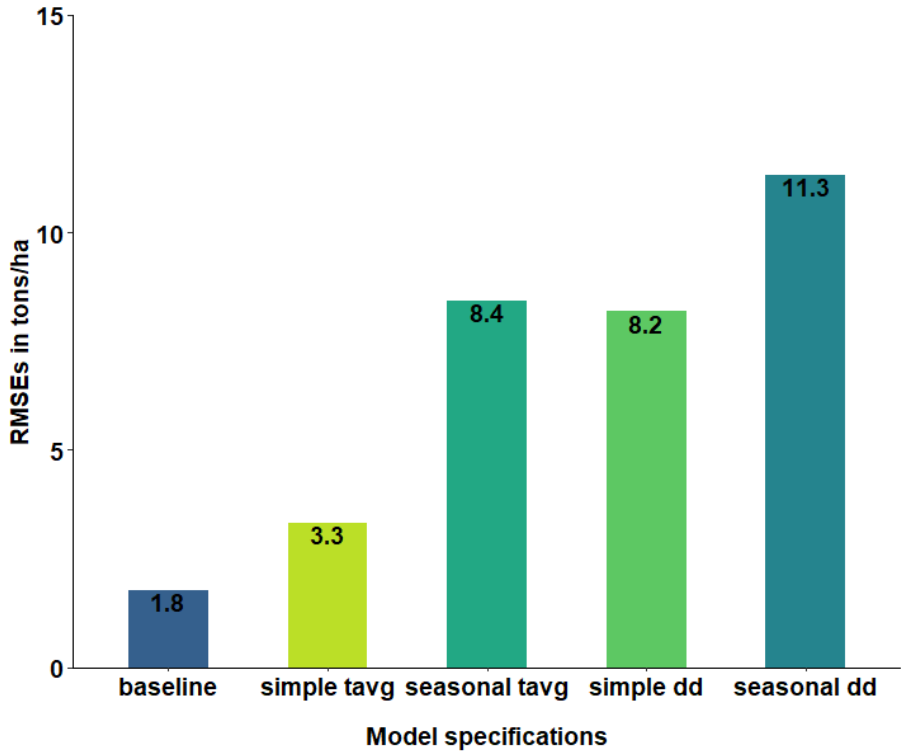

Figure 11. Out-of-sample prediction comparison for multiple model specifications

Figure 11 shows the RMSE results, and the baseline model exhibits the lowest level of error by a substantial margin. That indicates the baseline model outperforms the other four alternatives in predicting yields. One of the most striking results is that the simple average temperature model ("simple tavg") performs better than the other more "sophisticated" models that include seasonally defined variables ("seasonal tavg" and "seasonal dd"). This highlights the fact that at least in our case models using degree-day variables calculated based on a single threshold temperature of 0 ºC, a common practice in the literature (Dreccer et al. 2018; Yang et al. 2015; Yi et al. 2016), does not do a good job of fitting the climate responses of winter wheat.

In Appendix B, we further show that the baseline estimates pass a suite of robustness checks with respect to various lengths of the growing period, inclusion/exclusion of certain seasons,

alternative temperature threshold settings for use in computing degree days, and wider geographic coverage, as well as statistical inference constructed from bootstrapping.

Short-run impacts, long-run impacts, and adaptations

As we have discussed previously, the panel data model with fixed effects has been criticized for its inability to reflect long-run impacts. Several hybrid approaches have been developed in the literature, such as the long difference model (Burke and Emerick 2016) and the multistage model (Butler and Huybers 2013; Kolstad and Moore 2020). These approaches essentially exploit cross-sectional variation and thus require a large number of counties to obtain reliable estimates (usually containing data for over 1000 counties in most applications).[31] Unfortunately, we only have 352 counties.[32]

Recently, Mérel and Gammans (2021) proposed a method to estimate short- and long-run impacts by adding "climate penalty" terms to the conventional panel data model in the form of $\beta(x_{it}-\mu_i)^2$. Here x_{it} denote weather variables (i.e., temperature, degree-days, etc.) for year t at location i; μ_i indicates the climate in location i calculated by averaging the weather variable across the study period, thus $(x_{it}-\mu_i)^2$ measures the *squared* distance between weather realization and the local climate; β is the associated coefficient and is expected to be negative indicating penalties for deviating from the local climate (the underlying assumption is that farm practices are adapted to/optimized for the long-run climate, thus deviation from the climate would harm

[31]The long difference model is a cross-sectional comparison of changes over time (a long period) in which unobserved characteristics are canceled out (Burke and Emerick 2016; Chen and Gong 2020). The multistage method models the county-level response as a function of local climate (Auffhammer 2018; Butler and Huybers 2013; Carleton et al. 2020; Heutel, Miller, and Molitor 2020). A more recent work uses a panel error-correction model (ECM) to distinguish short-run and long-run impacts, i.e., see (Wing, De Cian, and Mistry 2021).

[32]We did run the long-difference regressions with multiple specifications. However, the results were sensitive to the choice of period over which we averaged the data.

agricultural productivity). Conditional on the contemporaneous *weather realization*, locations with an underlying climate closer to that realization will have higher yields than locations for which that realization happens to be unusual. In the long run, we expect such penalties to be removed by adaptations. In a special scenario where adaptations are instantaneous, there will be no penalty (i.e., $\beta = 0$).[33]

In our case, taking *DDhigh_fall*$_{it}$ as an example, $\beta_4^{fall} DDhigh\_fall_{it}$ in the baseline equation (4) becomes

(8) $$\beta_4^{fall,1} DDhigh\_fall_{it} + \beta_4^{fall,2} (DDhigh\_fall_{it} - \overline{DDhigh\_fall_i})^2$$

Where $\overline{DDhigh\_fall_i}$ is the average of $DDhigh\_fall_{it}$ across the study period (1981-2015), representing the climate in county i.[34] In this case, $\beta_4^{fall,1}$ indicates the long-run responses to climate, whereas the short-run impacts are determined by the long-run impacts *plus* the climate penalty ($\beta_4^{fall,2} (DDhigh\_fall_{it} - \overline{DDhigh\_fall_i})^2$)[35].

It should be noted that while $\beta_4^{fall,1}$ in equation (8) can be interpreted as the *marginal* long-run climate impacts, such *marginal* interpretation for short-run impacts is not immediately clear, because the climate penalty term depends on the actual weather realization and the local climate. The adaptation effects are then revealed by comparing the yield projections with long-run impacts and short-run impacts.

---

[33]Mérel and Gammans (2021) make it clear that, conditional on weather, the squared weather-climate difference represents a shock due to diverging underlying climate rather than a shock due to unanticipated weather given climate.

[34]We also tried characterizing this climate variable using a 5- and 15-year moving average respectively, however, the subsequent regression results were not robust nor consistent with the theoretical justification and our expectations.

[35]Note that, in addition to the climate penalties characterized by the squared term, we also ran regressions with alternative specifications. Particularly, we replaced the squared term with an absolute value term, i.e., $\beta_4^{fall,2} | DDhigh\_fall_{it} - \overline{DDhigh\_fall_i} |$. The results indicate that the coefficients on the original climate variables (i.e., $DDhigh\_fall_{it}$) remain largely unchanged, whereas the coefficients on the absolute value penalties terms are all negative with their magnitudes differing from that in the regression with squared penalty terms.

While the climate penalty terms could be added for each climate variable, we are particularly interested in the adaptation effects in response to the most evident yield reduction drivers that are recovered by our baseline model estimation (i.e., *DDhigh_fall* and *Frez_spring*). The results are shown in Table 5 below (note that only coefficients of key variables are reported). Column (1) refers to the estimation of the baseline panel data model. Column (2) contains the results with climate penalty terms added only for *DDhigh_fall* and *Frez_spring* and Column (3) with penalty terms added for all degree-day variables, respectively.

As can be seen from the table, the coefficients associated with the climate penalty terms are all negative which meets the expectation. Compared with the baseline estimates, long-run impacts indicate smaller marginal damages. For instance, yield reductions induced by 10 degree-days increase in *DDhigh_fall* decrease from 11.4% in the baseline model to 7.0% in the model with climate penalty terms (column 2), whereas freezing damages in the spring reduce from 11.3% to 8.8% (column 2). Additionally, estimations with penalty terms added o for nly*DDhigh_fall* and *Frez_spring* are quite consistent with the estimations for the case with climate penalty terms added for all degree-day variables (column 2 versus column 3). Finally, as indicated previously, the *marginal* short-run impacts are not directly revealed in Table 5 (i.e., no such coefficients or combination of coefficients can be interpreted as so).

The interpretation of results here is slightly different from those of the long difference model (Burke and Emerick 2016; Chen and Gong 2020). Specifically, applications that use the long difference model directly consider estimates from the conventional panel model (i.e., the baseline model in our case) as the short-run impacts and estimates from the long difference model as the long-run impacts. Nevertheless, the long-run adaptation effects are recovered in a similar way which we will illustrate in the following sections.

Table 5. The regression results with climate penalty terms

	Winter wheat yields		
	Baseline estimate	Climate penalty	Full penalty
	(1)	(2)	(3)
DDhigh_fall	-0.114*** (0.021)	-0.070*** (0.022)	-0.088*** (0.024)
Frez_spring	-0.113*** (0.019)	-0.088*** (0.017)	-0.074*** (0.016)
DDhigh_fall_penalty		-0.065*** (0.020)	-0.081*** (0.025)
Frez_spring_ penalty		-0.029** (0.013)	-0.027** (0.013)
County fixed effect	Yes	Yes	Yes
Linear time trend	Yes	Yes	Yes
Quadratic time trend	Yes	Yes	Yes
Observations	8,867	8,867	8,867
Adjusted R^2	0.527	0.528	0.531

Note: Standard errors are clustered at the county-level and are shown in the parentheses. *p<0.1; **p<0.05; ***p<0.01.

What do we expect for climate change impacts on winter wheat?

Two interesting questions emerge while considering the climate change impacts on winter wheat. First, we have shown that heat in the fall and freezing days in the spring are the most evident drivers of yield reduction. Climate change characterized by increasing temperatures not only increases the intensity and duration of hot days but also reduces the number of freezing days (De Winne and Peersman 2021). Thus, it is not immediately clear what the overall impacts of climate change would be for winter wheat. Second, if climate change damages are expected, how much of the damages could be alleviated through adaptations then?

To answer the first question, we project yield consequences with and without freezing variables under a range of uniform warming scenarios (1 ºC to 5 ºC temperature increase in relative to 1981-2015) to make our results comparable with previous studies (Asseng et al. 2015; Liu et al. 2016; Tack, Barkley, and Nalley 2015). Specifically, we first apply a uniform temperature increase in all counties across the entire growing period, and then we recalculate the degree-day variables.

Following that, we use the ***long-run*** estimates to project future yield. Formally, taking *DDhigh_fall* as an example,

(9) $$\Delta LR = \beta_4^{fall,1} * \Delta DDhigh\_fall$$

Where ΔLR is the percentage changes in yield that are attributable to changes in *DDhigh_fall* (i.e., $\Delta DDhigh\_fall$). $\beta_4^{fall,1}$ is the estimated long-run impact (column 2 in Table 5).

The results are shown in Figure 12. In that figure, "All degree-day variables" denotes the yield projections with all degree-day variables, whereas "Omit freezing" indicates the yield projection without the consideration of terms capturing freezing effects (*Frez_fall*, *DDlow_winter*, and *Frez_spring*).

Two basic findings emerge. First, the potential yield increases stemming from the reduction in freezing days largely offset the yield decreases from the added heat. Ignoring this leads to estimates that overstate the damages of warming. For instance, under a 1 ºC uniform warming scenario, yield forecasts ignoring freezing effects show a yield reduction of 4.1% whereas projections accounting for the freezing effects show weak gains in yield (0.4%). More surprisingly, from a long-run perspective where adaptation is in place, even larger yield benefits are expected as temperatures increase.

Second, the "Omit freezing" projections are largely consistent with previous findings from modeling efforts where freezing impacts are not explicitly considered. For instance, an ensemble projection made by 30 crop simulation models at 30 agricultural sites indicates a global yield reduction of 6% (compared with our 4.1% yield reduction) under a 1 ºC uniform warming scenario

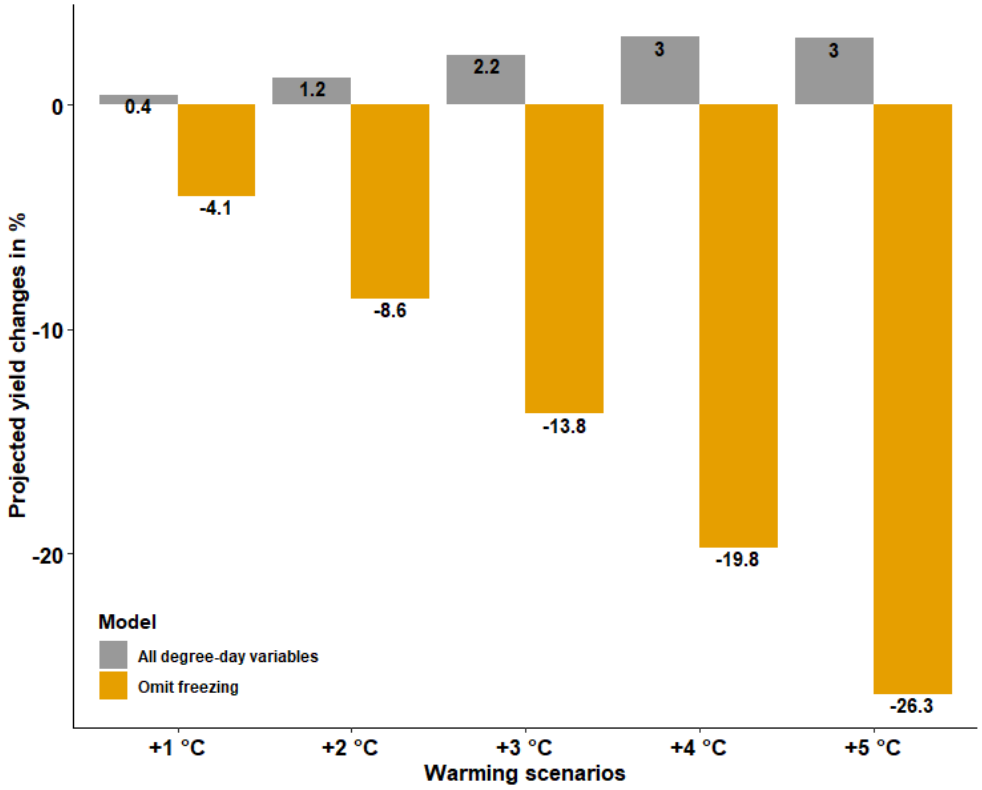

Figure 12. Projected yield consequences under a range of uniform warming scenarios

(Asseng et al. 2015).[36] Only 7 out of those 30 simulation models take advantage of the freezing information. For winter wheat in China, Liu et al. (2016) find a yield reduction of 3.0% under a 1 ºC uniform warming scenario. On the empirical side, Chen, Chen, and Xu (2016), using a temperature bin model with no freezing variables, conclude a winter wheat yield reduction of 11.9% in 2070-2099 relative to 1980-2010 in China under a climate change scenario of A1F1,[37] which translates to a temperature increase of 3 ºC - 4 ºC (IPCC 2007). This empirical projection is

[36]By performing a meta-analysis of process-based crop simulation models, Wilcox and Makowski (2014) concluded a 3.3 ± 0.8% declined in wheat yield with a 1 ºC increase in local temperature. Based on historical regressions and simulation studies, Fischer, Byerlee, and Edmeades (2014) reported an average of 5.9% wheat yield decline with 1 ºC warming.

[37]According to (Chen, Chen, and Xu 2016), the yield reduction is not statistically significant when projected with only temperature and precipitation changes. They highlight the importance of taking account of "secondary climatic variables" in climate change assessments (i.e., wind speed, solar radiation, etc.), in which case Chen, Chen, and Xu (2016) conclude a yield reduction of 18.3%.

again in line with our "Omit freezing" projections. Overall, the consistency between our "Omit freezing" projections and the results of previous studies supports the importance of considering freezing effects when evaluating climate change impacts on winter wheat yields.

In addition to uniform warming scenarios, in Figure B5-B6 we show yield projections using Shared Socioeconomic Pathways (which are scenarios to replace the Representative Concentration Pathways in the sixth assessment of IPCC). There we find larger sensitivity estimates when freezing is not considered (even higher yield gains are expected in the "All degree-day variables" case compared with uniform warming).

How large are the adaptation potentials?

We have shown weak yield gains in the projections with long-run impacts. An important question that arises is what are the roles of long-run adaptations in the impact assessments? To answer this question, we compare the projections derived from short-run and long-run impacts. The former is estimated as follows. Taking *DDhigh_fall* as an example,

$$\begin{aligned}\Delta SR &= \beta_4^{fall,1} * \Delta DDhigh\_fall + \beta_4^{fall,2} * (\Delta DDhigh\_fall)^2 \\ &= \Delta LR + \beta_4^{fall,2} * (\Delta DDhigh\_fall)^2\end{aligned} \tag{10}$$

Where ΔSR is the short-run percentage changes in yield that are attributable to changes in *DDhigh_fall* and is the sum of long-run impacts and the climate penalty term. It should be noted that equation (10) uses a simplified version of climate penalty terms which are represented by direct changes in climate, i.e., $\beta_4^{fall,2} * (\Delta DDhigh\_fall)^2$. This is slightly different from the estimation model in equation (8), where the climate penalty measures the distance between weather realization and local climate. The rest of the notation is as defined in association with

equation (8). In this section, we focus on differences between short and long-run impacts thus do projections with all degree-day variables (i.e., we do not exclude freezing variables).

The results are shown in Figure 13 below. In the figure, "short-run" and "long-run" refer to the yield projections with short-run and long-run impacts, respectively. The long-run adaptation effects are essentially the difference between long-run projections and short-run projections. "baseline panel" refers to the yield consequences using the estimation of the baseline panel model.

We can see in the figure that the adaptation effects are substantial and even reverse the sign of climate change impacts. Under 1-5 ºC uniform warming scenarios, projections with long-run impacts indicate small yield gains ranging from 0.4%-3%, whereas those with short-run impacts result in yield reductions from 1.1% to 32.6%. Taking the year 2019 as a reference, the yield reductions translate to winter wheat production losses of 1.5 to 43.5 million tons with revenue losses up to 17.3 billion US dollars (FAOSTAT 2021).

Similar evidence is found in (Chen and Gong 2020) in which the authors use the long difference model and focus on agricultural total factor productivity (TFP) in China. They found that long-run adaptation has mitigated 37.9% of the short-run effects of extreme exposure on TFP. Differing from winter wheat in our study, Chen and Gong (2020) concluded that, regardless of adaptations, future climate change still triggers a substantial loss in China's TFP.

Another interesting finding is that the projections with baseline panel model roughly line between projections with short-run impacts and long-run impacts. The evidence becomes more obvious in scenarios with higher temperature increases. For instance, with a 3 ºC uniform warming, projections with short-run, baseline panel model, and long-run respectively indicate yield changes of -4.9%, -2.1%, and 2.2%. This finding is consistent with Mérel and Gammans (2021)'s argument that estimates from a conventional panel data model represent a weighted average of short-run and

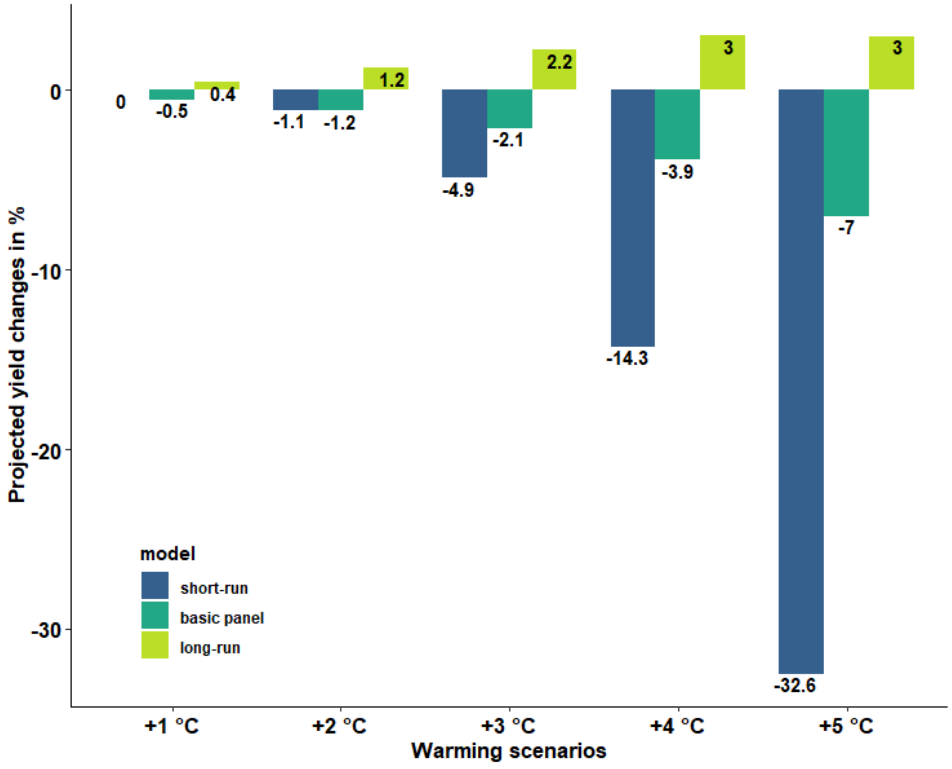

Figure 13. Yield projections with short-run impacts, basic panel estimates, and long-run impacts, respectively

long-run impacts with the weight on the long-run impacts increasing with the share of overall weather variation attributable to cross-sectional differences.[38] With that being said, applications that directly compare the estimates from the long difference model with that from a conventional model might undermine the effects of long-run adaptations. Lastly, it also should be noted that regardless of how the long-run adaptation effects are revealed (i.e., either through climate penalty terms as in this paper or the long different model as in (Burke and Emerick 2016; Chen and Gong 2020), they are always estimated from historical data and thus entail historical actions. But

[38]To be more precise, this argument holds perfectly for models with nonlinear long-run effect (i.e., a model with linear and quadratic average temperature). In our setting, we assume *linear* relationships between yield and degree-day variables. Nonetheless, based on the empirical evidence in the future yield projection part, the argument holds in our case.

adaptations in the future could be substantially different from what we have observed nowadays, especially given the rapid engagement of information technology in the agricultural sector (Oyinbo et al. 2021).

Conclusion

The agriculture sector is quite vulnerable to climate change because temperature and precipitation are key determinants of crop yields. Here we analyze climate change impacts on winter wheat, one of the most widely planted cereal crops globally. We find heat in the fall and freezing days in the early spring are the most important drivers of yield reductions. In particular, from a long-run perspective, a 10 degree-days increase in conditions over 24 ºC in the fall decreases yields by 7.0%, and a 10 degree-days increase in freezing temperatures in the spring decreases them by 8.8%. Most importantly, our yield projections with various climate change scenarios highlight the importance of accounting for reductions in freezing days at least in our winter wheat case. When such effects are omitted, the projected climate change impacts on winter wheat are significantly larger and portend yield reductions, i.e., 4.1%-26.3% reduction as opposed to 0.4%-3.0% yield gains under projections from models with such terms. Finally, we also find the inclusion of terms that reflect adaptation effects yields substantial changes in projected yields that in cases even reverse the sign of the climate change impacts.

CHAPTER IV

ENVIRONMENTAL ASSESSMENT OF THE PROPOSED MIBR PLATFORM AND MARKET IMPLICATIONS FOR CARBON FIBER

Climate change poses real risks to agricultural production, and many are considering ways that agriculture may participate in reducing the magnitude of future climate change. One such means is enhanced production of bioenergy (biofuel). The IPCC special report on 1.5 ℃ warming indicates that in 2050, biofuel will still be as important as a means of transportation displacing carbon-emitting fossil fuels (IPCC 2018).

First generation biofuels, derived mainly from food crops, have been extensively developed. However, due to their lower greenhouse gas emission efficiency (McCarl 2008) along with competition with food supply and indirect land use change effects (Koizumi 2015), the focus is now shifting toward second generation biofuels (Falano, Jeswani, and Azapagic 2014). These fuels are produced from lignocellulosic biomass in the form of crop wastes/residues, forest products/residues municipal wastes, and energy crops (Nanda et al. 2015). Falano, Jeswani, and Azapagic (2014) concluded that compared to fossil fuel and first-generation ethanol, ethanol from lignocellulosic biomass is more sustainable.[39]

Nevertheless, lignocellulosic biorefineries still face challenges in terms of profitability (i.e. high production cost) and sustainability (i.e. energy-intensive processes) (ElMekawy et al. 2013; Philippini et al. 2020; Fernando et al. 2006). More importantly, today almost all biological

[39]The overall environmental benefits of bioenergy should always be considered carefully, especially in the regard of climate change mitigation. Unexpected negative side effects may occur along with the biofuel production. For instance, a recent study conclude that bioenergy with carbon capture and storage (BECCS), an important negative emissions technology, may double the global area and population living under severe water stress and even exceed the impact of climate change, mainly due to the additional irrigation requirement for biomass plantations (Stenzel et al. 2021).

processing platforms for lignocellulosic conversion result in significant lignin-containing waste streams with about 30-40% used to supply biorefinery thermal requirements (Souto, Calado, and Pereira 2018). The remaining 60-70% of the lignin stream is generally either a) utilized for power generation which is low in value and inefficient in carbon conversion or b) conveyed to disposal (Li et al. 2019; Li et al. 2019; Liu et al. 2019). Thus, the production of value-added byproducts, such as carbon fiber, biopigments, biopolymers, etc., from the lignin-containing wastes has been attracting increased attention.

Improved lignin use in a Multi-Stream Integrated Biorefinery (MIBR) is proposed to address the challenges of lignin use, profitability, and greenhouse gas efficiency. The MIBR platform would utilize the lignin-containing biorefinery waste as feedstock for high-value bioproducts (carbon fiber, asphalt binder modifiers, lipid for biodiesel, bioplastics, etc.), which offers a significant opportunity to enhance operational efficiency, reduce cost, minimize carbon emission, and maximize the sustainability of lignocellulosic biofuels (Xie et al. 2019; Li et al. 2019; Li et al. 2019; Li et al. 2020; Zhao et al. 2020; Arreola-Vargas et al. 2021; Li et al. 2021; Liu et al. 2021). Previous studies suggest that lignin-based carbon fiber production coupled with a biorefinery may provide $2400 to $3600 added value per dry ton of biomass for vehicle application (Langholtz et al. 2014). Furthermore, compared to producing ethanol alone, the addition of lignin-derived carbon fiber per year in the US could reduce fossil fuel consumption by 2-5 billion liters and reduce CO2 emissions by about 6.7 million tons (Langholtz et al. 2014).

Despite the potential benefits argued in the literature, the real environmental performance of the proposed MIBR platform is yet to be fully estimated. Thus, one goal of this chapter is to evaluate the environmental impacts of MIBR considering the addition of valuable byproducts and compare that with the traditional biorefineries where cellulosic ethanol is the only product.

Concerns also arise from the market reactions to the introduction of lignin waste-based byproducts. Normally the ethanol market is much larger than the byproduct market. For instance, while bioethanol goes to the large liquid fuel market (355 billion US dollars in 2019 - EIA 2020), the global market for carbon fiber, one of the byproducts, was estimated at roughly 3 billion US dollars (Witten et al. 2018). In this spirit, it is worth asking how the prices of byproducts like carbon fiber would change after a sudden increase in supply in association with biorefinery production. It is possible that the additional supply of lignin-based byproducts will overwhelm the demand, and in turn, a sharp price decline is expected, a pattern that has been documented in the bioglycerol market.[40] Moreover, if commercializing the byproducts takes years to complete, it is worthwhile investigating how large the potential of the future market would be. This is important because low-cost byproducts may create new demand from industries/regions where the products were not widely used due to previous high costs. Thus, it is desirable to perform relevant market analysis for the byproducts to gauge market reactions as well as future market development, which is the second goal of the chapter.

The chapter proceeds as follows. We first briefly introduce the proposed MIBR platform.[41] We then build life cycle assessment (LCA) models to evaluate the environmental impacts (mainly carbon dioxide-equivalent GHG emissions) of the platform and compare that with emissions from the conventional petroleum-based counterparts. Third, we perform market analysis for carbon fiber with respect to its demand, supply, cost, and price. Additionally, we examine how the market

[40]Ma and Hanna (1999) stated that glycerol, a valuable byproduct from the production of biodiesel, is the primary option to be considered to lower the cost of biodiesel. Along with the boom of biodiesel, the glycerol byproduct flooded the market. The global supply of glycerol increased sharply from 0.6 million tons in 2006 to over 2 million tons in 2011 and the following years. Ciriminna et al. (2014) reported that the price for refined glycerol decreased from about 4000€/ton in year 2000 to less than €450/ton in early 2010, when the price of crude glycerol went to €0 per ton which made the glycerol a product with no economic values.

[41]Please note that in this chapter, we use MIBR platform and MIBR system interchangeably.

prices would change in response to the introduction of lignin-based supplies based on demand elasticities. Finally, we conclude the chapter.

An introduction to the MIBR platform

In this thesis, the terminology MIBR refers to the processes arising from a research project funded by the United States Department of Energy (DOE 2018). The project addresses one of the most challenging issues in lignocellulosic biofuel: the utilization of biorefinery lignin-containing wastes in producing value-added byproducts. As noted in the introduction, traditional lignocellulosic biorefining focuses on ethanol, which has limited value-added byproduct streams. MIBR aims to add valuable byproducts by developing fractionation, conversion, and processing technologies that will be used to produce byproducts like carbon fiber, asphalt binder modifier, and lipid for biodiesel, to name a few, from lignin-containing biorefinery wastes (Liu et al. 2021; Arreola-Vargas et al. 2021; Li et al. 2021). In addition to advances in technologies and profitability, MIBR is also expected to gain emission credits from the production of lignin-based byproducts by replacing fossil fuel-based counterparts.

MIBR activity embodies three major processes, namely the pretreatment of lignocellulosic biomass, the hydrolysis of biomass to produce cellulosic ethanol, and fractionation - fermentation processes that produce byproducts from the lignin-containing wastes. Note that while biomass could be wood, energy crops, forest, and farm residuals, etc., MIBR treats corn stover as the main feedstock. Figure 14 below shows all the processes involved in the platform.

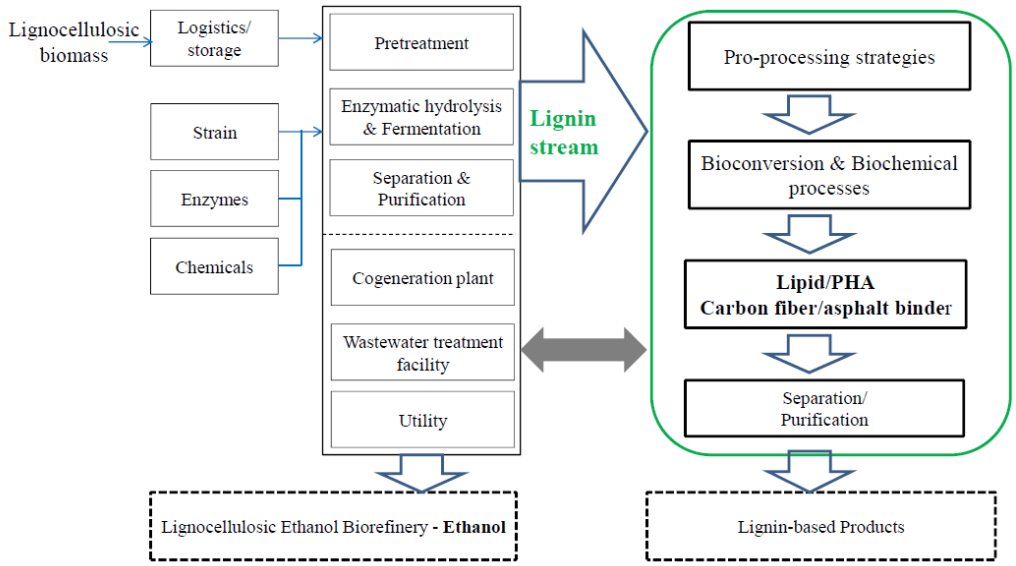

Figure 14. Main processes in the MIBR platform

Specifically, in the first step milled corn stover is slurried into a dilute acid reactor. After a targeted time and temperature, the slurry is flashed and cooled down, followed by the separation of solid and liquid streams.[42] This step corresponds to the pretreatment of biomasses.

In the second step, cellulase enzymes are added to the solid streams from step one to convert the remaining cellulose and hemicellulose to fermentable sugars, and these sugars together with the liquid streams from step one are transferred to a fermentable sugar platform to produce ethanol. This step refers to the hydrolysis of biomass and the production of cellulosic ethanol.

What follows are steps to filter out the suspended solid lignin residuals (i.e., so-called lignin-containing wastes). These solids move to step three where the solids will be reslurried and exposed to enzymes and mediator fractionation or other fractionation methods, before being separated again

[42]Currently, the most effective pretreatment strategies based on bioconversion performance developed at lab scale involves acid pretreatment at 120 degrees followed by alkaline processing.

either on a filter press or via centrifugation. The separation results in water-soluble and -insoluble lignin residuals. The water-soluble lignin streams are used to feed aerobic fermentation to produce either lipid for biodiesel (Xie et al. 2019) or PHAs (Polyhydroxyalkanoates, a form of bioplastic) (Liu et al. 2019; Liu et al. 2021). The broth (i.e., the residuals from the fermentation process) will then be processed to remove the oil and cell mass to purify the remaining water-soluble lignin which will be collected to produce asphalt binder modifiers (Xie et al. 2017). Finally, the water-insoluble high molecular weight lignin will be washed and collected to produce carbon fiber (Li et al. 2021; 2019).

In summary, the MIBR platform will lead to a main product of cellulosic ethanol and multiple possible byproducts, namely, lignin-based carbon fiber, lipid for biodiesel, asphalt binder modifier, or PHAs. At the end of the project, which product stream to scale up will depend on the overall environmental and economic performance of the platform. Finally, it should be noted that while we built LCA models that cover all byproduct scenarios, we focus on lignin-based carbon fiber and PHAs partially due to limited data availability for the rest of the byproducts.

LCA analysis on the MIBR platform

The life cycle assessment (LCA) method has been extensively used to evaluate the environmental impacts of the production of a specific product (Gerbinet, Belboom, and Léonard 2014; Levasseur et al. 2010; Cherubini, Strømman, and Ulgiati 2011). Such analysis has been standardized and coded in the International Organization for Standardization (ISO) with ISO 14040:2006 and ISO 14044:2006. A standard LCA includes the definition of the goal and scope of the LCA, a life cycle

inventory data phase (LCI), a life cycle impact assessment (LCIA) phase, and an interpretation of the results (ISO 2016).[43]

LCA applications on lignin-based byproducts (i.e., carbon fiber) are limited in the literature, mainly because the byproduct production practices are by no means mature (Hermansson 2020). For instance, according to Hermansson, Janssen and Svanström (2019), only one comprehensive analysis was found for lignin-based biorefinery byproducts of carbon fiber in Das (2011).

In this chapter, based on the data collected from the MIBR platform, we built LCA models to measure environmental impacts. We developed two scenarios regarding the main MIBR product one based on cellulosic ethanol and the other based on carbon fiber. The identification of the main product plays an important role in LCA analysis because the main product bears most of the emissions, especially when adopting the displacement method for emission allocation, which we will discuss in detail below. Naturally, for a process producing cellulosic ethanol from corn stover, ethanol is the main product, and that is the first scenario in our LCA analysis. In the second scenario, we treat lignin-based carbon fiber as the main product given carbon fiber's high economic values and potentially large environmental advantages over the PAN-based fibers (Witten et al. 2018; Das 2011; Janssen et al. 2019).

System boundary and the functional unit

We perform a "cradle to gate" LCA analysis; that is the system boundary starts from the collection of corn stover, the transportation of corn stover from the field to the biorefinery plant, the production of chemical inputs used in the process, as well as the required energy input, as shown

[43]Note that according to ISO, the rest of the phases include reporting and critical review of the LCA, limitations of the LCA, the relationship between the LCA phases, and conditions for use of value choices and optional elements. See https://www.iso.org/standard/37456.html.

in Figure 14. In other words, the LCA results take account of emissions emitted from all important processes that are involved during the production of the main product as well as the byproducts. We do not cover the environmental impacts during the end-use stage of the main or byproducts, nor any recycling of the products. For the analysis where ethanol is the main product, the functional unit is defined as 1 gallon of produced ethanol. When carbon fiber is the main product, we use 1 kg of carbon fiber.

Process and input data

Process and input data came from a number of sources. Much of the needed data were adopted from the GREET[44] (Greenhouse gases, Regulated Emissions, and Energy use in Transportation) database developed by the Argonne National Laboratory (we used the latest version released in October 2021, i.e., GREET2021). The GREET database was developed particularly for life cycle analysis in the United States and has been widely used in the literature (Wong et al. 2021; Woertz et al. 2014; Anderson et al. 2018; Pegallapati and Frank 2016; Burnham et al. 2012). Two standard DOE developed biorefinery processes exist in GREET, namely, corn stover at the conversion plant and corn stover to ethanol.[45] The first process models the collection of corn stover from the field, the transportation of corn stover to the biorefinery plants,[46] and the necessary pretreatment of corn stover. The second process is the key process that covers the production of ethanol from corn stover. The MIBR LCA model was built by integrating the process producing byproducts with those two processes that already exist in GREET. The input and output lists are shown in Table 6 below.

[44]The software can be downloaded from https://greet.es.anl.gov/index.php?content=greetdotnet.

[45]This process is called "DOE-Ethanol from Corn Stover" in GREET. See Canter et al. (2016) and Wang et al. (2012) for a detailed description of the process.

[46]GREET assumes the transportation distance is roughly 53 miles indicating that the field is close to the biorefinery plants.

Table 6. The input and output information

Feedstock	
Corn stover (kg)	11.3
Chemical input	
Cellulase (g)	466.9
Sulfuric acid (g)	1133.9
Ammonia (g)	47.2
Corn steep liquor (g)	136.2
Diammonium phosphate (g)	14.7
Sodium hydroxide (g)	200.1
Calcium oxide (g)	64.8
Sodium citrate (g)	4.0
Citric acid (g)	3.7
Sodium phosphate (g)	1400.8
Hydrochloric acid (g)	205.1
Electricity (kWh)	11.2
Glucose (g)	246.8
Specific input for producing carbon fiber	
Polyacrylonitrile (PAN) (g)	1000
Lignin powder from MIBR (g)	1000
Nature gas (MJ)	6.7
Electricity (kWh)	20.5
Output	
Ethanol (gallon)	1
PHA (g)	1000
Lignin-based carbon fiber (g)	1000

MIBR uses 11.33 kg corn stover to produce 1 gallon ethanol (this setup was aligned to the standard corn stover to ethanol process in GREET), which also results in 2.2 kg of lignin-containing biorefinery wastes (i.e., 20% of biomass ends up to wastes). The platform reaches a 50% solubilization rate; meaning that 2.2 kg of biorefinery wastes will be fractionated to 1.1 kg of a *water-soluble* lignin stream and a 1.1 kg *water-insoluble* lignin stream. The soluble lignin stream will enter the fermentation process to produce PHAs. The remaining 1.1 kg of water-insoluble lignin will be used to produce *lignin powder* which will be blended with PAN at a ratio of 1:1 to produce carbon fiber. Throughout the process, there are several important assumptions worth highlighting.

First, experience shows the quantities of needed chemical inputs stated in MIBR are generally overestimated given they were derived from lab-scale experiments. For instance, 11.33 kg corn stover is said to require roughly 1.1 kg sulfuric acid in MIBR (Liu et al. 2019), whereas, in GREET's corn stover to ethanol process, the quantity is only 0.3 kg. Since MIBR is essentially an extension to the conventional corn stover to ethanol process, such a high level of sulfuric acid consumption seems unrealistic. Nevertheless, the analysis forms an upper bound for the LCA results, which could be helpful for decision-making. On the other hand, the project is still ongoing, and the inputs will be further optimized in the future.

Second, we aligned the electricity usage in MIBR to that in Das (2011). In that paper, energy requirements for cooling water and lignin drying are 3.38 kWh per kg of lignin. In our application, 11.33 kg of corn stover leads to roughly 2.2 kg of lignin-containing biorefinery wastes. Thus, the electricity consumption is at least 7.4 kWh. We further took into account the electricity usage (3.8 kWh) during PHA fermentation which was estimated based on the equipment power consumption and the time for conditioning. This yields a total electricity consumption figure of 11.2 kWh for processing the 11.33 kg corn stover.

Third, we assumed the blending rate for lignin powder with PAN to occur at a ratio of 1:1 to produce carbon fiber and assumed the carbon fiber yield was 50% of the PAN and lignin powder weight. That means 1 kg of lignin powder and 1 kg of PAN were needed to produce 1 kg of carbon fiber. The blending with PAN is to improve mechanical properties as 100% lignin-based fibers have been found to produce less than desirable mechanical properties (Souto, Calado, and Pereira 2018). The electricity usage during the carbon fiber production process is reported in Table 6 (i.e., 20.5 kWh for 1 kg of carbon fiber). This is comparable with that amount given in the

Environmental Footprint database (i.e., 23 kWh) - a standard LCA inventory database widely used in Europe.[47]

Lastly, in terms to deal with multiple gases, we used the 100-year Global Warming Potential measured as heat-trapping capacity over 100 years (GWP100) relative to that of CO2 (US EPA 2016). GWP100 will be used to transform overall emissions into kg of CO2 equivalent emissions.[48]

Allocation method for byproducts

One of the critical issues in LCA analysis is to determine the allocation method used to allocate environmental impacts (i.e., emissions) among the main product and any byproducts. There are several methods widely used in the literature, mass/energy-based method (also called physical partitioning), economic value-based method (economic partitioning), and displacement method (system expansion) (Wardenaar et al. 2012; Luo et al. 2009; Svanes, Vold, and Hanssen 2011; Huang, Spray, and Parry 2013; Hermansson, Janssen, and Svanström 2020).

The mass/energy-based method allocates environmental impacts according to the mass/energy content of the main product and byproduct. The economic value-based method allocates the impacts based on the gross sale values (i.e., the produced quantity times the sale price). The displacement method, on the other hand, is particularly suitable when the byproducts are expected to displace conventional inputs (usually carbon intensive).

In the MIBR case, we expect the MIBR lignin-based carbon fiber to displace PAN-based carbon fiber at a lower emission rate. In using the displacement method, we need a displacement ratio. For instance, a ratio of 1:1 assumes 1 kg of lignin-based carbon fiber replaces (displaces) the

[47]The database can be freely downloaded from https://nexus.openlca.org/database/Environmental%20Footprints. The carbon fiber production process is called "Carbon fibre production, production mix, at plant, technology mix, 100% active substance".

[48]Individual GHG emissions are aggregated to kg of CO2 equivalent emissions (CO2e) using the 2007 Intergovernmental Panel on Climate Change (IPCC) 100-year global warming potentials (CO2 = 1, CH4 = 25 and N2O = 298) (IPCC 2007).

use of 1 kg of PAN-based product. The replaced emissions will be deducted from the net MIBR platform emissions and those allocated to the main product (i.e., ethanol). Similarly, if carbon fiber is considered the main product, we assume the byproduct ethanol displaces petroleum-based fuels (i.e., gasoline).

One of the advantages of the displacement method is it does not involve actual allocations as in the mass and economic value-based method because in some cases these two methods are not reliable. However, it should be noted that there is no consensus of which methods should be used (Wardenaar et al. 2012) and high sensitivity of environmental impacts to allocation methods have been reported in the literature (Kim and Dale 2002; Malça and Freire 2006; Beer and Grant 2007).[49]

For the MIBR platform, we primarily use the displacement method. We do this because we deem it is more relevant to the project as we expect to obtain emission credits from the production of lignin-based byproducts. Table 7 above shows the displacement ratios.

[49]Nevertheless, International Organization for Standardization (ISO) introduces a hierarchical approach for dealing with byproducts. The ISO 14044 allocation procedure (clause 4.3.4.2) recommends the displacement method as a first step to skip from actual allocation as in the mass and economic value-based methods. In case allocation cannot be avoided ISO prescribes mass/energy-based method as a second step (Wardenaar et al. 2012). As a third step, when physical partitioning cannot be established, ISO suggests allocation in a way that reflects another (i.e., economic) relationship between the different products (Wardenaar et al. 2012).

Table 7. The displacement ratios between lignin-based products and their counterparts

Byproducts from the MIBR platform	Alternatives to be displaced
1 kg of lignin-based carbon fiber	1 kg of PAN-based carbon fiber
1 kg of PHAs	1 kg high-density polyethylene (HDPE)
1 gallon of ethanol from corn stover	1 gallon of gasoline

Note: The processes for producing PAN-based carbon fiber, HDPE, and gasoline are "Carbon Fiber Production", "Final HDPE Product: Combined", and "Gasoline Blendstock from Crude Oil for Use in US Refineries", respectively, in GREET2021.

LCA analysis results

In this section, we first report the LCA results for the MIBR system where ethanol is the main product. Following that, we focus on lignin-based carbon fiber and compare its environmental impacts with that of PAN-based products.

Environmental impacts of the MIBR with ethanol being the main product

Figure 15 below shows the environmental impacts in terms of CO2 equivalent emissions associated with producing one gallon of ethanol from corn stover. We compare the emissions across multiple biorefinery processes, as shown in the horizontal axis. "DOE standard" refers to the standard process in GREET that transforms corn stover to ethanol. It should be noted that 1.79 kWh of electricity is generated during the process.[50] Such electricity is treated as a byproduct and is handled with the displacement method (i.e., displacing electricity mix on the grid in the United States). "DOE standard w/o electricity" is identical to the "DOE standard" process except that no electricity is generated. "MIBR with LP and PHAs" refers to the process in which *lignin powder* and PHAs are produced as byproducts. That means we did not include the production of carbon fiber and the derived lignin powder from the MIBR platform is expected to displace PAN.

[50]This was adjusted from 2.41 kWh in GREET2020. See more updates on GREET in (Wang et al. 2021).

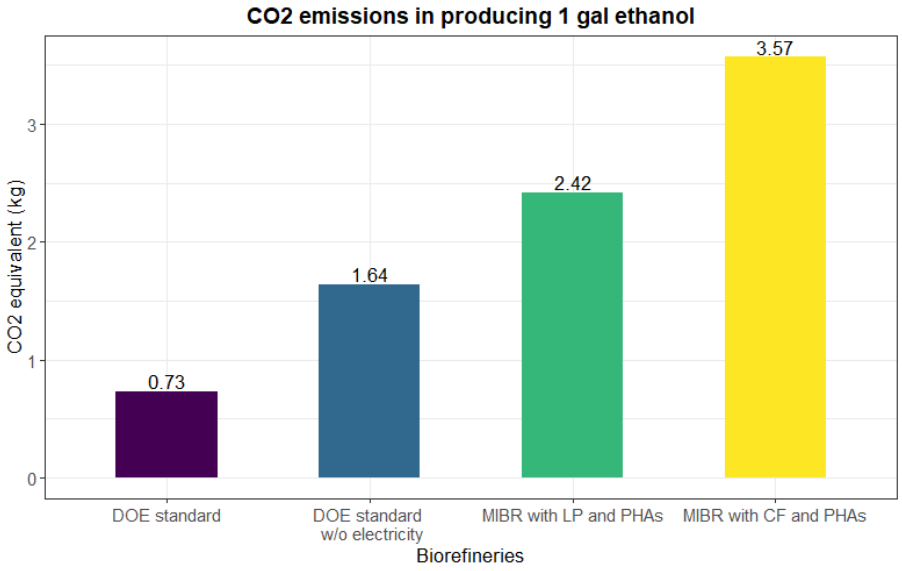

Figure 15. CO2 emissions per gallon of produced ethanol

In contrast, "MIBR with CF and PHAs" takes account of the production of carbon fiber from lignin powder and is expected to directly displace PAN-based fibers.

Several important findings emerge. First, taking the "DOE standard w/o electricity" as a reference, we observed greater emissions in both MIBR processes. In the case of lignin powder and PHAs, 1 gallon ethanol is associated with 2.42 kg CO2 equivalent emissions, an increase of 47.6% from that in the reference process. When we further integrated the production of carbon fiber into the MIBR platform, 1 gallon ethanol creates 3.57 kg CO2 emissions, an increase of 117% from the reference process. The emission increases are mainly due to the chemical inputs used in the MIBR processes. However, as we have mentioned in previous sections, we feel the inputs are overestimated to a certain extent. Consequently, the emissions reported in Figure 1 should be treated as an upper bound.

Second, we observed large emission differences between "MIBR with LP and PHAs" and "MIBR with CF and PHAs". Specifically, emissions from the latter are significantly higher than

those of the former. This implies that energy input-related emissions in the carbon fiber production process outweigh the displaced PAN-related emissions. This finding is consistent with the literature as carbon fiber production is highly energy-intensive.

Third, we noticed that the emissions from "DOE standard" are significantly lower than that from "DOE standard w/o electricity". We also found the DOE standard was somewhat of an outlier with lower emissions estimates compared with other estimates, as shown in

Table 8. For instance, based on biorefineries in Southwestern Michigan, Cronin et al. (2017) estimated emissions were at the level of 4.41 kg CO2 when producing one gallon of ethanol from corn stover, compared with an estimate of 0.73 kg that is reported in GREET2021. In Cronin et al. (2017), co-generated electricity reduced emissions reducing by about 50% meaning without that the emission level will be about 6.6 kg. In contrast, "DOE standard w/o electricity" reported an emission level of 1.64 kg which again is much lower.

Large variations in emission levels are not uncommon in LCA analysis. The variations could be largely attributable to different assumptions across applications. For instance, Obnamia et al. (2019) compared emissions estimates for US Midwest-based corn stover based ethanol production across three life cycle databases, GHGenius 4.03a (a database developed for Canada), GREET 2013, and GREET 2015. When default settings are adopted, they found emission levels from the three sources were 2.75 kg, 0.82 kg, and 0.17 kg per gallon ethanol, a range of over 16 times the lowest estimate. The authors found that while there were multiple differing assumptions (i.e., nitrogen fertilizer, on/off-site enzyme production, and material/energy inputs included/excluded) that contribute to the differences in the emissions estimates with the major factor being the assumptions on electricity offsets.

Table 8. A comparison of emissions reported in GREET2021 and the literature

Sources	Allocation method	Kg CO2 equivalent per gallon ethanol
DOE standard in GREET	Electricity displacement	0.73
DOE standard w/o electricity in GREET	No electricity	1.64
(Kaufman et al. 2010)	Electricity displacement	1.20
(Muñoz et al. 2014)	Electricity displacement	1.78
(Zhao, Ou, and Chang 2016)	Electricity displacement	3.43
(Cronin et al. 2017)	Electricity Displacement	4.41
USLCI database developed by NREL	No electricity	12.45

Note: USLCI is a United States-based LCA inventory database developed by the National Renewable Energy Laboratory (NREL). It can be downloaded from https://www.lcacommons.gov/.

Lastly, it should be noted that our LCA analysis is based on the assumption that all lignin-containing wastes are used to produce lignin-based byproducts. However, in practice, roughly 30%-40% of the wastes[51] will be burned to meet thermal requirements (such as generating electricity), which may reduce electricity usage from the grid and consequently lower emissions during the production of byproducts.

Environmental impacts when carbon fiber is treated as the main product

In the above section, we treated ethanol as the main product. However, lignin-based carbon fiber could be more valuable and become the main product. For the process where carbon fiber is the main product, we considered it replacing PAN in carbon fiber production and for the byproduct, we assumed gasoline was replaced by the produced cellulosic ethanol. It also should be noted that we assumed the carbon fiber production process for lignin is similar to that used for PAN (Das 2011), especially in the more energy-intensive stages (i.e. oxidation, carbonization, and graphitization in Figure 16).

The LCA results as well as the comparison with findings in the literature are shown in Table 9. We estimate that 1 kg of lignin-based carbon fiber is associated with 19.5 kg of CO2 emissions.

[51]This percentage was obtained from personal communications with Dr. Joshua Yuan (the PI of the MIBR project).

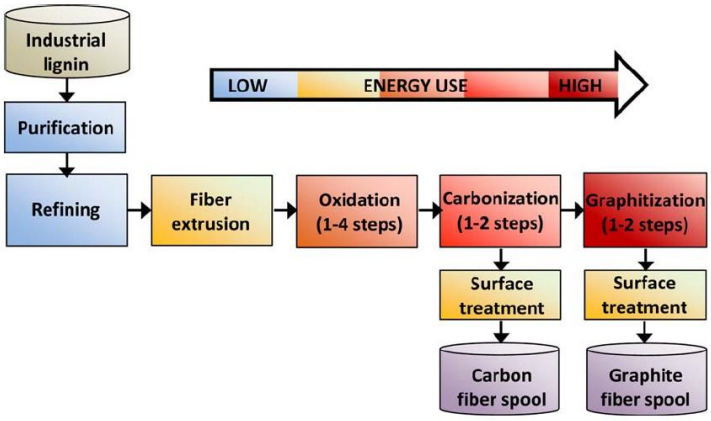

Figure 16. A general process for producing carbon fiber from lignin

Note: This figure was adopted from (Baker and Rials 2013).

We also find 1 kg of PAN-based carbon fiber in GREET2021 is associated with 19.1 kg CO2 emissions which are even lower than that of the lignin-based products. The same PAN-based process in GREET2020 was, however, associated with 38 kg of emissions. The notable emission reduction in the PAN-based process is due to updates in inventory data in GREET, particularly for the production of ammonia and propylene, which are necessary precursors for PAN (Iyer and Kelly 2021). In other words, GREET2021 adopted much "greener" processes than those assumed in GREET2020.

Since the LCA analysis is based on the latest version of GREET2021, naturally, we used processes in that version as references for comparison. Although we did not observe significant environmental advantages of lignin-based carbon fiber over PAN-based counterparts using data from GREET2021, our lignin-based results still outperformed other estimates we found in the literature, which report emissions ranging from 31 kg CO2 to 38 kg CO2 per kg of PAN-based carbon fiber (Das 2011; Keoleian et al. 2012; Janssen et al. 2019), indicating the lignin-based products reduced emissions by 35.4% - 64.2%. Our results are also comparable with findings in Das (2011)'s comprehensive LCA study on lignin-based carbon fiber. Besides, as we have

Table 9. Emissions (in kg CO2) per kg of carbon fiber produced

Scenarios	(Das 2011)	GREET	OpenLCA	(Janssen et al. 2019)	MIBR (50% lignin + 50% PAN)
PAN-based carbon fiber	31.0	19.1	31.0		
Lignin-based carbon fiber	24.2			1.5	19.5

Note: The OpenLCA database can be downloaded from the website: https://nexus.openlca.org/database/Environmental%20Footprints. The emission of 19.1 kg in GREET is based on GREET2021. In GREET2020 the emission was 38 kg. 31 kg of emissions in OpenLCA is based on the process of "Carbon fibre production, production mix, at plant, technology mix, 100% active substance" in the PEF database.

repeatedly argued, the inputs in MIBR could be optimized to a certain extent under industrial scale production levels which may further reduce the associated emissions.

It is also worth noting that environmental benefits from low-cost lignin-based carbon fiber could be larger because being cheaper can increase application replacing heavier materials and reducing fossil fuel use in a wide variety of industries, including but not limited to aerospace, automotive, wind energy, and the leisure department. In this regard, the potential environmental benefits are significant. Taking Boeing B767 as an example, replacing 50% of structural elements with carbon fiber-reinforced polymer lightens the plane weight by 20% and can achieve life-cycle CO2 emission reductions of 1400 tons (Onishi 2012).

Market analysis for carbon fiber

This section addresses the second objective of the chapter, which is to conduct market analysis for carbon fiber. Such analysis sheds light on market potential in the future.

Carbon fiber has a number of desirable mechanical properties such as high strength to weight ratios, resistance to corrosion, good tensile strength, fire resistance, etc., which are attractive to a variety of industrial sectors including aerospace, automotive, wind energy, and sports and leisure department (van Grootel et al. 2020; Das et al. 2016). Nonetheless, carbon fiber has not been

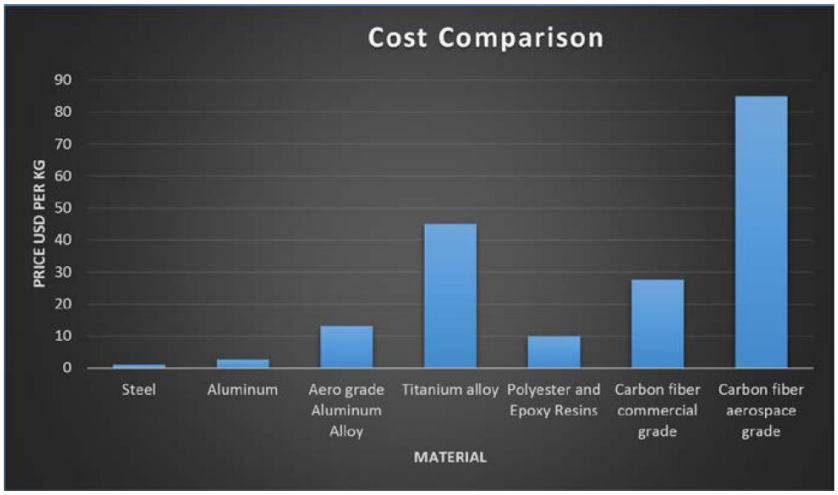

Figure 17. Cost comparisons across different composite materials (2012)

Note: The figure was adopted from (Shama et al. 2018).

widely used in practice, mainly because of its high cost (Shama et al. 2018; Holmes 2017). Figure 17 displays a price comparison across different materials. There we see that carbon fiber price is significantly higher than that for traditional materials it might replace like steel and aluminum which still dominate the current market. For instance, the prices for aerospace-grade carbon fiber remain high ranging from $80 to $120/kg (van Grootel et al. 2020; Witten, Kraus, and Kühnel 2015).

Regardless of its high cost, carbon fiber as a traditional material replacement has a promising future, partially due to the increasingly stringent environmental regulations. More importantly, carbon fiber prices have been steadily decreasing, mainly because of technical innovation. For instance, the average price of carbon fiber was estimated at $38/kg in 2018, a 7.3% reduction from that in 2012 (Industry Expert 2013). The price of carbon fibers used in wind energy and automotive industry which do not require as high-performance characteristics as carbon fiber used in the aerospace sector is substantially lower ranging between $20 and 30/kg (Lucintel 2012; Kozarsky et al. 2011). Further decreases in carbon fiber prices are likely to expand its usages replacing other

traditional and heavier materials in turn reducing costs of moving goods that incorporate those materials and consequent emissions.

Demand projections for carbon fiber

The carbon fiber market has been steadily expanding for more than ten years, as shown in Figure 18. Global demand for carbon fiber was estimated to reach 98 thousand tons and 120.5 thousand tons in 2020 and 2022, with market values estimated at 3.5 billion and 4.4 billion dollars, respectively (Witten et al. 2018). While demand projections vary substantially across studies, they all assume high compound annual growth rates (CAGR) ranging from 10% to 15% (Kozarsky et al. 2011; Red and Zimm 2012; Souto, Calado, and Pereira 2018; Witten et al. 2018). It should be noted that over 95% of carbon fiber is processed into carbon composites, mainly carbon fiber reinforced polymer (CFRP), which has an even larger market size and its demand was estimated to reach 127.8 thousand tons in 2018, accounting for 83% of the overall carbon composite market (Witten et al. 2018).

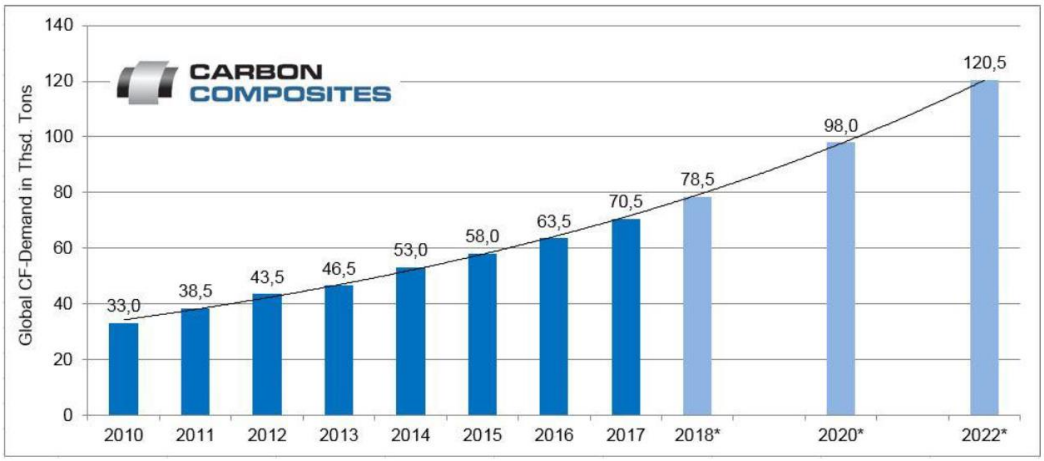

Figure 18. The projections of global carbon fiber demand

Note: The figure was adopted from (Witten et al. 2018).

In terms of the regional distribution of demand, North America led the market and accounted for 33% of global demand in 2018, followed by Europe (27%) and Asia (24%, excluding Japan which accounted for 11% of the global demand). In the future, demand increases from emerging economies such as China and India are expected to outpace that in North America and Europe and finally take the lead.

In terms of the demand by application sectors, currently aviation and aerospace (including defense) are still the largest segments, accounting for 36% of global consumption, as reported in Figure 19.[52] The automotive (24%) and wind energy (13%) sectors have been argued to have the largest demand potentials and are expected to lead the growth of carbon fiber demand in the future (Kozarsky et al. 2011; Langholtz et al. 2014). For instance, DOE's FreedomCAR program fosters

[52]Again, estimates vary across studies. For instance, Shama et al. (2018) stated that the aerospace and defense sector consumed 16% of global carbon fiber production, and the number was 13% for sports sector, 9% for marine sector, 7% for transportation sector, and 55% for other industry (i.e., wind energy). Nonetheless, the agreement has been reached that the transportation sector and wind sector contain the largest growth potential, with CAGR of 14.2% and 14.5%, respectively (Roy 2018).

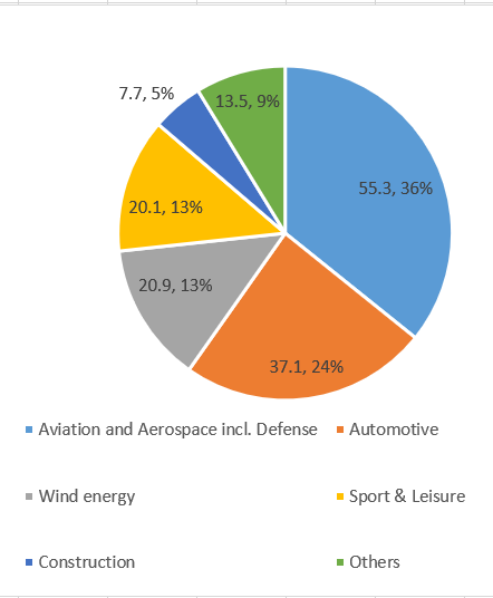

Figure 19. Carbon fiber consumption by sectors

Note: Data were obtained from (Witten et al. 2018). In the pie chart, the first number indicates consumption in thousand tons, whereas the second number reports the percentage.

the development of low-cost automotive-grade carbon fiber as its highest materials research priority (Sullivan 2006).

The supply capacity of carbon fiber

The information on carbon fiber supply is very limited. According to Witten et al. (2018), the estimated production capacity has reached 149.3 thousand tons as of 2018, a size that is 90.2% larger than the estimated demand (78.5 thousand tons). The Toray group owned the largest share of the total capacity (31.8%) in the world, as can be seen from Figure 20. It is worth noting that the estimates of capacity assume production plants that perfectly run year round and do not account for any downtime, such as holidays, maintenance, etc. (i.e., "theoretical capacity"). We argue that the current capacity can meet the demand, but a significant oversupply is unlikely to occur. More importantly, ongoing investment in facilities and higher real values of the utilization rates endorse a still promising carbon fiber market.

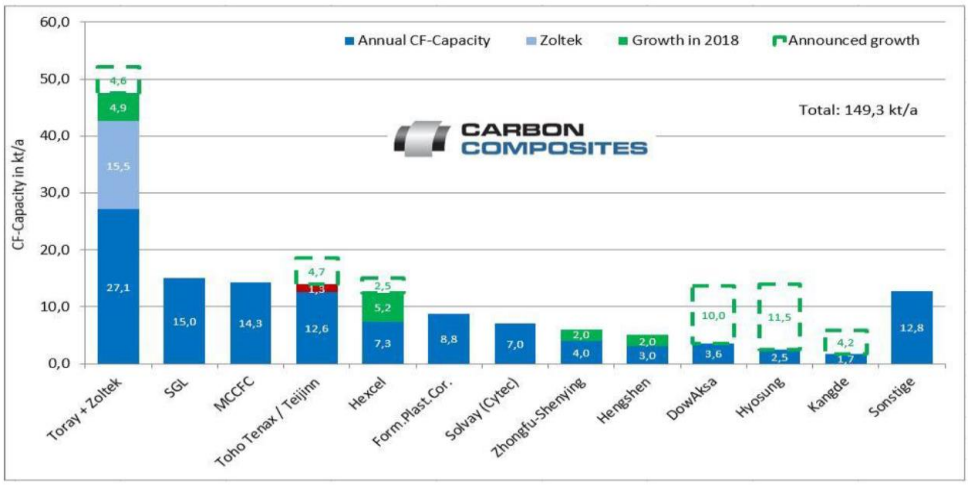

Figure 20. The theoretical supply capacity of carbon fiber in 2018

Note: The figure was adopted from (Witten et al. 2018).

The costs and prices of carbon fiber

The prices of carbon fiber have been decreasing during recent years, though slowly. The estimated average price in 2012 was $40.99/kg, with the highest prices in small-tow[53] products mainly applied in the aerospace industry ($75/kg-$100/kg) (Industry Expert 2013), whereas large-tow products applied in wind energy and automotive industry exhibited moderate and low prices ($20/kg-$30/kg) (Lucintel 2012; Kozarsky et al. 2011). Recent market analysis revealed an average carbon fiber price ranging from $14/kg to $18/kg[54] in 2020.

It should be noted that those are estimated prices and may not be representative of the real prices which are more volatile due to the precursor's connection to the global crude oil market (Das et al. 2016). Currently, over 90% of the world's total carbon fiber is produced from PAN,

[53]Tow refers to grouped fiber filaments. Typically, the diameter of carbon fiber filaments is between 5 µm and 8 µm and they are grouped into tows containing 5000-50000 filaments, known as 5K – 50K (Taylor 2000). 24K and 50K are the most common products in the market. Small tow products are superior to large tows in terms of mechanical properties.

[54]See from https://www.jinjiuyi.net/news/whats-the-price-of-carbon-fiber-sheet.html and https://smicomposites.com/carbon-fiber-cost-factors-that-influence-the-most/.

which is derived from oil refineries (Yusof and Ismail 2012; Newcomb 2016). Carbon fiber is sold in the form of sheets, plates, or tubes, and the prices highly depend on the size of the product (height, width, and thickness) and the grade of carbon fiber (either small-tow, such as 24K or large-tow like 50K).

Analyses show that carbon fiber prices are most sensitive to utility and precursor costs, as displayed in Figure 21 below. In fact, the production of carbon fiber (at least PAN-based carbon fiber) is much more energy-intensive than conventional materials such as steel and aluminum. For example, the production of automotive used carbon fiber is estimated to be 4.6 times more energy-intensive than conventional steel (Suzuki and Takahashi 2005; Naskar and Warren 2012).[55] The precursor cost (i.e., PAN) represents the largest share of the total production cost, approximately 50% to 55% (Ellringmann et al. 2015; Das and Warren 2012; Nunna et al. 2019).

The price of PAN starts from $2.2/kg, and the derived carbon fiber cost is above $12.25/kg, generally being over $20/kg (Das 2011; Naskar and Warren 2012; Ellringmann et al. 2015). This is where lignin-based carbon fibers gain advantages over their PAN-based counterpart. Taking the MIBR as an example, the lignin from biorefinery wastes has a cost that is significantly lower than PAN (Li et al. 2019). DOE has estimated that the cost for a suitable lignin precursor, including the required processing and an adjustment for a carbon fiber yield of 55%, would end up at $1.52/kg, resulting in a carbon fiber cost of $6.27/kg (Gill et al. 2017). On the other hand, it has been argued that a reduction of 50% in the production cost (roughly down to $10-15/kg) would significantly increase the opportunities of carbon fiber usage in a wider range of applications (Ellringmann et al. 2016; Baker and Rials 2013). The FreedomCAR estimated that if carbon fiber technologies are

[55]The most energy-intensive processes are oxidation and carbonization, which account for 15% and 23% of the total production cost, respectively (Mainka et al. 2015).

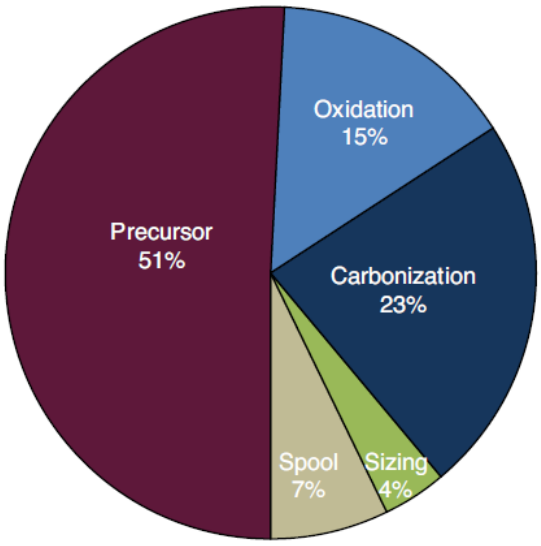

Figure 21. The distribution of carbon fiber production cost

Note: The figure was adopted from (Mainka et al. 2015).

fully developed and implemented in high volume, it could reduce the bulk cost of automotive-grade carbon fiber to between $3 and $5 per pound (that is $6.6 to $11 per kg) (Sullivan 2006) or less than half the current cost.

Market responses to lignin-based carbon fiber

We know from the pure cost/price analysis that carbon fiber sales prospects are promising. However, one important question remains is that how the market will react to industrial-sized volumes of lignin-based carbon fibers from the MIBR platform. This is by no means easy to evaluate given the fact that the carbon fiber market is far from mature and still actively growing plus quality is a factor. Additionally, detailed data on the market are not publicly accessible (mostly commercial). Nevertheless, in this section, we attempt to address the question based on estimated market conditions and associated demand elasticities.

Data limitations prevent us from rigorously estimating the demand elasticity of carbon fiber. Alternatively, we turn to the so-called "arc elasticity", which requires less data (Allen and Lerner 1934; Nichol 1931). Specifically, arc elasticity is calculated as follows.

$$\varepsilon = \frac{\frac{q_2 - q_1}{(q_1 + q_2)/2}}{\frac{p_2 - p_1}{(p_1 + p_2)/2}} \tag{11}$$

Where q_1 and q_2 are demand quantities at two time points, and p_1 and p_2 are associated prices. Although demand and price data are available from multiple market analyses, we feel it makes more sense to estimate the elasticity using data from the same source, given market estimations vary across studies. We chose to use data from Shama et al. (2018)[56] which reports both estimated (projected) demands and prices for carbon fiber for the years from 2012 to 2020. We used data points in 2012 and 2017 with demands of 40 thousand tons and 80 thousand tons, and prices of \$30/kg and \$20/kg, respectively. It should be noted that while Shama et al. (2018)'s estimates on demand are comparable with others (Kozarsky et al. 2011; Red and Zimm 2012; Souto, Calado, and Pereira 2018; Witten et al. 2018), their estimates on carbon fiber prices are considerably lower. For instance, Shama et al. (2018) suggested that carbon fiber prices would reach \$10/kg in 2020 and even \$8/kg in 2021, whereas the current market in 2020-2021 reported a price between \$14/kg and \$18/kg.

With the data points in 2012 and 2017, we estimated a demand elasticity of -1.7, indicating the demand for carbon fiber is elastic (i.e., demand is sensitive to price changes). This finding is in line with expectations due to the existence of many substitutes (i.e., glass fiber, steel, aluminum,

[56]Figure 3 in (Shama et al. 2018) plots the estimated (projected) demands and prices for carbon fiber from 2012 to 2020.

etc.). To derive price responses to lignin-based carbon fiber from MIBR, we rearranged equation (11) and obtained the formula below.

(12) $$\varepsilon = \frac{\Delta q / q}{\Delta p / p} = \frac{\Delta q}{\Delta p} \times \frac{p}{q} \Rightarrow \Delta p = p \times \frac{\Delta q}{q} \times \frac{1}{\varepsilon}$$

Where Δq and Δp indicate changes in quantity and price, respectively. From equation (12), we can see that price response depends on the current market size q , price p, changes in demand Δq, and demand elasticity.

Taking the year 2021 as a reference, we assumed a market size of 160 thousand tons (Shama et al. 2018; Mordor Intelligence 2021) and a market price of $18/kg. On the MIBR side, the platform size we considered would process 1 dry ton corn stover per day,[57] resulting in 200 kg lignin-containing biorefinery wastes and consequently leading to 100 kg lignin-based carbon fiber per day. Assuming no breaks in production, the platform can produce 36 tons per year, which is almost neglectable compared with the current market size of 160 thousand tons. Based on equation (12), the price changes to such small increases in supply are trivial (i.e., $0.002/kg). Additionally, another important factor to consider is the increasing demand. Although market analysis has adjusted the compound annual growth rates of the carbon fiber market downward from 10%-15% to around 5%-6%, they all expected the market to bounce back to normal in 2021-2022. Thus, we expect additional supplies from MIBR could be easily absorbed by the increasing demand without disturbing the market prices.

Despite the analysis above, it should be noted that the designed capacity of the MIBR refinery setup we are examining is significantly lower than the capacity of a real biorefinery plant. Today

[57]The scale-up of MIBR will be performed by the ICM Inc.

in the United States an average commercial ethanol plant produces about 89 million gallons of ethanol annually from about 32 million bushels of corn (EIA 2021).[58] Assuming a corn yield of 171 bushels per acre (USDA NASS 2021), that amount of corn needs to be harvested from 187000 acres of land, resulting in about 766700 dry tons of corn stover per year (based on a ratio of 4.1 tons/acre in Wang et al. 2013).

In other words, an "industrial-sized" corn stover ethanol plant with a capacity comparable to a corn ethanol plant will be more than 2000 times larger than the sample MIBR platform we are using data on. Such a plant will generate 76 thousand tons of lignin-based carbon fiber per year, which is nearly half of the estimated global carbon fiber demand in 2021. According to equation (12), these additional supplies would decrease the carbon fiber price by $5/kg, a reduction of 28% from the current price of $18/kg. This would pose significant challenges to the profitability of lignin-based byproducts scaled up from the MIBR platform.

Moreover, the Energy Independence and Security Act (EISA) set a goal of producing 21 billion gallons of lignocellulosic ethanol by 2022. This would require 235 plants of the average-sized 89-million-gallon plants discussed above and they would generate 17.8 million tons of lignin-based carbon fiber, a quantity that is 111 times larger than the current market. Under this level of production, the current market would be overwhelmed, and prices would collapse. Clearly, for widespread production, there would need to be substantial increases in the use of carbon fiber in many manufacturing endeavors, or there would need to be other uses for the lignin with carbon fiber only being a small part of the byproduct usage.

[58]The calculation involves several assumptions. According to U.S. Energy Information Administration (EIA), the average ethanol plant capacity reached 89 million gallons per year. Based on a corn ethanol yield of 0.365 bushels per gallon, in GREET2021, that means an average-sized ethanol plant would consume 32 million bushels per year.

Conclusion

In this chapter, we answered two critical questions regarding the environmental performance of the proposed MIBR platform and the market potential of lignin-based carbon fiber.

In the first part of the chapter, we estimate emission impacts by building LCA models that cover the entirety of the platform. In doing this we developed two product scenarios focusing on cellulosic ethanol and carbon fiber, respectively, as the main product. The results reveal that when cellulosic ethanol is treated as the main product (i.e., the scenario where lignin-based carbon fiber and PHAs are expected to replace PAN-based products and petroleum-based plastics, respectively), the MIBR does not exhibit significant environmental advantages over the standard DOE corn stover to ethanol process. Specifically, 1 gallon ethanol in MIBR is associated with 2.42 kg CO2 equivalent emissions, an increase of 47.6% from that in the reference DOE process. We argue that the current estimates should be considered as an upper bound on MIBR emissions because the chemical inputs are likely overestimated.

On the other hand, when lignin-based carbon fiber is treated as the main product (that means ethanol is treated as a byproduct and is expected to replace gasoline), our results demonstrate an emission level of 19.5 kg per kg of lignin-based carbon fiber produced from MIBR, indicating an emission reduction ranging from 35.4% - 64.2% relative to PAN-based counterparts, which is comparable to that in the literature.

The goal of the MIBR was to reduce CO2 emissions by 10% relative to the current processes. Our findings indicate meeting such a goal seems unrealistic given our estimates indicating an emission increase of 47.6%. However, we do feel confident that MIBR emission reductions could

be enhanced through optimizations of chemical inputs and improvements in carbon yields. We also find some evidence that the GREET-based estimates may be optimistic.

In the second part of the chapter, we perform market analyses for carbon fiber's demand, supply capacity, prices, and costs. There is some need to cautiously consider the market size and price response. First, we find theoretical supply capacity was 90.2% larger than the estimated demand (in 2018) and that might portend a market that was overwhelmed by industrial-scale production. Second, we do see signs that the carbon fiber market is still promising, signaled by steady increases in investment in capacity. Third, we see potentials for market expansion given that a major barrier to extensive applications of carbon fiber in the industry remains its high cost and we believe lignin-based fiber could be much cheaper to produce. Fourth, as more and more stringent environmental regulations are applied, we expect carbon fiber demand will continue to grow at compound annual growth rates of over 10%. Fifth, our results show that additional supplies from the small MIBR platform are negligible compared with the overall market size and would barely impact the market price of carbon fiber. However, additional carbon fiber supplies from an industrial scale corn stover based ethanol plant with a capacity level comparable with a single current average sized corn ethanol plant will reduce the price by 28% to $13/kg, and production at a national scale representative of the volumes anticipated in EISA would collapse the market price. This poses challenges to the profitability of lignin-based carbon fiber with a need for developing alternative byproducts or a need for a great expansion in carbon fiber usage.

CHAPTER V

CONCLUSIONS AND FUTURE RESEARCH

Conclusion

In this dissertation, we cover two general topics related to climate change: The impacts of climate change and the means to mitigate it.

In Chapter 2 (the first essay), we examine the impacts of climate change and air pollution (surface ozone) on crop yields jointly in the United States. This is done for corn, soybeans, spring wheat, winter wheat, barley, cotton, peanuts, rice, sorghum, and sunflower.

We find significant negative impacts of ozone exposure on most of the crops we examined, which is largely consistent with experimental studies. However, there are two exceptions. First, our results suggest that winter wheat is not sensitive to ozone exposure, as opposed to chamber studies, which label winter wheat as one of the most ozone-sensitive crops. Second, we confirm the existing empirical evidence that corn tends to be more sensitive than soybeans, which again contradicts chamber experiments. Our results also show that climate change exacerbates ozone damages for ozone-sensitive crops, particularly for soybeans and spring wheat. On the other hand, drought mitigation alleviates ozone damages.

Mid-21st century projections indicate that climate change would increase ozone concentrations in the agricultural regions by 36% for spring crops. Consequently, elevations in ozone would decrease yields by 0.1% to 1.8%, which is significantly lower than the yield reductions caused directly by climate change (i.e., 5.2% to 25.5%).

In Chapter 3 (the second essay), we analyze climate change impacts on winter wheat, one of the most widely planted cereal crops globally. To better characterize climate impacts, we divide

winter wheat's growing period into three seasons, corresponding to distinct growing stages. Doing this allows us to identify important climate impacts that are possibly overlooked in existing studies.

We find heat in the fall and freezing days in the early spring are the most important drivers of yield reductions. Most importantly, our yield projections with various climate change scenarios highlight the importance of accounting for reductions in freezing days. When such effects are omitted, the projected climate change impacts on winter wheat are significantly larger and portend yield reductions, i.e., 4.1%-26.3% reduction as opposed to 0.4%-3.0% yield gains under projections from models with such terms. Finally, the introduction of "climate penalty" terms enables us to differentiate the short-run and long-run climate impacts, leading to the estimation of adaptation effects. We find substantial adaptation effects that could even reverse the sign of the climate change impacts on winter wheat.

In Chapter 4 (the third essay), we answer two critical questions regarding the environmental performance of the proposed MIBR platform and the market potential of carbon fiber.

We build LCA models to measure the overall emissions in the process. In doing this we develop two product scenarios focusing on cellulosic ethanol and carbon fiber, respectively, as the main product. The results reveal that when cellulosic ethanol is treated as the main product, the MIBR does not exhibit significant environmental advantages over the standard DOE corn stover to ethanol process. We argue that the current estimates should be considered as an upper bound on MIBR emissions because the chemical inputs are likely overestimated. On the other hand, when lignin-based carbon fiber is treated as the main product, our results demonstrate an emission reduction ranging from 35.4% - 64.2% of MIBR, relative to PAN-based counterparts.

We also perform market analyses for carbon fiber's demand, supply capacity, prices, costs, and possible market reactions to the introduction of lignin-based products. Although we find

theoretical supply capacity was 90.2% larger than the estimated demand (in 2018), we do see signs indicating a promising carbon fiber market. We expect carbon fiber demand will continue to grow at compound annual growth rates of over 10%.

On the market penetration side, our results show that additional supplies from the MIBR platform are neglectable compared with the overall market size and can barely impact the market price of carbon fiber. However, additional carbon fiber supplies from a corn stover ethanol plant with a capacity level comparable with a corn ethanol plant will reduce the price by 28% to $13/kg, posing challenges to the profitability of lignin-based byproducts.

Limitations and future research

Naturally, some limitations characterize this research and could be improved in the future. Here we choose to highlight some of them.

In Chapter 2, we used two sources for ozone: USEPA observations and simulated data. The problem with the latter is its biases. Although we performed simple yet solid corrections, the problem still exists. To be more detailed, since we used the mean differences between observed and simulated data to correct, it will make the corrected data coverage to the mean. In other words, regions with extreme incidences (either low or high ozone levels) will have large measurement errors after correction, attenuating the power of our estimations.

This concern was raised by Dr. Kazuhiko Kobayashi from The University of Tokyo, who kindly provided us with new data sources for ozone that are measured at the crop canopy height. For future research, we aim to take advantage of the new data and extend the current work by considering other air pollution variables, i.e., aerosols (PM2.5). The inclusion of aerosols in the assessment is important because there are projections of more frequent heatwaves and higher aerosol episodes for developing countries.

We have multiple limitations in Chapter 3. First, we made a strong assumption on irrigation, (i.e., we assume the study region is rain-fed for winter wheat), due to the lack of reliable irrigation data. However, the assumption may not perfectly hold in reality, because studies have indicated intensive irrigation activities in those regions. Currently, we are still looking for potential solutions to address this concern.

The second concern is about the winter wheat yield data we used in the chapter. As noted in Figure 8, there was a huge discontinuous increase in yields in 1990, which is very strange and unlikely to happen in the absence of natural disasters.[59] To address this concern, we ran robustness checks with data restricted to 1991-2015 and the results were consistent with that derived from the full sample. Nevertheless, it still makes sense to pin down the specific reasons which caused the sudden jump in yields.

The third concern in Chapter 3 is that we only included temperature and precipitation variables in the model. However, several studies have emphasized the importance of secondary variables (i.e., relative humidity, wind speed, solar radiation, and potential evaporation). We plan to address this concern while revising the paper.

Lastly, there is a common concern in Chapter 2 and Chapter 3; that is we were unable to account for the CO2 fertilization effect. It is difficult to do so because CO2 is well mixed in the atmosphere, thus with limited spatial variation but common increases over time which are difficult to break from technological progress. Free-Air Carbon Dioxide Enrichment (FACE) is a method commonly used by ecologists and plant biologists to estimate those fertilization effects.

In Chapter 4, the major limitation is the accuracy of the data collected for LCA analysis. As we have repeatedly addressed in the chapter, those data tend to be overestimated. Some of the data

[59]We appreciate the comments from two anonymous reviewers on this issue.

were obtained via personal communication with the group members who constructed the MIBR platform. However, it should be noted that input usages (particularly electricity consumption) during the process largely depend on the device and conditioning time. We are working on developing methods to produce more accurate data. Another direction for future efforts is to unify the LCA and TEA analyses. The results should be derived from a common ground, including consistent assumptions and input usages.

REFERENCES

Adams, Richard M, and Bruce A McCarl. 1985. “Assessing the Benefits of Alternative Ozone Standards on Agriculture: The Role of Response Information.” *Journal of Environmental Economics and Management* 12 (3): 264–76. doi:10.1016/0095-0696(85)90034-8.

Ainsworth, Elizabeth A. 2008. “Rice Production in a Changing Climate: A Meta-Analysis of Responses to Elevated Carbon Dioxide and Elevated Ozone Concentration.” *Global Change Biology* 14 (7): 1642–50. doi:10.1111/j.1365-2486.2008.01594.x.

Ainsworth, Elizabeth A., Craig R. Yendrek, Stephen Sitch, William J. Collins, and Lisa D. Emberson. 2012. “The Effects of Tropospheric Ozone on Net Primary Productivity and Implications for Climate Change.” *Annual Review of Plant Biology* 63 (1): 637–61. doi:10.1146/annurev-arplant-042110-103829.

Allen, R. G. D., and A. P. Lerner. 1934. “The Concept of Arc Elasticity of Demand.” *The Review of Economic Studies* 1 (3). [Oxford University Press, Review of Economic Studies, Ltd.]: 226–30. doi:10.2307/2967486.

Amin, Nawahda. 2013. “Effect of Ozone on the Relative Yield of Rice Crop in Japan Evaluated Based on Monitored Concentrations.” *Water, Air, & Soil Pollution* 225 (1): 1797. doi:10.1007/s11270-013-1797-5.

Amundson, R.G., R.J. Kohut, A.W. Schoettle, R.M. Raba, and P.B. Reich. 1987. “Correlative Reductions in Whole-Plant Photosynthesis and Yield of Winter Wheat Caused by Ozone.” *Physiology and Biochemistry* 77 (1): 75–79.

Anderson, Ryan, Deepak Keshwani, Ashu Guru, Haishun Yang, Suat Irmak, and Jeyamkondan Subbiah. 2018. “An Integrated Modeling Framework for Crop and Biofuel Systems Using the DSSAT and GREET Models.” *Environmental Modelling & Software* 108 (October): 40–50. doi:10.1016/j.envsoft.2018.07.004.

Arreola-Vargas, Jorge, Xianzhi Meng, Yun-yan Wang, Arthur J. Ragauskas, and Joshua S. Yuan. 2021. “Enhanced Medium Chain Length-Polyhydroxyalkanoate Production by Co-Fermentation of Lignin and Holocellulose Hydrolysates.” *Green Chemistry* 23 (20). Royal Society of Chemistry: 8226–37. doi:10.1039/D1GC02725E.

Asseng, S., F. Ewert, P. Martre, R. P. Rötter, D. B. Lobell, D. Cammarano, B. A. Kimball, et al. 2015. “Rising Temperatures Reduce Global Wheat Production.” *Nature Climate Change* 5 (2): 143–47. doi:10.1038/nclimate2470.

Asseng, S., F. Ewert, C. Rosenzweig, J. W. Jones, J. L. Hatfield, A. C. Ruane, K. J. Boote, et al. 2013. “Uncertainty in Simulating Wheat Yields under Climate Change.” *Nature Climate Change* 3 (9): 827–32. doi:10.1038/nclimate1916.

Auffhammer, Maximilian. 2018. “Climate Adaptive Response Estimation: Short And Long Run Impacts Of Climate Change On Residential Electricity and Natural Gas Consumption Using Big Data.” Working Paper 24397. Working Paper Series. National Bureau of Economic Research. doi:10.3386/w24397.

Auffhammer, Maximilian, Patrick Baylis, and Catherine H. Hausman. 2017. “Climate Change Is Projected to Have Severe Impacts on the Frequency and Intensity of Peak Electricity Demand across the United States.” *Proceedings of the National Academy of Sciences* 114 (8). National Academy of Sciences: 1886–91. doi:10.1073/pnas.1613193114.

Auffhammer, Maximilian, Solomon M. Hsiang, Wolfram Schlenker, and Adam Sobel. 2013. “Using Weather Data and Climate Model Output in Economic Analyses of Climate Change.” *Review of Environmental Economics and Policy* 7 (2): 181–98. doi:10.1093/reep/ret016.

Avnery, Shiri, Denise L. Mauzerall, Junfeng Liu, and Larry W. Horowitz. 2011a. “Global Crop Yield Reductions Due to Surface Ozone Exposure: 1. Year 2000 Crop Production Losses and Economic Damage.” *Atmospheric Environment* 45 (13): 2284–96. doi:10.1016/j.atmosenv.2010.11.045.

———. 2011b. “Global Crop Yield Reductions Due to Surface Ozone Exposure: 2. Year 2030 Potential Crop Production Losses and Economic Damage under Two Scenarios of O3 Pollution.” *Atmospheric Environment* 45 (13): 2297–2309. doi:10.1016/j.atmosenv.2011.01.002.

Baker, Darren A., and Timothy G. Rials. 2013. “Recent Advances in Low-Cost Carbon Fiber Manufacture from Lignin.” *Journal of Applied Polymer Science* 130 (2): 713–28. doi:10.1002/app.39273.

Barreca, Alan, Karen Clay, Olivier Deschênes, Michael Greenstone, and Joseph S. Shapiro. 2015. “Convergence in Adaptation to Climate Change: Evidence from High Temperatures and Mortality, 1900-2004.” *American Economic Review* 105 (5): 247–51. doi:10.1257/aer.p20151028.

Barreca, Alan, Karen Clay, Olivier Deschenes, Michael Greenstone, and Joseph S. Shapiro. 2016. “Adapting to Climate Change: The Remarkable Decline in the US Temperature-Mortality Relationship over the Twentieth Century.” *Journal of Political Economy* 124 (1). The University of Chicago Press: 105–59. doi:10.1086/684582.

Barreca, Alan I. 2012. “Climate Change, Humidity, and Mortality in the United States.” *Journal of Environmental Economics and Management* 63 (1): 19–34. doi:10.1016/j.jeem.2011.07.004.

Beer, Tom, and Tim Grant. 2007. “Life-Cycle Analysis of Emissions from Fuel Ethanol and Blends in Australian Heavy and Light Vehicles.” *Journal of Cleaner Production*, From Cleaner Production to Sustainable Production and Consumption in Australia and New Zealand: Achievements, Challenges, and Opportunities, 15 (8): 833–37. doi:10.1016/j.jclepro.2006.07.003.

Bell, Michelle L., Richard Goldberg, Christian Hogrefe, Patrick L. Kinney, Kim Knowlton, Barry Lynn, Joyce Rosenthal, Cynthia Rosenzweig, and Jonathan A. Patz. 2007. “Climate Change, Ambient Ozone, and Health in 50 US Cities.” *Climatic Change* 82 (1): 61–76. doi:10.1007/s10584-006-9166-7.

Biswas, D. K., and G. M. Jiang. 2011. “Differential Drought-Induced Modulation of Ozone Tolerance in Winter Wheat Species.” *Journal of Experimental Botany* 62 (12): 4153–62. doi:10.1093/jxb/err104.

Blanc, Elodie, and Wolfram Schlenker. 2017. “The Use of Panel Models in Assessments of Climate Impacts on Agriculture.” *Review of Environmental Economics and Policy* 11 (2): 258–79. doi:10.1093/reep/rex016.

Boddiger, David. 2007. “Boosting Biofuel Crops Could Threaten Food Security.” *The Lancet* 370 (9591). Elsevier: 923–24. doi:10.1016/S0140-6736(07)61427-5.

Boucher, O., S. Denvil, A. Caubel, and M.A. Foujols. 2019. “IPSL IPSL-CM6A-LR Model Output Prepared for CMIP6 ScenarioMIP Ssp460 (Version 20191121).” *Earth System Grid Federation*. doi:https://doi.org/10.22033/ESGF/CMIP6.5268.

Burke, Marshall, and Kyle Emerick. 2016. “Adaptation to Climate Change: Evidence from US Agriculture.” *American Economic Journal: Economic Policy* 8 (3): 106–40. doi:10.1257/pol.20130025.

Burke, Marshall, Felipe González, Patrick Baylis, Sam Heft-Neal, Ceren Baysan, Sanjay Basu, and Solomon Hsiang. 2018. “Higher Temperatures Increase Suicide Rates in the United States and Mexico.” *Nature Climate Change* 8 (8). Nature Publishing Group: 723–29. doi:10.1038/s41558-018-0222-x.

Burke, Marshall, Solomon M. Hsiang, and Edward Miguel. 2015. “Global Non-Linear Effect of Temperature on Economic Production.” *Nature* 527 (7577). Nature Publishing Group: 235–39. doi:10.1038/nature15725.

Burnham, Andrew, Jeongwoo Han, Corrie E. Clark, Michael Wang, Jennifer B. Dunn, and Ignasi Palou-Rivera. 2012. “Life-Cycle Greenhouse Gas Emissions of Shale Gas, Natural Gas, Coal, and Petroleum.” *Environmental Science & Technology* 46 (2). American Chemical Society: 619–27. doi:10.1021/es201942m.

Butler, Ethan E., and Peter Huybers. 2013. “Adaptation of US Maize to Temperature Variations.” *Nature Climate Change* 3 (1): 68–72. doi:10.1038/nclimate1585.

Canter, Christina E., Jennifer B. Dunn, Jeongwoo Han, Zhichao Wang, and Michael Wang. 2016. “Policy Implications of Allocation Methods in the Life Cycle Analysis of Integrated Corn and Corn Stover Ethanol Production.” *BioEnergy Research* 9 (1): 77–87. doi:10.1007/s12155-015-9664-4.

Cao, Weixing, and Dale N. Moss. 1989. “Temperature Effect on Leaf Emergence and Phyllochron in Wheat and Barley.” *Crop Science* 29 (4): 1018–21. doi:https://doi.org/10.2135/cropsci1989.0011183X002900040038x.

Carleton, Tamma A., Amir Jina, Michael T. Delgado, Michael Greenstone, Trevor Houser, Solomon M. Hsiang, Andrew Hultgren, et al. 2020. “Valuing the Global Mortality Consequences of Climate Change Accounting for Adaptation Costs and Benefits.” w27599. National Bureau of Economic Research. doi:10.3386/w27599.

Carter, Colin A., Xiaomeng Cui, Aijun Ding, Dalia Ghanem, Fei Jiang, Fujin Yi, and Funing Zhong. 2017. “Stage-Specific, Nonlinear Surface Ozone Damage to Rice Production in China.” *Scientific Reports* 7 (March): 44224. doi:10.1038/srep44224.

Chen, Chi-Chung, Bruce A. McCarl, and David E. Schimmelpfennig. 2004. “Yield Variability as Influenced by Climate: A Statistical Investigation.” *Climatic Change* 66 (1): 239–61. doi:10.1023/B:CLIM.0000043159.33816.e5.

Chen, Shuai, Xiaoguang Chen, and Jintao Xu. 2016. “Impacts of Climate Change on Agriculture: Evidence from China.” *Journal of Environmental Economics and Management* 76 (March): 105–24. doi:10.1016/j.jeem.2015.01.005.

Chen, Shuai, and Binlei Gong. 2020. “Response and Adaptation of Agriculture to Climate Change: Evidence from China.” *Journal of Development Economics*, August, 102557. doi:10.1016/j.jdeveco.2020.102557.

Chen, Xiaoguang, and Madhu Khanna. 2013. “Food vs. Fuel: The Effect of Biofuel Policies.” *American Journal of Agricultural Economics* 95 (2): 289–95. doi:10.1093/ajae/aas039.

Cherubini, Francesco, Anders Hammer Strømman, and Sergio Ulgiati. 2011. “Influence of Allocation Methods on the Environmental Performance of Biorefinery Products—A Case Study.” *Resources, Conservation and Recycling* 55 (11): 1070–77. doi:10.1016/j.resconrec.2011.06.001.

Ciriminna, Rosaria, Cristina Della Pina, Michele Rossi, and Mario Pagliaro. 2014. “Understanding the Glycerol Market.” *European Journal of Lipid Science and Technology* 116 (10): 1432–39. doi:https://doi.org/10.1002/ejlt.201400229.

Cook, Benjamin I., Toby R. Ault, and Jason E. Smerdon. 2015. “Unprecedented 21st Century Drought Risk in the American Southwest and Central Plains.” *Science Advances* 1 (1). American Association for the Advancement of Science: e1400082. doi:10.1126/sciadv.1400082.

Cronin, Keith R., Troy M. Runge, Xuesong Zhang, R. César Izaurralde, Douglas J. Reinemann, and Julie C. Sinistore. 2017. “Spatially Explicit Life Cycle Analysis of Cellulosic Ethanol Production Scenarios in Southwestern Michigan.” *BioEnergy Research* 10 (1): 13–25. doi:10.1007/s12155-016-9774-7.

Da, Yabin, Yangyang Xu, and Bruce McCarl. 2021. “Effects of Surface Ozone and Climate on Historical (1980–2015) Crop Yields in the United States: Implication for Mid-21st Century Projection.” *Environmental and Resource Economics*, November, In press. doi:10.1007/s10640-021-00629-y.

Das, Sujit. 2011. “Life Cycle Assessment of Carbon Fiber-Reinforced Polymer Composites.” *The International Journal of Life Cycle Assessment* 16 (3): 268–82. doi:10.1007/s11367-011-0264-z.

Das, Sujit, and D Warren. 2012. “Technical Cost Modeling-Life Cycle Analysis Basis for Program Focus.” *Oak Ridge National Laboratory, Oak Ridge, TN*.

Das, Sujit, Josh Warren, Devin West, and Susan M. Schexnayder. 2016. “Global Carbon Fiber Composites Supply Chain Competitiveness Analysis.” ORNL/SR-2016/100 | NREL/TP-6A50-66071. CEMAC.

Davis, Lucas W., and Paul J. Gertler. 2015. “Contribution of Air Conditioning Adoption to Future Energy Use under Global Warming.” *Proceedings of the National Academy of Sciences* 112 (19). National Academy of Sciences: 5962–67. doi:10.1073/pnas.1423558112.

De Winne, Jasmien, and Gert Peersman. 2021. “The Adverse Consequences of Global Harvest and Weather Disruptions on Economic Activity.” *Nature Climate Change* 11 (8): 665–72. doi:10.1038/s41558-021-01102-w.

Debaje, S. B. 2014. “Estimated Crop Yield Losses Due to Surface Ozone Exposure and Economic Damage in India.” *Environmental Science and Pollution Research* 21 (12): 7329–38. doi:10.1007/s11356-014-2657-6.

Dell, Melissa, Benjamin F. Jones, and Benjamin A. Olken. 2012. “Temperature Shocks and Economic Growth: Evidence from the Last Half Century.” *American Economic Journal: Macroeconomics* 4 (3): 66–95. doi:10.1257/mac.4.3.66.

———. 2014. “What Do We Learn from the Weather? The New Climate-Economy Literature.” *Journal of Economic Literature* 52 (3): 740–98. doi:10.1257/jel.52.3.740.

Deryng, Delphine, Declan Conway, Navin Ramankutty, Jeff Price, and Rachel Warren. 2014. “Global Crop Yield Response to Extreme Heat Stress under Multiple Climate Change Futures.” *Environmental Research Letters* 9 (3). IOP Publishing: 034011. doi:10.1088/1748-9326/9/3/034011.

Deryugina, Tatyana, Garth Heutel, Nolan H. Miller, David Molitor, and Julian Reif. 2019. “The Mortality and Medical Costs of Air Pollution: Evidence from Changes in Wind Direction.” *American Economic Review* 109 (12): 4178–4219. doi:10.1257/aer.20180279.

Deschênes, Olivier, and Michael Greenstone. 2007. “The Economic Impacts of Climate Change: Evidence from Agricultural Output and Random Fluctuations in Weather.” *American Economic Review* 97 (1): 354–85. doi:10.1257/aer.97.1.354.

———. 2011. “Climate Change, Mortality, and Adaptation: Evidence from Annual Fluctuations in Weather in the US.” *American Economic Journal: Applied Economics* 3 (4): 152–85. doi:10.1257/app.3.4.152.

DOE. 2018. “CX-101107 Multi-Stream Integrated Biorefinery.” May. https://www.energy.gov/nepa/downloads/cx-101107-multi-stream-integrated-biorefinery.

Dreccer, M. Fernanda, Justin Fainges, Jeremy Whish, Francis C. Ogbonnaya, and Victor O. Sadras. 2018. “Comparison of Sensitive Stages of Wheat, Barley, Canola, Chickpea and Field Pea to Temperature and Water Stress across Australia.” *Agricultural and Forest Meteorology* 248 (January): 275–94. doi:10.1016/j.agrformet.2017.10.006.

EIA. 2020a. “Form EIA-860 Detailed Data with Previous Form Data (EIA-860A/860B).” https://www.eia.gov/electricity/data/eia860/.

———. 2020b. “Use of Gasoline - U.S. Energy Information Administration (EIA).” April. https://www.eia.gov/energyexplained/gasoline/use-of-gasoline.php.

———. 2021. “U.S. Fuel Ethanol Plant Production Capacity.” September. https://www.eia.gov/petroleum/ethanolcapacity/index.php.

Ellringmann, Tim, Christian Wilms, Moritz Warnecke, Gunnar Seide, and Thomas Gries. 2015. “Carbon Fiber Production Costing: A Modular Approach:” *Textile Research Journal*, April. doi:10.1177/0040517514532161.

———. 2016. “Carbon Fiber Production Costing: A Modular Approach.” *Textile Research Journal* 86 (2). SAGE Publications Ltd STM: 178–90. doi:10.1177/0040517514532161.

ElMekawy, Ahmed, Ludo Diels, Heleen De Wever, and Deepak Pant. 2013. "Valorization of Cereal Based Biorefinery Byproducts: Reality and Expectations." *Environmental Science & Technology* 47 (16). American Chemical Society: 9014–27. doi:10.1021/es402395g.

Emberson, L. D., P. Büker, M. R. Ashmore, G. Mills, L. S. Jackson, M. Agrawal, M. D. Atikuzzaman, et al. 2009. "A Comparison of North American and Asian Exposure–Response Data for Ozone Effects on Crop Yields." *Atmospheric Environment* 43 (12): 1945–53. doi:10.1016/j.atmosenv.2009.01.005.

Falano, Temitope, Harish K. Jeswani, and Adisa Azapagic. 2014. "Assessing the Environmental Sustainability of Ethanol from Integrated Biorefineries." *Biotechnology Journal* 9 (6): 753–65. doi:10.1002/biot.201300246.

Fan, Jing-Li, Yabin Da, Bin Zeng, Hao Zhang, Zhu Liu, Na Jia, Jue Liu, et al. 2020. "How Do Weather and Climate Change Impact the COVID-19 Pandemic? Evidence from the Chinese Mainland." *Environmental Research Letters*. doi:10.1088/1748-9326/abcf76.

FAOSTAT. 2021. "Food and Agriculture Organization of the United Nations." http://www.fao.org/faostat/en/#data.

Feng, Zhaozhong, Tingjian Hu, Amos P. K. Tai, and Vicent Calatayud. 2020. "Yield and Economic Losses in Maize Caused by Ambient Ozone in the North China Plain (2014–2017)." *Science of The Total Environment* 722 (June): 137958. doi:10.1016/j.scitotenv.2020.137958.

Feng, Zhaozhong, Kazuhiko Kobayashi, Pin Li, Yansen Xu, Haoye Tang, Anhong Guo, Elena Paoletti, and Vicent Calatayud. 2019. "Impacts of Current Ozone Pollution on Wheat Yield in China as Estimated with Observed Ozone, Meteorology and Day of Flowering." *Atmospheric Environment* 217 (November): 116945. doi:10.1016/j.atmosenv.2019.116945.

Fernando, Sandun, Sushil Adhikari, Chauda Chandrapal, and Naveen Murali. 2006. "Biorefineries: Current Status, Challenges, and Future Direction." *Energy & Fuels* 20 (4). American Chemical Society: 1727–37. doi:10.1021/ef060097w.

Fezzi, Carlo, and Ian Bateman. 2015. "The Impact of Climate Change on Agriculture: Nonlinear Effects and Aggregation Bias in Ricardian Models of Farmland Values." *Journal of the Association of Environmental and Resource Economists* 2 (1). The University of Chicago Press: 57–92. doi:10.1086/680257.

Fick, Stephen E., and Robert J. Hijmans. 2017. "WorldClim 2: New 1-Km Spatial Resolution Climate Surfaces for Global Land Areas." *International Journal of Climatology* 37 (12): 4302–15. doi:https://doi.org/10.1002/joc.5086.

Fiore, Arlene M., Vaishali Naik, Dominick V. Spracklen, Allison Steiner, Nadine Unger, Michael Prather, Dan Bergmann, et al. 2012. "Global Air Quality and Climate." *Chemical Society Reviews* 41 (19). The Royal Society of Chemistry: 6663–83. doi:10.1039/C2CS35095E.

Fischer, R.A., D. Byerlee, and G. Edmeades. 2014. *Crop Yield and Food Security: Will Yield Increases Continue to Feed the World?* Canberra: ACIAR.

Fuhrer, J., L. Skärby, and M. R. Ashmore. 1997. “Critical Levels for Ozone Effects on Vegetation in Europe.” *Environmental Pollution* 97 (1): 91–106. doi:10.1016/S0269-7491(97)00067-5.

Gerbinet, Saïcha, Sandra Belboom, and Angélique Léonard. 2014. “Life Cycle Analysis (LCA) of Photovoltaic Panels: A Review.” *Renewable and Sustainable Energy Reviews* 38 (October): 747–53. doi:10.1016/j.rser.2014.07.043.

Godzinski, Alexandre, and Milena Suarez Castillo. 2021. “Disentangling the Effects of Air Pollutants with Many Instruments.” *Journal of Environmental Economics and Management*, June, 102489. doi:10.1016/j.jeem.2021.102489.

Graff Zivin, Joshua, and Matthew Neidell. 2014. “Temperature and the Allocation of Time: Implications for Climate Change.” *Journal of Labor Economics* 32 (1). The University of Chicago Press: 1–26. doi:10.1086/671766.

Griliches, Zvi. 1979. “Sibling Models and Data in Economics: Beginnings of a Survey.” *Journal of Political Economy* 87 (5, Part 2). The University of Chicago Press: S37–64. doi:10.1086/260822.

Grootel, Alexander van, Jiyoun Chang, Brian L. Wardle, and Elsa Olivetti. 2020. “Manufacturing Variability Drives Significant Environmental and Economic Impact: The Case of Carbon Fiber Reinforced Polymer Composites in the Aerospace Industry.” *Journal of Cleaner Production* 261 (July): 121087. doi:10.1016/j.jclepro.2020.121087.

Guarin, Jose Rafael, Lisa Emberson, David Simpson, Ixchel M. Hernandez-Ochoa, Diane Rowland, and Senthold Asseng. 2019. “Impacts of Tropospheric Ozone and Climate Change on Mexico Wheat Production.” *Climatic Change*, May. doi:10.1007/s10584-019-02451-4.

Guarin, Jose Rafael, Belay Kassie, Alsayed M. Mashaheet, Kent Burkey, and Senthold Asseng. 2019. “Modeling the Effects of Tropospheric Ozone on Wheat Growth and Yield.” *European Journal of Agronomy* 105 (April): 13–23. doi:10.1016/j.eja.2019.02.004.

He, Jie, Kun Yang, Wenjun Tang, Hui Lu, Jun Qin, Yingying Chen, and Xin Li. 2020. “The First High-Resolution Meteorological Forcing Dataset for Land Process Studies over China.” *Scientific Data* 7 (1). Nature Publishing Group: 25. doi:10.1038/s41597-020-0369-y.

Hermansson, Frida. 2020. “Assessing the Future Environmental Impact of Lignin-Based and Recycled Carbon Fibres in Composites Using Life Cycle Assessment.” Chalmers Tekniska Hogskola (Sweden).

Hermansson, Frida, Matty Janssen, and Magdalena Svanström. 2019. “Prospective Study of Lignin-Based and Recycled Carbon Fibers in Composites through Meta-Analysis of Life Cycle Assessments.” *Journal of Cleaner Production* 223 (June): 946–56. doi:10.1016/j.jclepro.2019.03.022.

———. 2020. “Allocation in Life Cycle Assessment of Lignin.” *The International Journal of Life Cycle Assessment* 25 (8): 1620–32. doi:10.1007/s11367-020-01770-4.

Heutel, Garth, Nolan H. Miller, and David Molitor. 2020. “Adaptation and the Mortality Effects of Temperature Across U.S. Climate Regions.” *The Review of Economics and Statistics*, June. MIT Press, 1–33. doi:10.1162/rest_a_00936.

Holman, Johnathon D., Alan J. Schlegel, Curtis R. Thompson, and Jane E. Lingenfelser. 2011. "Influence of Precipitation, Temperature, and 56 Years on Winter Wheat Yields in Western Kansas." *Crop Management* 10 (1): 0–0. doi:10.1094/CM-2011-1229-01-RS.

Holmes, Mark. 2017. "Lowering the Cost of Carbon Fiber." *Reinforced Plastics* 61 (5): 279–83. doi:10.1016/j.repl.2017.02.001.

Hong, Chaopeng, Qiang Zhang, Yang Zhang, Steven J. Davis, Dan Tong, Yixuan Zheng, Zhu Liu, Dabo Guan, Kebin He, and Hans Joachim Schellnhuber. 2019. "Impacts of Climate Change on Future Air Quality and Human Health in China." *Proceedings of the National Academy of Sciences* 116 (35): 17193–200. doi:10.1073/pnas.1812881116.

Hsiang, Solomon. 2016. "Climate Econometrics." *Annual Review of Resource Economics* 8 (1): 43–75. doi:10.1146/annurev-resource-100815-095343.

Hu, Tingjian, Shuo Liu, Yansen Xu, Zhaozhong Feng, and Vicent Calatayud. 2019. "Assessment of O3-Induced Yield and Economic Losses for Wheat in the North China Plain from 2014 to 2017, China." *Environmental Pollution*, December, 113828. doi:10.1016/j.envpol.2019.113828.

Huang, Kaixing, Hong Zhao, Jikun Huang, Jinxia Wang, and Christopher Findlay. 2020. "The Impact of Climate Change on the Labor Allocation: Empirical Evidence from China." *Journal of Environmental Economics and Management* 104 (November): 102376. doi:10.1016/j.jeem.2020.102376.

Huang, Yaoxian, Jonathan E. Hickman, and Shiliang Wu. 2018. "Impacts of Enhanced Fertilizer Applications on Tropospheric Ozone and Crop Damage over Sub-Saharan Africa." *Atmospheric Environment* 180 (May): 117–25. doi:10.1016/j.atmosenv.2018.02.040.

Huang, Yue, Alan Spray, and Tony Parry. 2013. "Sensitivity Analysis of Methodological Choices in Road Pavement LCA." *The International Journal of Life Cycle Assessment* 18 (1): 93–101. doi:10.1007/s11367-012-0450-7.

Industry Expert. 2013. "Carbon Fibers and Carbon Fiber Reinforced Plastics (CFRP): A Global Market Overview."

IPCC. 2007. "Climate Change 2007: The Physical Science Basis. Contribution of Working Group I to the Fourth Assessment Report of the Intergovernmental Panel on Climate Change [Solomon, S., D. Qin, M. Manning, Z. Chen, M. Marquis, K.B. Averyt, M. Tignor and H.L. Miller (Eds.)." https://www.ipcc.ch/site/assets/uploads/2018/05/ar4_wg1_full_report-1.pdf.

———. 2018. "Global Warming of 1.5°C. An IPCC Special Report on the Impacts of Global Warming of 1.5°C above Pre-Industrial Levels and Related Global Greenhouse Gas Emission Pathways, in the Context of Strengthening the Global Response to the Threat of Climate Change, Sustainable Development, and Efforts to Eradicate Poverty." https://www.ipcc.ch/sr15/download/.

ISO. 2016. "ISO 14040:2006 Environmental Management - Life Cycle Assessment - Principles and Framework." *ISO*. https://www.iso.org/cms/render/live/en/sites/isoorg/contents/data/standard/03/74/37456.html.

Iyer, R.K., and J.C. Kelly. 2021. “Update of the Carbon Fiber Pathway in GREET2021.” Argonne National Laboratory.

Jacob, Daniel J., and Darrell A. Winner. 2009. “Effect of Climate Change on Air Quality.” *Atmospheric Environment*, Atmospheric Environment - Fifty Years of Endeavour, 43 (1): 51–63. doi:10.1016/j.atmosenv.2008.09.051.

Janssen, Matty, Eva Gustafsson, Linda Echardt, Johan Wallinder, and Jens Wolf. 2019. “Life Cycle Assessment of Lignin-Based Carbon Fibres.” In . Dubrovnik, Croatia. https://research.chalmers.se/publication/512897/file/512897_Fulltext.pdf.

Kaufman, Andrew S., Paul J. Meier, Julie C. Sinistore, and Douglas J. Reinemann. 2010. “Applying Life-Cycle Assessment to Low Carbon Fuel Standards—How Allocation Choices Influence Carbon Intensity for Renewable Transportation Fuels.” *Energy Policy*, Special Section on Carbon Emissions and Carbon Management in Cities with Regular Papers, 38 (9): 5229–41. doi:10.1016/j.enpol.2010.05.008.

Keoleian, Gregory, Shelie Miller, Robert De Kleine, Andrew Fang, and Janet Mosley. 2012. “Life Cycle Material Data Update for GREET Model.” CSS12-12. Center for Sustainable Systems, University of Michigan.

Khan, S., and G. Soja. 2003. “Yield Responses of Wheat to Ozone Exposure as Modified by Drought-Induced Differences in Ozone Uptake.” *Water, Air, and Soil Pollution* 147 (1): 299–315. doi:10.1023/A:1024577429129.

Kim, Seungdo, and Bruce E. Dale. 2002. “Allocation Procedure in Ethanol Production System from Corn Grain i. System Expansion.” *The International Journal of Life Cycle Assessment* 7 (4): 237. doi:10.1007/BF02978879.

Kjellstrom, Tord, R. Sari Kovats, Simon J. Lloyd, Tom Holt, and Richard S. J. Tol. 2009. “The Direct Impact of Climate Change on Regional Labor Productivity.” *Archives of Environmental & Occupational Health* 64 (4). Routledge: 217–27. doi:10.1080/19338240903352776.

Koizumi, Tatsuji. 2015. “Biofuels and Food Security.” *Renewable and Sustainable Energy Reviews* 52 (December): 829–41. doi:10.1016/j.rser.2015.06.041.

Kolstad, Charles D., and Frances C. Moore. 2020. “Estimating the Economic Impacts of Climate Change Using Weather Observations.” *Review of Environmental Economics and Policy* 14 (1). The University of Chicago Press: 1–24. doi:10.1093/reep/rez024.

Kozarsky, Ross, Michael Holman, Aaron Wirshba, and Leon Hulli. 2011. “Carbon Fiber and Beyond: The $26 Billion World of Advanced Composites.” LRMI-R-11-3. Luxresearch.

Kukal, Meetpal S., and Suat Irmak. 2018. “U.S. Agro-Climate in 20 Th Century: Growing Degree Days, First and Last Frost, Growing Season Length, and Impacts on Crop Yields.” *Scientific Reports* 8 (1): 1–14. doi:10.1038/s41598-018-25212-2.

Lal, Shyam, Sethuraman Venkataramani, Manish Naja, Jagdish Chandra Kuniyal, Tuhin Kumar Mandal, Pradip Kumar Bhuyan, Kandikonda Maharaj Kumari, et al. 2017. “Loss of Crop Yields in India Due to Surface Ozone: An Estimation Based on a Network of Observations.” *Environmental Science and Pollution Research* 24 (26): 20972–81. doi:10.1007/s11356-017-9729-3.

Langholtz, Matthew, Mark Downing, Robin Graham, Fred Baker, Alicia Compere, William Griffith, Raymond Boeman, and Martin Keller. 2014. “Lignin-Derived Carbon Fiber as a Co-Product of Refining Cellulosic Biomass.” *SAE International Journal of Materials and Manufacturing* 7 (1): 115–21. doi:10.4271/2013-01-9092.

Lee, E. H., D. T. Tingey, and W. E. Hogsett. 1988. “Evaluation of Ozone Exposure Indices in Exposure-Response Modeling.” *Environmental Pollution (Barking, Essex: 1987)* 53 (1–4): 43–62. doi:10.1016/0269-7491(88)90024-3.

Levasseur, Annie, Pascal Lesage, Manuele Margni, Louise Deschênes, and Réjean Samson. 2010. “Considering Time in LCA: Dynamic LCA and Its Application to Global Warming Impact Assessments.” *Environmental Science & Technology* 44 (8). American Chemical Society: 3169–74. doi:10.1021/es9030003.

Li, Binquan, Wei Zhou, Yaoyang Zhao, Qin Ju, Zhongbo Yu, Zhongmin Liang, and Kumud Acharya. 2015. “Using the SPEI to Assess Recent Climate Change in the Yarlung Zangbo River Basin, South Tibet.” *Water* 7 (10): 5474–86. doi:10.3390/w7105474.

Li, Jiamin, Shinobu Inanaga, Zhaohu Li, and A. Egrinya Eneji. 2005. “Optimizing Irrigation Scheduling for Winter Wheat in the North China Plain.” *Agricultural Water Management* 76 (1): 8–23. doi:10.1016/j.agwat.2005.01.006.

Li, Qiang, Cheng Hu, Mengjie Li, Phuc Truong, Jinghao Li, Hao-Sheng Lin, Mandar T. Naik, et al. 2021. “Enhancing the Multi-Functional Properties of Renewable Lignin Carbon Fibers via Defining the Structure–Property Relationship Using Different Biomass Feedstocks.” *Green Chemistry* 23 (10). Royal Society of Chemistry: 3725–39. doi:10.1039/D0GC03828H.

Li, Qiang, Cheng Hu, Mengjie Li, Phuc Truong, Mandar T. Naik, Dwarkanath Prabhu, Leo Hoffmann, William L. Rooney, and Joshua S. Yuan. 2020. “Discovering Biomass Structural Determinants Defining the Properties of Plant-Derived Renewable Carbon Fiber.” *IScience* 23 (8): 101405. doi:10.1016/j.isci.2020.101405.

Li, Qiang, Mengjie Li, Hao-Sheng Lin, Cheng Hu, Phuc Truong, Tan Zhang, Hung-Jue Sue, Yunqiao Pu, Arthur J. Ragauskas, and Joshua S. Yuan. 2019. “Non-Solvent Fractionation of Lignin Enhances Carbon Fiber Performance.” *ChemSusChem* 12 (14): 3249–56. doi:https://doi.org/10.1002/cssc.201901052.

Li, Xiaolu, Yucai He, Libing Zhang, Zhangyang Xu, Haoxi Ben, Matthew J. Gaffrey, Yongfu Yang, et al. 2019. “Discovery of Potential Pathways for Biological Conversion of Poplar Wood into Lipids by Co-Fermentation of Rhodococci Strains.” *Biotechnology for Biofuels* 12 (1): 60. doi:10.1186/s13068-019-1395-x.

Li, Yating, William A. Pizer, and Libo Wu. 2019. “Climate Change and Residential Electricity Consumption in the Yangtze River Delta, China.” *Proceedings of the National Academy of Sciences* 116 (2). National Academy of Sciences: 472–77. doi:10.1073/pnas.1804667115.

Liu, Bing, Senthold Asseng, Christoph Müller, Frank Ewert, Joshua Elliott, David B. Lobell, Pierre Martre, et al. 2016. “Similar Estimates of Temperature Impacts on Global Wheat Yield by Three Independent Methods.” *Nature Climate Change* 6 (12). Nature Publishing Group: 1130–36. doi:10.1038/nclimate3115.

Liu, Xiang, and Ankur R. Desai. 2021. “Significant Reductions in Crop Yields from Air Pollution and Heat Stress in the United States.” *Earth’s Future* accepted manuscript: e2021EF002000. doi:10.1029/2021EF002000.

Liu, Zhi-Hua, Naijia Hao, Yun-Yan Wang, Chang Dou, Furong Lin, Rongchun Shen, Renata Bura, et al. 2021. “Transforming Biorefinery Designs with ‘Plug-In Processes of Lignin’ to Enable Economic Waste Valorization.” *Nature Communications* 12 (1): 3912. doi:10.1038/s41467-021-23920-4.

Liu, Zhi-Hua, Rosemary K. Le, Matyas Kosa, Bin Yang, Joshua Yuan, and Arthur J. Ragauskas. 2019. “Identifying and Creating Pathways to Improve Biological Lignin Valorization.” *Renewable and Sustainable Energy Reviews* 105 (May): 349–62. doi:10.1016/j.rser.2019.02.009.

Liu, Zhi-Hua, Somnath Shinde, Shangxian Xie, Naijia Hao, Furong Lin, Man Li, Chang Geun Yoo, Arthur J. Ragauskas, and Joshua S. Yuan. 2019. “Cooperative Valorization of Lignin and Residual Sugar to Polyhydroxyalkanoate (PHA) for Enhanced Yield and Carbon Utilization in Biorefineries.” *Sustainable Energy & Fuels* 3 (8). The Royal Society of Chemistry: 2024–37. doi:10.1039/C9SE00021F.

Lobell, David B., and Senthold Asseng. 2017. “Comparing Estimates of Climate Change Impacts from Process-Based and Statistical Crop Models.” *Environmental Research Letters* 12 (1): 015001. doi:10.1088/1748-9326/aa518a.

Lobell, David B, and Jennifer A Burney. 2021. “Cleaner Air Has Contributed One-Fifth of U.S. Maize and Soybean Yield Gains since 1999.” *Environmental Research Letters*. doi:10.1088/1748-9326/ac0fa4.

Lobell, David B., Wolfram Schlenker, and Justin Costa-Roberts. 2011. “Climate Trends and Global Crop Production Since 1980.” *Science* 333 (6042): 616–20. doi:10.1126/science.1204531.

Lucintel. 2012. “Growth Opportunities in the Global Carbon Fiber Market: 2013-2018.” Irving, Texas.

Luedeling, Eike. 2020. “Producing Hourly Temperature Records for Agroclimatic Analysis.” May. https://cran.r-project.org/web/packages/chillR/vignettes/hourly_temperatures.html.

Luo, Lin, Ester van der Voet, Gjalt Huppes, and Helias A. Udo de Haes. 2009. “Allocation Issues in LCA Methodology: A Case Study of Corn Stover-Based Fuel Ethanol.” *The International Journal of Life Cycle Assessment* 14 (6): 529–39. doi:10.1007/s11367-009-0112-6.

Lv, Zunfu, Xiaojun Liu, Weixing Cao, and Yan Zhu. 2013. “Climate Change Impacts on Regional Winter Wheat Production in Main Wheat Production Regions of China.” *Agricultural and Forest Meteorology* 171–172 (April): 234–48. doi:10.1016/j.agrformet.2012.12.008.

Ma, Fangrui, and Milford A Hanna. 1999. “Biodiesel Production: A Review1Journal Series #12109, Agricultural Research Division, Institute of Agriculture and Natural Resources, University of Nebraska–Lincoln.1.” *Bioresource Technology* 70 (1): 1–15. doi:10.1016/S0960-8524(99)00025-5.

Ma, Mingchen, Yang Gao, Yuhang Wang, Shaoqing Zhang, L. Ruby Leung, Cheng Liu, Shuxiao Wang, et al. 2019. “Substantial Ozone Enhancement over the North China Plain from Increased Biogenic Emissions Due to Heat Waves and Land Cover in Summer 2017.” *Atmospheric Chemistry and Physics* 19 (19). Copernicus GmbH: 12195–207. doi:10.5194/acp-19-12195-2019.

Mainka, Hendrik, Olaf Täger, Enrico Körner, Liane Hilfert, Sabine Busse, Frank T. Edelmann, and Axel S. Herrmann. 2015. “Lignin – an Alternative Precursor for Sustainable and Cost-Effective Automotive Carbon Fiber.” *Journal of Materials Research and Technology* 4 (3): 283–96. doi:10.1016/j.jmrt.2015.03.004.

Malça, João, and Fausto Freire. 2006. “Renewability and Life-Cycle Energy Efficiency of Bioethanol and Bio-Ethyl Tertiary Butyl Ether (BioETBE): Assessing the Implications of Allocation.” *Energy*, ECOS 2004 - 17th International Conference on Efficiency, Costs, Optimization, Simulation, and Environmental Impact of Energy on Process Systems, 31 (15): 3362–80. doi:10.1016/j.energy.2006.03.013.

Mauzerall, Denise L., and Xiaoping Wang. 2001. “PROTECTING AGRICULTURAL CROPS FROM THE EFFECTS OF TROPOSPHERIC OZONE EXPOSURE: Reconciling Science and Standard Setting in the United States, Europe, and Asia.” *Annual Review of Energy and the Environment* 26 (1): 237–68. doi:10.1146/annurev.energy.26.1.237.

McCarl, Bruce A. 2008. “Choices Article - Bioenergy in a Greenhouse Mitigating World” 23 (1): 31–33.

McCarl, Bruce A., and Uwe A. Schneider. 2001. “Greenhouse Gas Mitigation in U.S. Agriculture and Forestry.” *Science* 294 (5551): 2481–82. doi:10.1126/science.1064193.

McCarl, Bruce A., Xavier Villavicencio, and Ximing Wu. 2008. “Climate Change and Future Analysis: Is Stationarity Dying?” *American Journal of Agricultural Economics* 90 (5): 1241–47. doi:https://doi.org/10.1111/j.1467-8276.2008.01211.x.

McGrath, Justin M., Amy M. Betzelberger, Shaowen Wang, Eric Shook, Xin-Guang Zhu, Stephen P. Long, and Elizabeth A. Ainsworth. 2015. “An Analysis of Ozone Damage to Historical Maize and Soybean Yields in the United States.” *Proceedings of the National Academy of Sciences* 112 (46): 14390–95. doi:10.1073/pnas.1509777112.

McIntosh, Craig T., and Wolfram Schlenker. 2006. “Identifying Non-Linearities in Fixed Effects Models.” https://gps.ucsd.edu/_files/faculty/mcintosh/mcintosh_research_identifying.pdf.

Mérel, Pierre, and Matthew Gammans. 2021. “Climate Econometrics: Can the Panel Approach Account for Long-Run Adaptation?” *American Journal of Agricultural Economics* 103 (4): 1207–38. doi:10.1111/ajae.12200.

Miller, Noah, Jesse Tack, and Jason Bergtold. 2021. “The Impacts of Warming Temperatures on US Sorghum Yields and the Potential for Adaptation.” *American Journal of Agricultural Economics*. doi:10.1111/ajae.12223.

Mills, G., A. Buse, B. Gimeno, V. Bermejo, M. Holland, L. Emberson, and H. Pleijel. 2007. “A Synthesis of AOT40-Based Response Functions and Critical Levels of Ozone for Agricultural and Horticultural Crops.” *Atmospheric Environment* 41 (12): 2630–43. doi:10.1016/j.atmosenv.2006.11.016.

Mills, Gina, Katrina Sharps, David Simpson, Håkan Pleijel, Malin Broberg, Johan Uddling, Fernando Jaramillo, et al. 2018. "Ozone Pollution Will Compromise Efforts to Increase Global Wheat Production." *Global Change Biology* 24 (8): 3560–74. doi:10.1111/gcb.14157.

Mills, Gina, Katrina Sharps, David Simpson, Håkan Pleijel, Michael Frei, Kent Burkey, Lisa Emberson, et al. 2018. "Closing the Global Ozone Yield Gap: Quantification and Cobenefits for Multistress Tolerance." *Global Change Biology* 24 (10): 4869–93. doi:10.1111/gcb.14381.

Mordor Intelligence. 2021. "Carbon Fiber Market - Growth, Trends, COVID-19 Impacts, and Forecasts (2021-2026)." Mordor Intelligence. https://www.researchandmarkets.com/reports/4536316/carbon-fiber-market-growth-trends-covid-19.

Muñoz, Ivan, Karin Flury, Niels Jungbluth, Giles Rigarlsford, Llorenç Milà i Canals, and Henry King. 2014. "Life Cycle Assessment of Bio-Based Ethanol Produced from Different Agricultural Feedstocks." *The International Journal of Life Cycle Assessment* 19 (1): 109–19. doi:10.1007/s11367-013-0613-1.

Nanda, Sonil, Ramin Azargohar, Ajay K. Dalai, and Janusz A. Kozinski. 2015. "An Assessment on the Sustainability of Lignocellulosic Biomass for Biorefining." *Renewable and Sustainable Energy Reviews* 50 (October): 925–41. doi:10.1016/j.rser.2015.05.058.

Narciso, G., P. Ragni, and A. Venturi. 1992. *Agrometeorological Aspects of Crops in Italy, Spain and Greece: A Summary Review for Common and Durum Wheat, Barley, Maize, Rice, Sugar Beet, Sunflower, Soya Bean, Rape, Potato, Tobacco, Cotton, Olive and Grape Crops*. Commission of the European Communities.

NASA. 2019. "M2T3NVASM: MERRA-2 Tavg3_3d_asm_Nv: 3d,3-Hourly,Time-Averaged,Model-Level,Assimilation,Assimilated Meteorological Fields V5.12.4." https://disc.gsfc.nasa.gov/datasets/M2T3NVASM_5.12.4/summary?keywords=tavg3_3d_asm_Nv%20(M2T3NVASM).

Naskar, A., and D. Warren. 2012. "Lower Cost Carbon Fiber Precursor." Oak Ridge, TN, USA, May.

National Bureau of Statistics. 2019. "The announcement of crop production data in 2019." December. http://www.stats.gov.cn/tjsj/zxfb/201912/t20191206_1715827.html.

Newcomb, Bradley A. 2016. "Processing, Structure, and Properties of Carbon Fibers." *Composites Part A: Applied Science and Manufacturing* 91 (December): 262–82. doi:10.1016/j.compositesa.2016.10.018.

Newell, Richard G., Brian C. Prest, and Steven E. Sexton. 2021. "The GDP-Temperature Relationship: Implications for Climate Change Damages." *Journal of Environmental Economics and Management* 108 (July): 102445. doi:10.1016/j.jeem.2021.102445.

Nichol, A. J. 1931. "Measures of Average Elasticity of Demand." *Journal of Political Economy* 39 (2). The University of Chicago Press: 249–55. doi:10.1086/254200.

NOAA. 2019. "FTP Sites for Climate Data." ftp://ftp.ncdc.noaa.gov/pub/data/cirs/climdiv/.

Nunna, Srinivas, Patrick Blanchard, Derek Buckmaster, Sam Davis, and Minoo Naebe. 2019. "Development of a Cost Model for the Production of Carbon Fibres." *Heliyon* 5 (10). doi:10.1016/j.heliyon.2019.e02698.

Obnamia, Jon Albert, Goretty M. Dias, Heather L. MacLean, and Bradley A. Saville. 2019. "Comparison of U.S. Midwest Corn Stover Ethanol Greenhouse Gas Emissions from GREET and GHGenius." *Applied Energy* 235 (February): 591–601. doi:10.1016/j.apenergy.2018.10.091.

Onishi, Moriyuki. 2012. "Toray's Business Strategy for Carbon Fiber Composite Materials."

Oyinbo, Oyakhilomen, Jordan Chamberlin, Tahirou Abdoulaye, and Miet Maertens. 2021. "Digital Extension, Price Risk, and Farm Performance: Experimental Evidence from Nigeria." *American Journal of Agricultural Economics* in press. doi:10.1111/ajae.12242.

Pegallapati, Ambica K., and Edward D. Frank. 2016. "Energy Use and Greenhouse Gas Emissions from an Algae Fractionation Process for Producing Renewable Diesel." *Algal Research* 18 (September): 235–40. doi:10.1016/j.algal.2016.06.019.

Philippini, Rafael Rodrigues, Sabrina Evelin Martiniano, Avinash P. Ingle, Paulo Ricardo Franco Marcelino, Gilda Mariano Silva, Fernanda Gonçalves Barbosa, Júlio César dos Santos, and Silvio Silvério da Silva. 2020. "Agroindustrial Byproducts for the Generation of Biobased Products: Alternatives for Sustainable Biorefineries." *Frontiers in Energy Research* 8. Frontiers. doi:10.3389/fenrg.2020.00152.

Pleijel, H., H. Danielsson, L. Emberson, M. R. Ashmore, and G. Mills. 2007. "Ozone Risk Assessment for Agricultural Crops in Europe: Further Development of Stomatal Flux and Flux–Response Relationships for European Wheat and Potato." *Atmospheric Environment* 41 (14): 3022–40. doi:10.1016/j.atmosenv.2006.12.002.

Porter, John R, and Megan Gawith. 1999. "Temperatures and the Growth and Development of Wheat: A Review." *European Journal of Agronomy* 10 (1): 23–36. doi:10.1016/S1161-0301(98)00047-1.

Pu, X., T. J. Wang, X. Huang, D. Melas, P. Zanis, D. K. Papanastasiou, and A. Poupkou. 2017. "Enhanced Surface Ozone during the Heat Wave of 2013 in Yangtze River Delta Region, China." *Science of The Total Environment* 603–604 (December): 807–16. doi:10.1016/j.scitotenv.2017.03.056.

Red, C., and P. Zimm. 2012. "2012 Global Market for Carbon Fiber Composites: Maintaining Competitiveness in the Evolving Materials Market." In . La Jolla, CA.

Riahi, Keywan, Detlef P. van Vuuren, Elmar Kriegler, Jae Edmonds, Brian C. O'Neill, Shinichiro Fujimori, Nico Bauer, et al. 2017. "The Shared Socioeconomic Pathways and Their Energy, Land Use, and Greenhouse Gas Emissions Implications: An Overview." *Global Environmental Change* 42 (January): 153–68. doi:10.1016/j.gloenvcha.2016.05.009.

Rosenzweig, Cynthia, Joshua Elliott, Delphine Deryng, Alex C. Ruane, Christoph Müller, Almut Arneth, Kenneth J. Boote, et al. 2014. "Assessing Agricultural Risks of Climate Change in the 21st Century in a Global Gridded Crop Model Intercomparison." *Proceedings of the National Academy of Sciences* 111 (9). National Academy of Sciences: 3268–73. doi:10.1073/pnas.1222463110.

Roy, Ashmita. 2018. “Carbon Fiber Market 2021.” Allied Market Research. https://www.alliedmarketresearch.com/carbon-fiber-market.

Ryerson, T. B., M. Trainer, J. S. Holloway, D. D. Parrish, L. G. Huey, D. T. Sueper, G. J. Frost, et al. 2001. “Observations of Ozone Formation in Power Plant Plumes and Implications for Ozone Control Strategies.” *Science* 292 (5517). American Association for the Advancement of Science: 719–23. doi:10.1126/science.1058113.

Sarofim, Marcus C., Stephanie T. Waldhoff, and Susan C. Anenberg. 2017. “Valuing the Ozone-Related Health Benefits of Methane Emission Controls.” *Environmental and Resource Economics* 66 (1): 45–63. doi:10.1007/s10640-015-9937-6.

Schauberger, Bernhard, Sotirios Archontoulis, Almut Arneth, Juraj Balkovic, Philippe Ciais, Delphine Deryng, Joshua Elliott, et al. 2017. “Consistent Negative Response of US Crops to High Temperatures in Observations and Crop Models.” *Nature Communications* 8 (January): 13931. doi:10.1038/ncomms13931.

Schlenker, Wolfram, W. Michael Hanemann, and Anthony C. Fisher. 2005. “Will U.S. Agriculture Really Benefit from Global Warming? Accounting for Irrigation in the Hedonic Approach.” *The American Economic Review* 95 (1): 395–406.

Schlenker, Wolfram, and Michael J. Roberts. 2009. “Nonlinear Temperature Effects Indicate Severe Damages to U.S. Crop Yields under Climate Change.” *Proceedings of the National Academy of Sciences* 106 (37): 15594–98. doi:10.1073/pnas.0906865106.

Šebela, David, Blake Bergkamp, Impa M. Somayanda, Allan K. Fritz, and S. V. Krishna Jagadish. 2020. “Impact of Post-Flowering Heat Stress in Winter Wheat Tracked through Optical Signals.” *Agronomy Journal* 112 (5): 3993–4006. doi:10.1002/agj2.20360.

Shama, Rao N., T.G.A. Simha, K.P. Rao, and Kumar G.V.V. Ravi. 2018. “Carbon Composites Are Becoming Competitive and Cost Effective.”

Sicard, Pierre, Alessandro Anav, Alessandra De Marco, and Elena Paoletti. 2017. “Projected Global Ground-Level Ozone Impacts on Vegetation under Different Emission and Climate Scenarios.” *Atmospheric Chemistry and Physics* 17 (19): 12177–96. doi:https://doi.org/10.5194/acp-17-12177-2017.

Singh Gill, Amaninder, Darian Visotsky, Laine Mears, and Joshua D. Summers. 2017. “Cost Estimation Model for Polyacrylonitrile-Based Carbon Fiber Manufacturing Process.” *Journal of Manufacturing Science and Engineering* 139 (4). doi:10.1115/1.4034713.

Slafer, Gustavo A., and H. M. Rawson. 1995. “Photoperiod × Temperature Interactions in Contrasting Wheat Genotypes: Time to Heading and Final Leaf Number.” *Field Crops Research* 44 (2): 73–83. doi:10.1016/0378-4290(95)00077-1.

Souto, Felipe, Veronica Calado, and Nei Pereira. 2018. “Lignin-Based Carbon Fiber: A Current Overview.” *Materials Research Express* 5 (7): 072001. doi:10.1088/2053-1591/aaba00.

SPEI. 2019. “The Global SPEI Database.” https://spei.csic.es/database.html.

Stenzel, Fabian, Peter Greve, Wolfgang Lucht, Sylvia Tramberend, Yoshihide Wada, and Dieter Gerten. 2021. “Irrigation of Biomass Plantations May Globally Increase Water Stress More than Climate Change.” *Nature Communications* 12 (1). Nature Publishing Group: 1512. doi:10.1038/s41467-021-21640-3.

Stern, Nicholas. 2007. *The Economics of Climate Change: The Stern Review*. Cambridge: Cambridge University Press. doi:10.1017/CBO9780511817434.

Sullivan, Rogelio A. 2006. “Automotive Carbon Fiber: Opportunities and Challenges.” *JOM* 58 (11): 77–79. doi:10.1007/s11837-006-0233-3.

Suzuki, Tetsuya, and Jun Takahashi. 2005. “Prediction of Energy Intensity of Carbon Fiber Reinforced Plastics for Mass-Produced Passenger Cars.” In . http://j-t.o.oo7.jp/publications/051129/S1-02.pdf.

Svanes, Erik, Mie Vold, and Ole Jørgen Hanssen. 2011. “Effect of Different Allocation Methods on LCA Results of Products from Wild-Caught Fish and on the Use of Such Results.” *The International Journal of Life Cycle Assessment* 16 (6): 512–21. doi:10.1007/s11367-011-0288-4.

Tack, Jesse, Andrew Barkley, and Nathan Hendricks. 2017. “Irrigation Offsets Wheat Yield Reductions from Warming Temperatures.” *Environmental Research Letters* 12 (11). IOP Publishing: 114027. doi:10.1088/1748-9326/aa8d27.

Tack, Jesse, Andrew Barkley, and Lawton Lanier Nalley. 2015. “Effect of Warming Temperatures on US Wheat Yields.” *Proceedings of the National Academy of Sciences* 112 (22): 6931–36. doi:10.1073/pnas.1415181112.

Tai, Amos P. K., Maria Val Martin, and Colette L. Heald. 2014. “Threat to Future Global Food Security from Climate Change and Ozone Air Pollution.” *Nature Climate Change* 4 (9): 817–21. doi:10.1038/nclimate2317.

Tai, Amos P. K., and Maria Val Martin. 2017. “Impacts of Ozone Air Pollution and Temperature Extremes on Crop Yields: Spatial Variability, Adaptation and Implications for Future Food Security.” *Atmospheric Environment* 169 (November): 11–21. doi:10.1016/j.atmosenv.2017.09.002.

Tan, Kaiyan, Guangsheng Zhou, Xiaomin Lv, Jianping Guo, and Sanxue Ren. 2018. “Combined Effects of Elevated Temperature and CO 2 Enhance Threat from Low Temperature Hazard to Winter Wheat Growth in North China.” *Scientific Reports* 8 (1). Nature Publishing Group: 4336. doi:10.1038/s41598-018-22559-4.

Taylor, R. 2000. “4.13 - Carbon Matrix Composites.” In *Comprehensive Composite Materials*, edited by Anthony Kelly and Carl Zweben, 387–426. Oxford: Pergamon. doi:10.1016/B0-08-042993-9/00100-5.

Trinh, Trong Anh. 2018. “The Impact of Climate Change on Agriculture: Findings from Households in Vietnam.” *Environmental and Resource Economics* 71 (4): 897–921. doi:10.1007/s10640-017-0189-5.

US EPA. 1996. “Air Quality Criteria for Ozone and Related Photochemical Oxidants Volume I of III (Final Report, 1996).” EPA/600/AP-93/004aF (NTIS PB94173127). https://cfpub.epa.gov/ncea/isa/recordisplay.cfm?deid=44375.

———. 2015. “Ground-Level Ozone Basics.” Overviews and Factsheets. *US EPA*. May 29. https://www.epa.gov/ground-level-ozone-pollution/ground-level-ozone-basics.

———. 2016. “Understanding Global Warming Potentials.” January 12. https://www.epa.gov/ghgemissions/understanding-global-warming-potentials.

———. 2019. “Pre-Generated Data Files from USEPA.” https://aqs.epa.gov/aqsweb/airdata/download_files.html.

———. 2020. “Air Quality - National Summary.” Data and Tools. *US EPA*. April. https://www.epa.gov/air-trends/air-quality-national-summary.

USDA NASS. 2010. “Field Crops Usual Planting and Harvesting Dates.” *Usual Planting and Harvesting Dates for U.S. Field Crops*. https://usda.library.cornell.edu/concern/publications/vm40xr56k?locale=en.

———. 2019. “Quick Stats.” https://quickstats.nass.usda.gov/.

———. 2020. “Crop Values 2019 Summary.” February. https://www.nass.usda.gov/Publications/Todays_Reports/reports/cpvl0220.pdf.

———. 2021. “Crop Production (October 2021).” ISSN: 1936-3737. https://downloads.usda.library.cornell.edu/usda-esmis/files/tm70mv177/qf85pc34p/vh53xv71m/crop1021.pdf.

USGCRP. 2018. “Fourth National Climate Assessment.” https://nca2018.globalchange.gov.

Verschuur, Jasper, Sihan Li, Piotr Wolski, and Friederike E. L. Otto. 2021. “Climate Change as a Driver of Food Insecurity in the 2007 Lesotho-South Africa Drought.” *Scientific Reports* 11 (1): 3852. doi:10.1038/s41598-021-83375-x.

Vicente-Serrano, Sergio M., Santiago Beguería, and Juan I. López-Moreno. 2010. “A Multiscalar Drought Index Sensitive to Global Warming: The Standardized Precipitation Evapotranspiration Index.” *Journal of Climate* 23 (7): 1696–1718. doi:10.1175/2009JCLI2909.1.

Wang, Michael, Amgad Elgowainy, Uisung Lee, Adarsh Bafana, Sudhanya Banerjee, and et al. 2021. “Summary of Expansiions and Updates in GREET2021.” ANL/ESD-21/16. Argonne National Laboratory. https://greet.es.anl.gov/files/greet-2021-summary.

Wang, Michael, Jeongwoo Han, Jennifer B. Dunn, Hao Cai, and Amgad Elgowainy. 2012. “Well-to-Wheels Energy Use and Greenhouse Gas Emissions of Ethanol from Corn, Sugarcane and Cellulosic Biomass for US Use.” *Environmental Research Letters* 7 (4). IOP Publishing: 045905. doi:10.1088/1748-9326/7/4/045905.

Wang, Zhichao, Jennifer B. Dunn, Jeongwoo Han, and Michael Q. Wang. 2013. “Material and Energy Flows in the Production of Cellulosic Feedstocks for Biofuels for the GREET Model.” ANL/ESD-13/9. Argonne National Laboratory. https://greet.es.anl.gov/files/feedstocks-13.

Wardenaar, Tjerk, Theo van Ruijven, Angelica Mendoza Beltran, Kathrine Vad, Jeroen Guinée, and Reinout Heijungs. 2012. “Differences between LCA for Analysis and LCA for Policy: A Case Study on the Consequences of Allocation Choices in Bio-Energy Policies.” *The International Journal of Life Cycle Assessment* 17 (8): 1059–67. doi:10.1007/s11367-012-0431-x.

West, J. Jason, Steven J. Smith, Raquel A. Silva, Vaishali Naik, Yuqiang Zhang, Zachariah Adelman, Meridith M. Fry, Susan Anenberg, Larry W. Horowitz, and Jean-Francois Lamarque. 2013. “Co-Benefits of Mitigating Global Greenhouse Gas Emissions for Future

Air Quality and Human Health." *Nature Climate Change* 3 (10): 885–89. doi:10.1038/nclimate2009.

Wilcox, Julia, and David Makowski. 2014. "A Meta-Analysis of the Predicted Effects of Climate Change on Wheat Yields Using Simulation Studies." *Field Crops Research* 156 (February): 180–90. doi:10.1016/j.fcr.2013.11.008.

Wing, Ian Sue, Enrica De Cian, and Malcolm N. Mistry. 2021. "Global Vulnerability of Crop Yields to Climate Change." *Journal of Environmental Economics and Management* 109 (September): 102462. doi:10.1016/j.jeem.2021.102462.

Witten, Elmar, T Kraus, and Michael Kühnel. 2015. "Composites Market Report 2015." *Market Developments, Trends, Outlook and Challenges*.

Witten, Elmar, Volker Mathes, Michael Sauer, and Michael Kuhnel. 2018. "Composites Market Report 2018." AVK Industrievereinigung Verstärkte Kunststoffe.

Woertz, Ian C., John R. Benemann, Niu Du, Stefan Unnasch, Dominick Mendola, B. Greg Mitchell, and Tryg J. Lundquist. 2014. "Life Cycle GHG Emissions from Microalgal Biodiesel – A CA-GREET Model." *Environmental Science & Technology* 48 (11). American Chemical Society: 6060–68. doi:10.1021/es403768q.

Wong, Eugene Yin Cheung, Danny Chi Kuen Ho, Stuart So, Chi-Wing Tsang, and Eve Man Hin Chan. 2021. "Life Cycle Assessment of Electric Vehicles and Hydrogen Fuel Cell Vehicles Using the GREET Model—A Comparative Study." *Sustainability* 13 (9). Multidisciplinary Digital Publishing Institute: 4872. doi:10.3390/su13094872.

Wooldridge. 2013. *Introductory Econometrics: A Modern Approach. 5th Ed*. 5th ed. Mason, OH: South-Western Cengage Learning.

Wooldridge, Jeffrey M. 2010. *Econometric Analysis of Cross Section and Panel Data*. Second Edition. Cambridge, Massachusetts: The MIT Press.

Xiao, Liujun, Leilei Liu, Senthold Asseng, Yuming Xia, Liang Tang, Bing Liu, Weixing Cao, and Yan Zhu. 2018. "Estimating Spring Frost and Its Impact on Yield across Winter Wheat in China." *Agricultural and Forest Meteorology* 260–261 (October): 154–64. doi:10.1016/j.agrformet.2018.06.006.

Xie, Lunyu, Sarah M. Lewis, Maximilian Auffhammer, and Peter Berck. 2019. "Heat in the Heartland: Crop Yield and Coverage Response to Climate Change Along the Mississippi River." *Environmental and Resource Economics* 73 (2): 485–513. doi:10.1007/s10640-018-0271-7.

Xie, Shangxian, Qiang Li, Pravat Karki, Fujie Zhou, and Joshua S. Yuan. 2017. "Lignin as Renewable and Superior Asphalt Binder Modifier." *ACS Sustainable Chemistry & Engineering* 5 (4). American Chemical Society: 2817–23. doi:10.1021/acssuschemeng.6b03064.

Xie, Shangxian, Su Sun, Furong Lin, Muzi Li, Yunqiao Pu, Yanbing Cheng, Bing Xu, et al. 2019. "Mechanism-Guided Design of Highly Efficient Protein Secretion and Lipid Conversion for Biomanufacturing and Biorefining." *Advanced Science* 6 (13): 1801980. doi:10.1002/advs.201801980.

Xiong, Wei, Ian P. Holman, Liangzhi You, Jie Yang, and Wenbin Wu. 2014. “Impacts of Observed Growing-Season Warming Trends since 1980 on Crop Yields in China.” *Regional Environmental Change* 14 (1): 7–16. doi:10.1007/s10113-013-0418-6.

Xu, Chonggang, Nate G. McDowell, Rosie A. Fisher, Liang Wei, Sanna Sevanto, Bradley O. Christoffersen, Ensheng Weng, and Richard S. Middleton. 2019. “Increasing Impacts of Extreme Droughts on Vegetation Productivity under Climate Change.” *Nature Climate Change* 9 (12): 948–53. doi:10.1038/s41558-019-0630-6.

Xu, Yangyang, Xiaokang Wu, Rajesh Kumar, Mary Barth, Chenrui Diao, Meng Gao, Lei Lin, Bryan Jones, and Gerald A. Meehl. 2020. “Substantial Increase in the Joint Occurrence and Human Exposure of Heatwave and High-PM Hazards Over South Asia in the Mid-21st Century.” *AGU Advances* 1 (2): e2019AV000103. doi:10.1029/2019AV000103.

Yang, Xiaoguang, Fu Chen, Xiaomao Lin, Zhijuan Liu, Hailin Zhang, Jin Zhao, Kenan Li, et al. 2015. “Potential Benefits of Climate Change for Crop Productivity in China.” *Agricultural and Forest Meteorology* 208 (August): 76–84. doi:10.1016/j.agrformet.2015.04.024.

Yao, Junqiang, Dilinuer Tuoliewubieke, Jing Chen, Wen Huo, and Wenfeng Hu. 2019. “Identification of Drought Events and Correlations with Large-Scale Ocean–Atmospheric Patterns of Variability: A Case Study in Xinjiang, China.” *Atmosphere* 10 (2): 94. doi:10.3390/atmos10020094.

Yi, Fujin, Jia-ao Feng, Yan-jun Wang, and Fei Jiang. 2020. “Influence of Surface Ozone on Crop Yield of Maize in China.” *Journal of Integrative Agriculture* 19 (2): 578–89. doi:10.1016/S2095-3119(19)62822-4.

Yi, Fujin, Fei Jiang, Funing Zhong, Xun Zhou, and Aijun Ding. 2016. “The Impacts of Surface Ozone Pollution on Winter Wheat Productivity in China – An Econometric Approach.” *Environmental Pollution* 208 (January): 326–35. doi:10.1016/j.envpol.2015.09.052.

Yusof, N., and A. F. Ismail. 2012. “Post Spinning and Pyrolysis Processes of Polyacrylonitrile (PAN)-Based Carbon Fiber and Activated Carbon Fiber: A Review.” *Journal of Analytical and Applied Pyrolysis* 93 (January): 1–13. doi:10.1016/j.jaap.2011.10.001.

Zampieri, M., A. Ceglar, F. Dentener, and A. Toreti. 2017. “Wheat Yield Loss Attributable to Heat Waves, Drought and Water Excess at the Global, National and Subnational Scales.” *Environmental Research Letters* 12 (6). IOP Publishing: 064008. doi:10.1088/1748-9326/aa723b.

Zarei, Abdol Rassoul, and Mohammad Mehdi Moghimi. 2019. “Modified Version for SPEI to Evaluate and Modeling the Agricultural Drought Severity.” *International Journal of Biometeorology* 63 (7): 911–25. doi:10.1007/s00484-019-01704-2.

Zhang, Hao, Yabin Da, Xian Zhang, and Jing-Li Fan. 2021. “The Impacts of Climate Change on Coal-Fired Power Plants: Evidence from China.” *Energy & Environmental Science*. Royal Society of Chemistry. doi:10.1039/D1EE01475G.

Zhang, Junxi, Yang Gao, Kun Luo, L. Ruby Leung, Yang Zhang, Kai Wang, and Jianren Fan. 2018. “Impacts of Compound Extreme Weather Events on Ozone in the Present and Future.” *Atmospheric Chemistry and Physics (Online)* 18 (13). European Geosciences Union. doi:10.5194/ACP-18-9861-2018.

Zhang, Liqiang, Weiwei Liu, Kun Hou, Jintai Lin, Chenghu Zhou, Xiaohua Tong, Ziye Wang, et al. 2019. "Air Pollution-Induced Missed Abortion Risk for Pregnancies." *Nature Sustainability* 2 (11): 1011–17. doi:10.1038/s41893-019-0387-y.

Zhang, Peng, Junjie Zhang, and Minpeng Chen. 2017. "Economic Impacts of Climate Change on Agriculture: The Importance of Additional Climatic Variables Other than Temperature and Precipitation." *Journal of Environmental Economics and Management* 83 (May): 8–31. doi:10.1016/j.jeem.2016.12.001.

Zhang, Tianyi, and Yao Huang. 2013. "Estimating the Impacts of Warming Trends on Wheat and Maize in China from 1980 to 2008 Based on County Level Data." *International Journal of Climatology* 33 (3): 699–708. doi:10.1002/joc.3463.

Zhao, Guangcai. 2010. "Study on Chinese Wheat Planting Regionalization (part one)." *Journal of Triticeae Crops* 30 (5): 886–95.

Zhao, Lili, Xunmin Ou, and Shiyan Chang. 2016. "Life-Cycle Greenhouse Gas Emission and Energy Use of Bioethanol Produced from Corn Stover in China: Current Perspectives and Future Prospectives." *Energy* 115 (November): 303–13. doi:10.1016/j.energy.2016.08.046.

Zhao, Zhi-Min, Zhi-Hua Liu, Yunqiao Joseph Pu, Xianzhi Meng, Jifei Xu, Joshua S. Yuan, and Arthur J. Ragauskas. 2020. "Emerging Strategies for Modifying Lignin Chemistry to Enhance Biological Lignin Valorization." *ChemSusChem* 13 (20). ChemPubSoc Europe. doi:10.1002/cssc.202001401.

Zhou, Haoran, Ming Xu, Ruixing Hou, Yunpu Zheng, Yonggang Chi, and Zhu Ouyang. 2018. "Thermal Acclimation of Photosynthesis to Experimental Warming Is Season-Dependent for Winter Wheat (Triticum Aestivum L.)." *Environmental and Experimental Botany* 150 (June): 249–59. doi:10.1016/j.envexpbot.2018.04.001.

Zilberman, David, Gal Hochman, Deepak Rajagopal, Steve Sexton, and Govinda Timilsina. 2013. "The Impact of Biofuels on Commodity Food Prices: Assessment of Findings." *American Journal of Agricultural Economics* 95 (2): 275–81. doi:10.1093/ajae/aas037.

APPENDIX A

EFFECTS OF SURFACE OZONE AND CLIMATE ON HISTORICAL (1980-2015) CROP YIELDS IN THE UNITED STATES: IMPLICATION FOR MID-21ST CENTURY PROJECTION

Addressing multi-collinearity issues [60]

Given we included a list of climatic variables (i.e., FDD, GDD, Tmax, SPEI) in our model, multi-collinearity issues could be potential threats to the estimation. To address these concerns, we calculated the variance inflation factor (VIF) for major crops (i.e., corn, soybeans, winter wheat, and spring wheat). VIF essentially measures how much of the variation in a variable could be explained by other variables (Wooldridge 2013). It is calculated as follows.

(A1) $$\mathrm{VIF}_j = 1/(1-R_j^2)$$

Where j stands for the variable (i.e., GDD), R_j^2 is the R^2 in the regression of variable j on other variables (i.e., FDD, Tmax, SPEI). If VIF_j is greater than 10 (this means over 90% of the variable's variation could be explained by other variables), then we say multi-collinearity is a "problem" for estimating the coefficient of that variable.

However, it should be noted that the choice of the cutoff is relatively arbitrary, as also discussed in (Wooldridge 2013). If the variable is conceived as a key determinant of the outcome, it should always be included in the model regardless of its VIF. More importantly, in theory, multi-collinearity should not be a major problem to the estimation unless variables are *perfectly* correlated (i.e., one independent variable is a perfect linear combination of some other independent variables), which is unlikely to encounter in practice.

[60] We thank one of the reviewers' comments on this issue.

We report VIFs for FDD, GDD, Tmax, and SPEI in Table A4 in this Appendix. VIFs for precipitation, FDD, and SPEI are well below 10. VIFs for GDD and Tmax are higher but mostly remain below the cutoff, except for the GDD of soybean which has a VIF of 11.3. Nevertheless, we do not feel that VIF with such a margin would be a major threat to our estimation.

Addressing the potential endogeneity of ozone[61]

In the main text, we argue that the endogeneity of ozone may not be a great concern in our yield regressions because yields are largely determined by weather conditions and farm management practices. To further verify this hypothesis, we performed two sets of robustness checks. We call the first a "socioeconomic test" following the argument that there may exist socioeconomic factors that could affect ozone and food supply simultaneously. One of such candidates is electricity consumption. On one hand, power consumption is an indicator of economic activities and population which either directly or indirectly affect food supplies; on the other hand, power generation is an important source of ozone precursors (Ryerson et al. 2001; US EPA 2015), and power plants are normally adjacent to regions with high power demand (EIA 2020a).

We thus introduced a suite of county-level power consumption data[62] (i.e., total consumption and sectoral consumption data, i.e., residential, commercial, and industrial sectors) to our model one at a time. The results are presented in Table A20-A23 in this Appendix. The estimation of ozone variables remains unchanged and power consumptions tend to play a minor role on yields (i.e., 1% increase in total power consumption increases corn yield by 0.1%).

We also performed a "physical test" with respect to the agricultural inputs. Specifically, fertilizer applications (i.e., nitrogen) could impact yield development as well as ozone formation

[61] We thank one of the reviewers' comments on this issue.

[62] Only state-level data (1990-2020) were available in EIA. We interpolated the data to county level based on county-level populations. The population data were obtained from the United States Census Bureau (https://data.census.gov/cedsci/).

(Huang, Hickman, and Wu 2018), thus bias may occur if fertilizer data are omitted in the estimation. To test this hypothesis, we introduced fertilizer application data[63] in our model and again the estimations on ozone variables barely changed. This finding is consistent with experiments conducted in sub-Saharan Africa, where the authors concluded that the impacts of ozone exposure induced by enhanced fertilizer applications are minimal (Huang, Hickman, and Wu 2018).

Climate change driven AOT40 projections

As noted in the main text, ozone projections do not directly come from the global climate model, instead, they are obtained via two steps. We first ran a panel data regression of AOT40 on the climate-relevant variables (FDD, GDD, Prec, and Tmax) based on historical county-level data in the United States. The model takes the form below.

$$\log(AOT40_{it}) = \rho_1 FDD_{it} + \rho_2 GDD_{it} + \rho_3 Prec_{it} + \rho_4 Tmax_{it} + \alpha_i + \delta_t + \varepsilon_{it} \quad \text{(A2)}$$

Where i and t indicates county and year. α_i refers to county-fixed effects, and δ_t denotes the year-fixed effect which captures yearly shocks. The underlying assumption is that ozone concentrations in a county would have changed similarly to another county if they have experienced a similar change in climate, after controlling for the county fixed effect and national-level yearly shocks. The regression results are provided in Table A24 in this Appendix. Overall, Tmax has the most significant effects on AOT40, because both Tmax and AOT40 are measured over the ozone sensitive period, while the other climate variables are calculated during the growing season.

[63] Fertilizer application data are limited in USDA NASS. The data used here are state-level fertilizer expenses measured in dollars. We interpolated the data to county level based on county-level acres of croplands which were obtained from USDA's census data in 2012.

We then combined equation (A1) with projections from the global climate model to obtain ozone projections driven by climate change only (Deschênes and Greenstone 2011; Li, Pizer, and Wu 2019).

$$
\begin{aligned}
AOT40_i^{ptg} &= \frac{\Delta AOT40_i}{AOT40_i} = \frac{AOT40_i'}{AOT40_i} - 1 \\
&= \frac{\exp(\hat{\rho}_1 FDD_i' + \hat{\rho}_2 GDD_i' + \hat{\rho}_3 Prec_i' + \hat{\rho}_4 Tmax_i')}{\exp(\hat{\rho}_1 FDD_i + \hat{\rho}_2 GDD_i + \hat{\rho}_3 Prec_i + \hat{\rho}_4 Tmax_i)} - 1 \\
&= \exp(\hat{\rho}_1 \Delta FDD_i + \hat{\rho}_2 \Delta GDD_i + \hat{\rho}_3 \Delta Prec_i + \hat{\rho}_4 \Delta Tmax_i) - 1
\end{aligned}
\tag{A3}
$$

Where $AOT40_i^{ptg}$ refers to the percentage change of AOT40 in the middle of the century (2048-2052), relative to 2015-2019. Δ denotes the changes in the respective variables. Variables with a prime indicate levels in the middle of the century. $\hat{\rho}_1$ to $\hat{\rho}_4$ represent the estimated coefficients in equation (A1). The change of AOT40 in the middle of the century can be easily obtained by multiplying the percentage change $AOT40_i^{ptg}$ by the levels of AOT40 in 2015-2019.

Note that the whole process of calculation was conducted separately for spring crops and winter wheat because they have different growing seasons and ozone-sensitive periods.

Supplementary figures

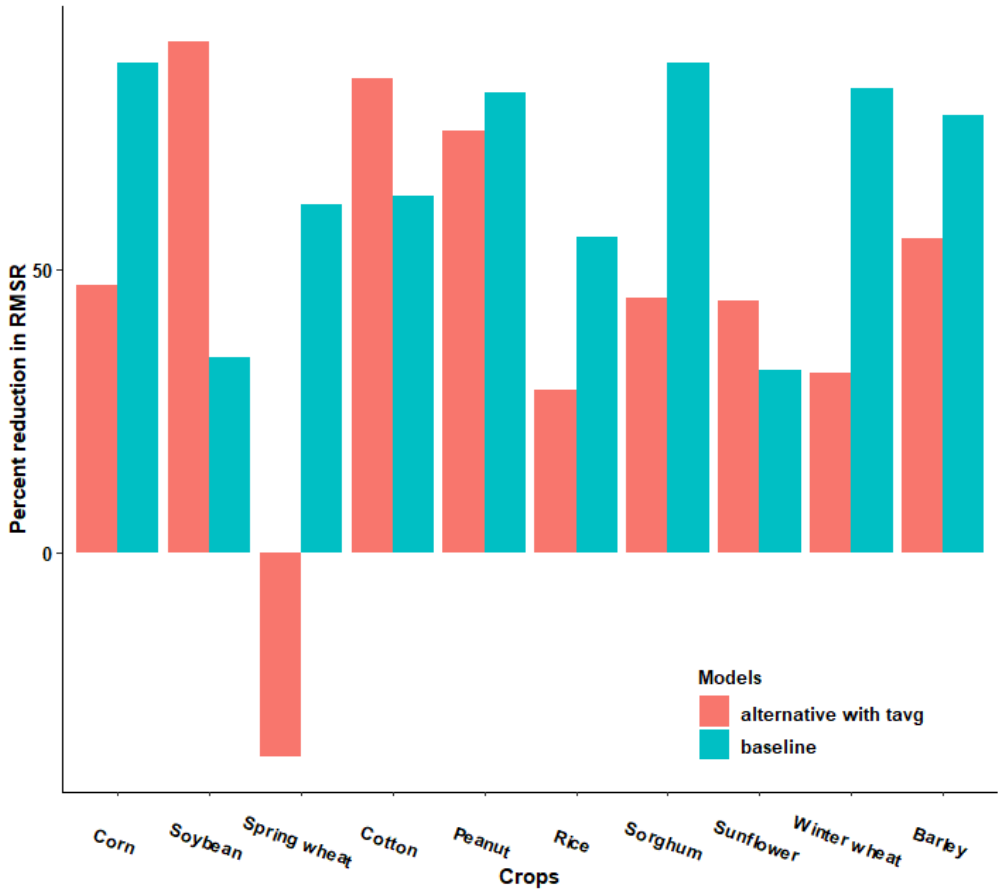

Figure A1. Out-of-sample cross-validations

Note: This figure depicts the percent reduction for RMSRs in our preferred model and the alternative model relative to the reference model in which only fixed effects and time trend variables are included. In the figure, "baseline" refers to our preferrable baseline model as in equation (1) in the main text. "alternative with tavg" indicates the alternative model with mean temperatures.

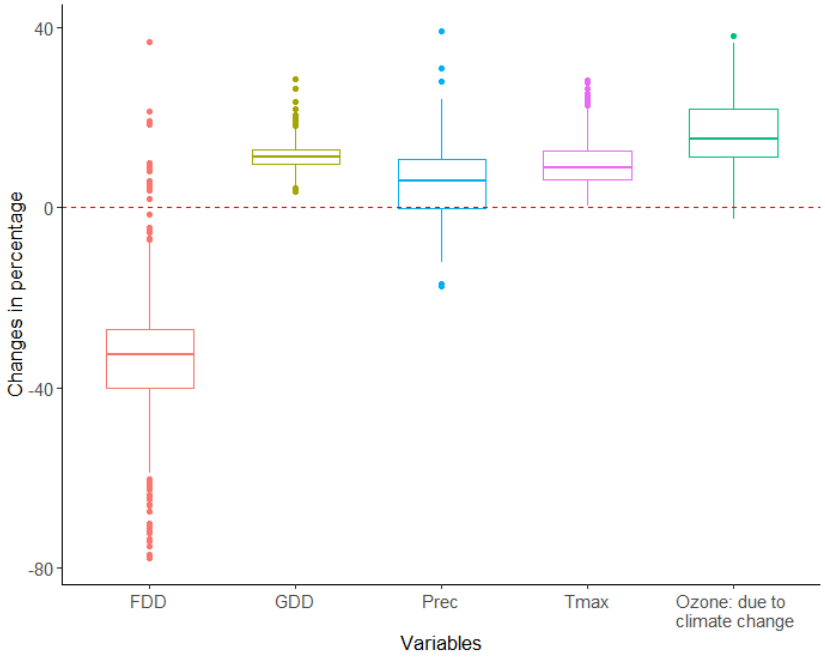

Figure A2. Future changes in climate conditions and climate change induced ozone changes for winter wheat

Note: This boxplot also reflects the distribution of changes across counties. Each box is defined by the upper and lower quartile, and the horizontal line within the box depicts the median. The endpoints for the whiskers are the upper and lower adjacent values, which are defined as the relevant quartile +/- three-halves of the interquartile range, and the dots refer to changes outside of the adjacent values.

Supplementary tables

Table A1. Winter Wheat Usual Planting and Harvesting Date by States

State	Planting date	Harvesting date	Ozone sensitive period
Colorado	September	July	April to June
Idaho	September	August	May to July
Illinois	October	June	March to May
Indiana	October	July	April to June
Kansas	September	July	April to June
Michigan	September	July	April to June
Missouri	October	June	March to May
Montana	September	August	May to July
Nebraska	September	July	April to June
Ohio	October	July	April to June
Oklahoma	September	June	March to May
Oregon	October	July	April to June
South Dakota	September	July	April to June
Texas	September	June	March to May
Washington	September	August	May to July

Note: Dates were obtained from the Field Crops Usual Planting and Harvesting Dates report from USDA (USDA NASS 2010).

Table A2. Summary statistics for the ten crops

Statistics	N	Mean	St. Dev.	Min	Max
Corn					
Yield (bushels/acre)	11,801	108.6	37.7	4.5	246.0
Harv (acres)	11,801	35,289.6	49,427.0	50	394,000
FDD (Celsius* days)	11,801	188.1	100.3	0.0	609.1
GDD (Celsius* days)	11,801	1,637.4	472.6	472.7	3,375.5
Prec (inches)	11,801	23.1	7.0	0.03	60.4
M7 (ppb)	10,228	49.1	8.4	4.8	101.8
AOT40 (ppm* hour)	11,801	12.3	6.5	0.0	59.7
SUM60 (ppm* hour)	11,801	17.5	12.3	0.0	102.6
W126 (ppm* hour)	11,801	14.6	9.6	0.003	91.9
Tmax (Celsius)	11,801	29.5	2.8	19.7	41.9
SPEI	11,801	0.05	0.6	-2.1	2.2
Soybean					
Yield (bushels/acre)	8,868	34.1	10.3	0.7	73.1
Harv (acres)	8,868	44,066.1	47,290.9	20	381,000
FDD (Celsius* days)	8,868	188.0	90.4	0.0	582.5
GDD (Celsius* days)	8,868	1,632.5	411.2	533.0	2,986.7
Prec (inches)	8,868	24.0	6.0	5.5	54.7
M7 (ppb)	7,772	49.2	7.7	4.8	101.8
AOT40 (ppm* hour)	8,868	12.4	6.1	0.0	59.7
SUM60 (ppm* hour)	8,868	17.5	11.8	0.0	102.6
W126 (ppm* hour)	8,868	14.6	9.0	0.003	91.9
Tmax (Celsius)	8,868	29.4	2.5	21.4	38.6
SPEI	8,868	0.1	0.6	-1.9	2.2
Spring wheat					
Yield (bushels/acre)	842	37.3	16.7	4	128
Harv (acres)	842	42,554.1	65,242.1	40.0	448,600.0
FDD (Celsius* days)	842	187.4	60.2	0.0	550.4
GDD (Celsius* days)	842	1,033.7	226.8	75.1	1,716.7
Prec (inches)	842	13.3	5.2	0.8	35.1
M7 (ppb)	842	43.2	7.8	11.2	66.0
AOT40 (ppm* hour)	842	8.0	5.4	0.0	29.3
SUM60 (ppm* hour)	842	9.1	9.4	0.0	46.6
W126 (ppm* hour)	842	8.5	7.0	0.2	41.2
Tmax (Celsius)	842	26.7	2.2	15.1	33.4
SPEI	842	0.1	0.6	-1.7	2.0
Winter wheat					
Yield (bushels/acre)	5,504	53.3	13.6	9.5	104.5

Harv (acres)	5,504	8,654.7	10,781.7	100	83,000
FDD (Celsius* days)	5,504	274.9	242.3	0.03	1,611.6
GDD (Celsius* days)	5,504	2,935.0	518.8	1,545.0	5,094.2
Prec (inches)	5,504	32.4	7.5	7.8	65.6
M7 (ppb)	5,504	45.7	5.3	12.1	67.7
AOT40 (ppm* hour)	5,504	9.6	3.8	0.0	28.5
SUM60 (ppm* hour)	5,504	11.5	7.2	0.0	50.0
W126 (ppm* hour)	5,504	10.2	5.2	0.1	40.1
Tmax (Celsius)	5,504	21.5	2.4	10.5	29.2
SPEI	5,504	0.1	0.6	-1.9	1.8
Barley					
Yield (bushels/acre)	3,173	61.1	15.6	7	128
Harv (acres)	3,173	3,557.9	7,932.4	10	107,000
FDD (Celsius* days)	3,173	140.3	81.1	0.0	536.5
GDD (Celsius* days)	3,173	1,280.1	368.0	102.0	2,451.1
Prec (inches)	3,173	10.4	4.5	0.1	30.4
M7 (ppb)	3,173	49.0	9.4	0.0	101.8
AOT40 (ppm* hour)	3,173	12.9	7.1	0.0	59.7
SUM60 (ppm* hour)	3,173	18.4	13.4	0.0	96.7
W126 (ppm* hour)	3,173	15.5	10.4	0.0	91.9
Tmax (Celsius)	3,173	27.7	2.6	16.4	37.4
SPEI	3,173	0.02	0.6	-1.6	2.0
Cotton					
Yield (lbs/acre)	1,446	642.1	252.8	96	1,621
Harv (acres)	1,446	14,816.9	20,721.6	10	142,900
FDD (Celsius* days)	1,446	16.7	18.6	0.0	97.6
GDD (Celsius* days)	1,446	2,118.9	252.8	1,533.4	2,957.1
Prec (inches)	1,446	12.2	5.3	1.0	32.4
M7 (ppb)	1,446	47.4	9.6	18.5	89.7
AOT40 (ppm* hour)	1,446	11.2	6.3	0.0	54.7
SUM60 (ppm* hour)	1,446	15.8	11.7	0.0	102.6
W126 (ppm* hour)	1,446	13.0	8.8	0.1	89.1
Tmax (Celsius)	1,446	32.6	1.7	28.7	39.1
SPEI	1,446	0.02	0.6	-1.5	1.8
Peanuts					
Yield (lbs/acre)	472	2,533.7	909.4	400	5,342
Harv (acres)	472	4,996.2	5,503.3	5	31,900
FDD (Celsius* days)	472	15.8	18.1	0	98
GDD (Celsius* days)	472	2,102.1	223.5	1,580.8	2,908.3
Prec (inches)	472	14.6	5.7	2.8	36.0
M7 (ppb)	472	47.4	8.5	23.1	70.6

AOT40 (ppm* hour)	472	11.0	6.2	0.3	30.1
SUM60 (ppm* hour)	472	15.5	11.6	0.0	49.5
W126 (ppm* hour)	472	13.0	8.9	0.4	43.2
Tmax (Celsius)	472	32.4	1.5	28.6	37.0
SPEI	472	-0.03	0.6	-1.5	1.7
Rice					
Yield (lbs/acre)	294	5,219.4	1,204.7	1,820	10,350
Harv (acres)	294	15,862.1	17,752.5	800	91,900
FDD (Celsius* days)	294	3.0	7.0	0	38
GDD (Celsius* days)	294	2,349.5	124.8	1,858.2	2,661.0
Prec (inches)	294	14.3	5.6	5.1	30.4
M7 (ppb)	294	40.1	7.7	21.5	62.4
AOT40 (ppm* hour)	294	7.9	4.2	0.9	21.2
SUM60 (ppm* hour)	294	11.2	7.1	0.0	34.8
W126 (ppm* hour)	294	9.7	5.8	0.8	29.7
Tmax (Celsius)	294	32.8	0.9	30.8	35.9
SPEI	294	0.1	0.6	-1.5	1.6
Sorghum					
Yield (bushels/acre)	1,955	62.3	20.4	9	127
Harv (acres)	1,955	12,429.5	31,543.4	40	270,000
FDD (Celsius* days)	1,955	42.1	42.6	0.0	249.6
GDD (Celsius* days)	1,955	1,954.8	363.4	1,006.0	2,981.4
Prec (inches)	1,955	11.3	4.7	1.0	30.0
M7 (ppb)	1,955	47.9	9.8	4.8	89.7
AOT40 (ppm* hour)	1,955	11.9	6.4	0.0	54.7
SUM60 (ppm* hour)	1,955	17.0	11.8	0.0	102.6
W126 (ppm* hour)	1,955	14.1	9.0	0.1	89.1
Tmax (Celsius)	1,955	31.8	2.2	25.2	38.5
SPEI	1,955	0.03	0.6	-1.6	1.8
Sunflower					
Yield (lbs/acre)	189	1,209.4	374.2	330	2,040
Harv (acres)	189	7,973.5	9,813.4	100	66,500
FDD (Celsius* days)	189	174.2	48.9	0.0	300.2
GDD (Celsius* days)	189	1,091.2	270.9	566.6	2,746.6
Prec (inches)	189	8.2	3.1	3.0	24.0
M7 (ppb)	189	41.1	5.0	24.5	59.1
AOT40 (ppm* hour)	189	5.1	3.2	0.3	20.1
SUM60 (ppm* hour)	189	2.8	4.4	0.0	31.2
W126 (ppm* hour)	189	4.3	3.1	0.5	23.2
Tmax (Celsius)	189	27.4	2.1	22.3	35.6
SPEI	189	0.04	0.6	-1.3	1.3

Table A3. Correlations among key variables for corn, soybean, spring wheat, and winter wheat

Corn									
	FDD	GDD	Prec	Tmax	SPEI	M7	AOT40	SUM60	W126
FDD									
GDD	-0.90***								
Prec	-0.25***	0.19***							
Tmax	-0.79***	0.93***	0.01						
SPEI	0.09***	-0.15***	0.39***	-0.31***					
M7	-0.09***	0.11***	-0.19***	0.30***	-0.34***				
AOT40	-0.05***	0.08***	-0.23***	0.25***	-0.36***	0.95***			
SUM60	-0.05***	0.08***	-0.22***	0.25***	-0.35***	0.91***	0.99***		
W126	-0.04***	0.07***	-0.23***	0.24***	-0.34***	0.91***	0.99***	0.99***	
Soybean									
	FDD	GDD	Prec	Tmax	SPEI	M7	AOT40	SUM60	W126
FDD									
GDD	-0.89***								
Prec	-0.30***	0.26***							
Tmax	-0.78***	0.93***	0.12***						
SPEI	0.12***	-0.18***	0.48***	-0.36***					
M7	-0.14***	0.19***	-0.16***	0.37***	-0.41***				
AOT40	-0.07***	0.12***	-0.22***	0.30***	-0.42***	0.95***			
SUM60	-0.07***	0.12***	-0.22***	0.29***	-0.41***	0.92***	0.99***		
W126	-0.04***	0.10***	-0.22***	0.27***	-0.40***	0.91***	0.99***	0.99***	
Spring wheat									
	FDD	GDD	Prec	Tmax	SPEI	M7	AOT40	SUM60	W126
FDD									
GDD	-0.75***								
Prec	-0.20***	0.12***							
Tmax	-0.48***	0.84***	-0.29***						
SPEI	0.10***	-0.21***	0.47***	-0.38***					
M7	-0.30***	0.57***	-0.26***	0.65***	-0.27***				
AOT40	-0.23***	0.51***	-0.18***	0.51***	-0.26***	0.92***			
SUM60	-0.19***	0.43***	-0.05	0.36***	-0.21***	0.80***	0.95***		
W126	-0.19***	0.45***	-0.08*	0.40***	-0.23***	0.84***	0.97***	0.99***	
Winter wheat									
	FDD	GDD	Prec	Tmax	SPEI	M7	AOT40	SUM60	W126
FDD									
GDD	-0.66***								
Prec	-0.24***	0.17***							
Tmax	-0.17***	0.70***	0.08***						

SPEI	0.13***	-0.12***	0.41***	-0.17***				
M7	-0.27***	0.32***	0.04**	0.41***	-0.28***			
AOT40	-0.23***	0.26***	0.02	0.40***	-0.31***	0.93***		
SUM60	-0.17***	0.20***	0.01	0.36***	-0.32***	0.84***	0.96***	
W126	-0.16***	0.20***	0	0.37***	-0.30***	0.86***	0.97***	0.98***

Note: *p<0.1; **p<0.05; ***p<0.01.

Table A4. VIF table for corn, soybean, spring wheat, and winter wheat

Crop	FDD	GDD	Prec	Tmax	SPEI
Corn	4.6	9.4	1.4	8.1	1.3
Soybean	5.3	**11.3**	1.5	8.0	1.9
Spring wheat	2.9	9.1	2.9	7.4	1.5
Winter wheat	3.1	5.5	1.4	3.6	1.4

Table A5. Estimations on Corn with the Four Ozone Indices

	Yield			
	M7	AOT40	SUM60	W126
Harv	0.0647***	0.0619***	0.0619***	0.0618***
	(0.0093)	(0.0093)	(0.0093)	(0.0094)
FDD	0.0003***	0.0003***	0.0003***	0.0003***
	(0.0001)	(0.0001)	(0.0001)	(0.0001)
GDD	13.4341***	13.5046***	13.5096***	13.6109***
	(1.0378)	(0.9577)	(0.9641)	(0.9604)
GDD^2	-0.8833***	-0.8875***	-0.8884***	-0.8955***
	(0.0717)	(0.0662)	(0.0666)	(0.0664)
Prec	0.0102***	0.0107***	0.0101***	0.0103***
	(0.0029)	(0.0026)	(0.0027)	(0.0027)
Prec^2	-0.0002***	-0.0002***	-0.0002***	-0.0002***
	(0.0001)	(0.0000)	(0.0001)	(0.0001)
Ozone	-0.0051***	-0.0082***	-0.0044***	-0.0056***
	(0.0006)	(0.0007)	(0.0004)	(0.0005)
Tmax	-0.1063***	-0.1076***	-0.1072***	-0.1080***
	(0.0043)	(0.0042)	(0.0042)	(0.0043)
SPEI	0.0638***	0.0597***	0.0602***	0.0603***
	(0.0059)	(0.0055)	(0.0055)	(0.0055)
Ozone*Tmax	-0.0006**	-0.0007**	-0.0003**	-0.0004**
	(0.0002)	(0.0003)	(0.0002)	(0.0002)
Ozone*SPEI	0.0071***	0.0088***	0.0047***	0.0056***
	(0.0007)	(0.0008)	(0.0004)	(0.0006)
Observations	10228	11801	11801	11801
Adjusted R^2	0.506	0.489	0.488	0.486

Note: Yield, Harv, and GDD are in log format. Linear and quadratic time trends were included in the regressions. Numbers in parenthesis are standard errors clustered at the county level. *p<0.1; **p<0.05; ***p<0.01.

Table A6. Estimations on Soybeans with the Four Ozone Indices

	Yield			
	M7	AOT40	SUM60	W126
Harv	0.0027	0.0024	0.0022	0.0024
	(0.0048)	(0.0049)	(0.0049)	(0.0049)
FDD	0.0003***	0.0003***	0.0003***	0.0003***
	(0.00005)	(0.00005)	(0.00005)	(0.00005)
GDD	10.2105***	11.0286***	11.0611***	11.0984***
	(0.9474)	(0.8803)	(0.8816)	(0.8827)
GDD^2	-0.6370***	-0.6946***	-0.6975***	-0.7000***
	(0.0653)	(0.0606)	(0.0607)	(0.0608)
Prec	0.0195***	0.0181***	0.0177***	0.0179***
	(0.0031)	(0.0027)	(0.0027)	(0.0028)
Prec^2	-0.0004***	-0.0004***	-0.0004***	-0.0004***
	(0.0001)	(0.0001)	(0.0001)	(0.0001)
Ozone	-0.0016***	-0.0038***	-0.0024***	-0.0028***
	(0.0005)	(0.0006)	(0.0003)	(0.0004)
Tmax	-0.0853***	-0.0828***	-0.0812***	-0.0823***
	(0.0040)	(0.0038)	(0.0038)	(0.0038)
SPEI	0.0882***	0.0874***	0.0872***	0.0875***
	(0.0046)	(0.0044)	(0.0044)	(0.0044)
Ozone*Tmax	-0.0013***	-0.0020***	-0.0010***	-0.0013***
	(0.0002)	(0.0002)	(0.0001)	(0.0002)
Ozone*SPEI	0.0048***	0.0057***	0.0028***	0.0036***
	(0.0006)	(0.0007)	(0.0003)	(0.0005)
Observations	7772	8868	8868	8868
Adjusted R^2	0.467	0.460	0.459	0.457

Note: Yield, Harv, and GDD are in log format. Linear and quadratic time trends were included in the regressions. Numbers in parenthesis are standard errors clustered at the county level. *p<0.1; **p<0.05; ***p<0.01.

Table A7. Estimations on Spring Wheat with the Four Ozone Indices

	Yield			
	M7	AOT40	SUM60	W126
Harv	0.0539***	0.0552***	0.0558***	0.0549***
	(0.0177)	(0.0174)	(0.0173)	(0.0173)
FDD	0.0004*	0.0005*	0.0005**	0.0005**
	(0.0002)	(0.0002)	(0.0002)	(0.0002)
GDD	9.7304***	8.4997***	7.9962***	8.1091***
	(2.4132)	(2.3881)	(2.3888)	(2.4195)
GDD^2	-0.6776***	-0.5891***	-0.5533***	-0.5623***
	(0.1795)	(0.1772)	(0.1770)	(0.1795)
Prec	0.0859***	0.0870***	0.0869***	0.0876***
	(0.0140)	(0.0139)	(0.0139)	(0.0139)
Prec^2	-0.0024***	-0.0024***	-0.0024***	-0.0025***
	(0.0004)	(0.0004)	(0.0004)	(0.0004)
Ozone	-0.0033	-0.0120***	-0.0074***	-0.0103***
	(0.0027)	(0.0037)	(0.0020)	(0.0026)
Tmax	-0.0990***	-0.0852***	-0.0842***	-0.0811***
	(0.0207)	(0.0203)	(0.0198)	(0.0198)
SPEI	-0.0702***	-0.0732***	-0.0731***	-0.0725***
	(0.0246)	(0.0243)	(0.0242)	(0.0243)
Ozone*Tmax	-0.0038***	-0.0053***	-0.0021***	-0.0034***
	(0.0008)	(0.0012)	(0.0006)	(0.0009)
Ozone*SPEI	0.0007	-0.0013	-0.0007	-0.0012
	(0.0029)	(0.0043)	(0.0024)	(0.0032)
Observations	812	812	812	812
Adjusted R^2	0.230	0.230	0.223	0.227

Note: Yield, Harv, and GDD are in log format. Linear and quadratic time trends were included in the regressions. Numbers in parenthesis are standard errors clustered at the county level. *p<0.1; **p<0.05; ***p<0.01.

Table A8. Estimations on Winter Wheat with the Four Ozone Indices

	Yield			
	M7	AOT40	SUM60	W126
Harv	0.0641***	0.0640***	0.0637***	0.0637***
	(0.0072)	(0.0072)	(0.0071)	(0.0071)
FDD	0.000003	0.0000	-0.000001	-0.000001
	(0.00002)	(0.0000)	(0.00002)	(0.00002)
GDD	13.4726***	13.4729***	13.6752***	13.6619***
	(1.6585)	(1.6646)	(1.6827)	(1.6790)
GDD^2	-0.8205***	-0.8207***	-0.8337***	-0.8329***
	(0.1046)	(0.1050)	(0.1061)	(0.1059)
Prec	0.0048	0.0049	0.0050	0.0050
	(0.0032)	(0.0032)	(0.0032)	(0.0032)
Prec^2	-0.0002***	-0.0002***	-0.0002***	-0.0002***
	(0.00004)	(0.0000)	(0.00004)	(0.00004)
Ozone	0.0028***	0.0027***	0.0002	0.0005
	(0.0007)	(0.0009)	(0.0005)	(0.0007)
Tmax	-0.0259***	-0.0251***	-0.0233***	-0.0235***
	(0.0027)	(0.0027)	(0.0027)	(0.0027)
SPEI	-0.0090**	-0.0101**	-0.0123***	-0.0122***
	(0.0044)	(0.0043)	(0.0043)	(0.0042)
Ozone*Tmax	-0.0001	-0.0004	0.0009***	0.0010***
	(0.0001)	(0.0003)	(0.0001)	(0.0002)
Ozone*SPEI	0.0086***	0.0085***	0.0093***	0.0093***
	(0.0011)	(0.0012)	(0.0011)	(0.0011)
Observations	5504	5504	5504	5504
Adjusted R^2	0.303	0.300	0.292	0.293

Note: Yield, Harv, and GDD are in log format. Linear and quadratic time trends were included in the regressions. Numbers in parenthesis are standard errors clustered at the county level. *p<0.1; **p<0.05; ***p<0.01.

Table A9. Estimations on Barley with the Four Ozone Indices

	Yield			
	M7	AOT40	SUM60	W126
Harv	0.016	0.016	0.016	0.016
	(0.011)	(0.011)	(0.011)	(0.011)
FDD	-0.0004***	-0.0004***	-0.0004***	-0.0004***
	(0.0001)	(0.0001)	(0.0001)	(0.0001)
GDD	1.736*	1.749*	1.775*	1.752*
	(0.971)	(0.994)	(1.018)	(0.998)
GDD^2	-0.154**	-0.154**	-0.156**	-0.155**
	(0.071)	(0.072)	(0.074)	(0.072)
Prec	0.021***	0.021***	0.021***	0.021***
	(0.008)	(0.008)	(0.008)	(0.008)
Prec^2	-0.001***	-0.001***	-0.001***	-0.001***
	(0.0003)	(0.0003)	(0.0003)	(0.0003)
Ozone	0.001	0.001	0.001	0.001
	(0.001)	(0.001)	(0.001)	(0.001)
Tmax	-0.020**	-0.020**	-0.022**	-0.020**
	(0.009)	(0.009)	(0.009)	(0.009)
SPEI	-0.009	-0.010	-0.010	-0.010
	(0.012)	(0.012)	(0.012)	(0.012)
Ozone*Tmax	-0.0001	0.0002	0.0001	0.0002
	(0.0003)	(0.0004)	(0.0002)	(0.0003)
Ozone*SPEI	-0.0003	0.001	0.0004	0.001
	(0.001)	(0.001)	(0.001)	(0.001)
Observations	3173	3173	3173	3173
Adjusted R^2	0.086	0.087	0.087	0.087

Note: Yield, Harv, and GDD are in log format. Linear and quadratic time trends were included in the regressions. Numbers in parenthesis are standard errors clustered at the county level. *p<0.1; **p<0.05; ***p<0.01.

Table A10. Estimations on Cotton with the Four Ozone Indices

	Yield			
	M7	AOT40	SUM60	W126
Harv	0.010	0.010	0.009	0.009
	(0.012)	(0.013)	(0.013)	(0.013)
FDD	-0.001	-0.001	-0.001	-0.001
	(0.001)	(0.001)	(0.001)	(0.001)
GDD	27.487**	31.089**	31.697**	32.070**
	(13.223)	(13.290)	(13.374)	(13.266)
GDD^2	-1.753**	-1.995**	-2.036**	-2.061**
	(0.866)	(0.870)	(0.876)	(0.869)
Prec	0.005	0.006	0.006	0.006
	(0.010)	(0.010)	(0.010)	(0.010)
Prec^2	-0.0005*	-0.001*	-0.001*	-0.001*
	(0.0003)	(0.0003)	(0.0003)	(0.0003)
Ozone	-0.002	-0.008***	-0.005***	-0.006***
	(0.001)	(0.002)	(0.001)	(0.002)
Tmax	-0.144***	-0.132***	-0.130***	-0.130***
	(0.020)	(0.019)	(0.019)	(0.019)
SPEI	-0.009	-0.010	-0.012	-0.010
	(0.023)	(0.023)	(0.024)	(0.023)
Ozone*Tmax	-0.001	-0.002	-0.001**	-0.002*
	(0.001)	(0.001)	(0.001)	(0.001)
Ozone*SPEI	0.005***	0.009***	0.005***	0.007***
	(0.001)	(0.002)	(0.001)	(0.001)
Observations	1446	1446	1446	1446
Adjusted R^2	0.230	0.241	0.248	0.245

Note: Yield, Harv, and GDD are in log format. Linear and quadratic time trends were included in the regressions. Numbers in parenthesis are standard errors clustered at the county level. *p<0.1; **p<0.05; ***p<0.01.

Table A11. Estimations on Peanuts with the Four Ozone Indices

	Yield			
	M7	AOT40	SUM60	W126
Harv	0.041	0.042	0.042	0.042
	(0.030)	(0.030)	(0.030)	(0.030)
FDD	0.0001	0.00002	0.00004	0.00003
	(0.001)	(0.001)	(0.001)	(0.001)
GDD	-9.173	-9.605	-9.610	-9.633
	(15.065)	(14.819)	(14.951)	(14.841)
GDD^2	0.611	0.635	0.635	0.637
	(0.993)	(0.977)	(0.986)	(0.979)
Prec	0.031**	0.030**	0.029**	0.029**
	(0.014)	(0.013)	(0.013)	(0.013)
Prec^2	-0.001***	-0.001***	-0.001**	-0.001**
	(0.0003)	(0.0003)	(0.0003)	(0.0003)
Ozone	-0.002	-0.005**	-0.003**	-0.004**
	(0.002)	(0.003)	(0.001)	(0.002)
Tmax	-0.056*	-0.048	-0.047	-0.047
	(0.033)	(0.033)	(0.032)	(0.033)
SPEI	0.015	0.013	0.012	0.013
	(0.034)	(0.034)	(0.034)	(0.034)
Ozone*Tmax	-0.0004	-0.001	-0.0003	-0.0003
	(0.001)	(0.002)	(0.001)	(0.001)
Ozone*SPEI	-0.001	-0.002	-0.001	-0.002
	(0.002)	(0.002)	(0.001)	(0.002)
Observations	472	472	472	472
Adjusted R^2	0.185	0.189	0.191	0.192

Note: Yield, Harv, and GDD are in log format. Linear and quadratic time trends were included in the regressions. Numbers in parenthesis are standard errors clustered at the county level. *p<0.1; **p<0.05; ***p<0.01.

Table A12. Estimations on Rice with the Four Ozone Indices

	Yield			
	M7	AOT40	SUM60	W126
Harv	0.041	0.038	0.039	0.039
	(0.044)	(0.046)	(0.045)	(0.045)
FDD	-0.001	-0.001	-0.001	-0.001
	(0.001)	(0.001)	(0.001)	(0.001)
GDD	-29.112	-23.024	-27.547	-28.473
	(32.586)	(31.213)	(32.237)	(32.314)
GDD^2	1.948	1.555	1.847	1.907
	(2.112)	(2.023)	(2.089)	(2.094)
Prec	0.010	0.010	0.010	0.010
	(0.011)	(0.012)	(0.011)	(0.011)
Prec^2	-0.0003	-0.0003	-0.0003	-0.0003
	(0.0003)	(0.0003)	(0.0003)	(0.0003)
Ozone	-0.002	-0.003**	-0.004	-0.003
	(0.002)	(0.001)	(0.003)	(0.002)
Tmax	-0.056**	-0.052**	-0.054**	-0.055**
	(0.022)	(0.022)	(0.023)	(0.022)
SPEI	-0.015	-0.017	-0.015	-0.016
	(0.029)	(0.030)	(0.030)	(0.030)
Ozone*Tmax	0.002	0.001	0.002	0.002
	(0.002)	(0.001)	(0.002)	(0.002)
Ozone*SPEI	-0.001	-0.001	-0.001	-0.001
	(0.002)	(0.002)	(0.004)	(0.002)
Observations	294	294	294	294
Adjusted R^2	0.426	0.423	0.425	0.423

Note: Yield, Harv, and GDD are in log format. Linear and quadratic time trends were included in the regressions. Numbers in parenthesis are standard errors clustered at the county level. *p<0.1; **p<0.05; ***p<0.01.

Table A13. Estimations on Sorghum with the Four Ozone Indices

	Yield			
	M7	AOT40	SUM60	W126
Harv	0.057***	0.057***	0.057***	0.057***
	(0.011)	(0.011)	(0.011)	(0.011)
FDD	0.0001	0.00004	0.00003	0.00004
	(0.0003)	(0.0003)	(0.0003)	(0.0003)
GDD	26.103***	26.659***	26.615***	26.517***
	(6.128)	(6.144)	(6.121)	(6.153)
GDD^2	-1.715***	-1.753***	-1.751***	-1.744***
	(0.411)	(0.412)	(0.411)	(0.413)
Prec	0.018***	0.018***	0.018***	0.018***
	(0.007)	(0.007)	(0.007)	(0.007)
Prec^2	-0.001***	-0.001***	-0.001***	-0.001***
	(0.0002)	(0.0002)	(0.0002)	(0.0002)
Ozone	-0.001	-0.003*	-0.002**	-0.002
	(0.001)	(0.001)	(0.001)	(0.001)
Tmax	-0.102***	-0.098***	-0.098***	-0.099***
	(0.013)	(0.013)	(0.013)	(0.013)
SPEI	-0.016	-0.017	-0.018	-0.017
	(0.022)	(0.022)	(0.022)	(0.022)
Ozone*Tmax	-0.0003	-0.001	-0.0005	-0.001
	(0.001)	(0.001)	(0.0005)	(0.001)
Ozone*SPEI	0.004***	0.006***	0.003***	0.003***
	(0.001)	(0.001)	(0.001)	(0.001)
Observations	1955	1955	1955	1955
Adjusted R^2	0.206	0.208	0.206	0.204

Note: Yield, Harv, and GDD are in log format. Linear and quadratic time trends were included in the regressions. Numbers in parenthesis are standard errors clustered at the county level. *p<0.1; **p<0.05; ***p<0.01.

Table A14. Estimations on Sunflower with the Four Ozone Indices

	Yield			
	M7	AOT40	SUM60	W126
Harv	0.039*	0.044**	0.043**	0.043**
	(0.021)	(0.020)	(0.019)	(0.019)
FDD	-0.001**	-0.001***	-0.001***	-0.001***
	(0.001)	(0.001)	(0.001)	(0.001)
GDD	13.271*	11.402*	12.605*	12.220*
	(6.927)	(6.207)	(6.592)	(6.444)
GDD^2	-1.008**	-0.875*	-0.963**	-0.934**
	(0.499)	(0.447)	(0.475)	(0.464)
Prec	0.095**	0.097**	0.099**	0.098**
	(0.045)	(0.045)	(0.045)	(0.045)
Prec^2	-0.007***	-0.007***	-0.007***	-0.007***
	(0.002)	(0.002)	(0.002)	(0.002)
Ozone	0.005	-0.008**	-0.007	-0.008
	(0.007)	(0.004)	(0.006)	(0.006)
Tmax	0.024	0.039*	0.039	0.037
	(0.029)	(0.023)	(0.025)	(0.025)
SPEI	0.213***	0.198**	0.202**	0.202**
	(0.076)	(0.085)	(0.082)	(0.082)
Ozone*Tmax	0.001	0.004	0.005	0.006
	(0.003)	(0.005)	(0.006)	(0.007)
Ozone*SPEI	0.023***	0.032***	0.034**	0.043***
	(0.006)	(0.011)	(0.013)	(0.015)
Observations	189	189	189	189
Adjusted R^2	0.206	0.199	0.213	0.209

Note: Yield, Harv, and GDD are in log format. Linear and quadratic time trends were included in the regressions. Numbers in parenthesis are standard errors clustered at the county level. *p<0.1; **p<0.05; ***p<0.01.

Table A15. Robustness checks with secondary climatic variables for corn

	Yield					
	Baseline	Relative humidity	Wind speed	Solar radiation	Potential evaporation	Full variables
	(1)	(2)	(3)	(4)	(5)	(6)
Harv	0.062***	0.062***	0.062***	0.062***	0.062***	0.062***
	(0.009)	(0.009)	(0.009)	(0.009)	(0.009)	(0.009)
FDD	0.0003***	0.0003***	0.0003***	0.0003***	0.0003***	0.0003***
	(0.0001)	(0.0001)	(0.0001)	(0.0001)	(0.0001)	(0.0001)
GDD	13.505***	13.519***	13.701***	13.513***	12.882***	11.552***
	(0.958)	(0.951)	(0.959)	(0.958)	(0.937)	(0.929)
GDD^2	-0.888***	-0.889***	-0.902***	-0.888***	-0.842***	-0.744***
	(0.066)	(0.066)	(0.066)	(0.066)	(0.065)	(0.064)
Prec	0.011***	0.011***	0.011***	0.010***	0.008***	0.012***
	(0.003)	(0.003)	(0.003)	(0.003)	(0.003)	(0.003)
Prec^2	-0.0002***	-0.0002***	-0.0002***	-0.0002***	-0.0002***	-0.0003***
	(0.0001)	(0.0001)	(0.0001)	(0.0001)	(0.0001)	(0.0001)
AOT40	-0.008***	-0.008***	-0.008***	-0.008***	-0.008***	-0.008***
	(0.001)	(0.001)	(0.001)	(0.001)	(0.001)	(0.001)
Tmax	-0.108***	-0.108***	-0.108***	-0.107***	-0.106***	-0.107***
	(0.004)	(0.004)	(0.004)	(0.004)	(0.004)	(0.004)
SPEI	0.060***	0.060***	0.059***	0.060***	0.061***	0.057***
	(0.005)	(0.006)	(0.005)	(0.006)	(0.006)	(0.005)
RH		-0.0002				-0.016***
		(0.001)				(0.002)
Wind			0.029***			0.050***
			(0.009)			(0.009)
Solar				-0.0003		0.001**
				(0.0003)		(0.0004)
Evp					-0.235***	-1.229***
					(0.066)	(0.151)
County FE	Yes	Yes	Yes	Yes	Yes	Yes
Linear trend	Yes	Yes	Yes	Yes	Yes	Yes
Quadratic trend	Yes	Yes	Yes	Yes	Yes	Yes
Observations	11,801	11,801	11,801	11,801	11,801	11,801
Adjusted R^2	0.468	0.468	0.469	0.468	0.469	0.474

Note: This table only presents regression results with AOT40. Yield, Harv, and GDD are in log format. Numbers in parenthesis are standard errors clustered at the county level. *p<0.1; **p<0.05; ***p<0.01.

Table A16. Robustness checks with secondary climatic variables for soybeans

	Yield					
	Baseline	Relative humidity	Wind speed	Solar radiation	Potential evaporation	Full variables
	(1)	(2)	(3)	(4)	(5)	(6)
Harv	0.002	0.003	0.002	0.002	0.003	0.003
	(0.005)	(0.005)	(0.005)	(0.005)	(0.005)	(0.005)
FDD	0.0003***	0.0003***	0.0003***	0.0003***	0.0003***	0.0003***
	(0.00005)	(0.00005)	(0.00005)	(0.00005)	(0.00005)	(0.00005)
GDD	11.029***	10.935***	11.063***	11.034***	10.667***	10.200***
	(0.880)	(0.864)	(0.884)	(0.883)	(0.859)	(0.897)
GDD^2	-0.695***	-0.688***	-0.697***	-0.695***	-0.669***	-0.634***
	(0.061)	(0.060)	(0.061)	(0.061)	(0.059)	(0.062)
Prec	0.018***	0.016***	0.018***	0.018***	0.016***	0.016***
	(0.003)	(0.003)	(0.003)	(0.003)	(0.003)	(0.003)
Prec^2	-0.0004***	-0.0003***	-0.0004***	-0.0004***	-0.0003***	-0.0003***
	(0.0001)	(0.0001)	(0.0001)	(0.0001)	(0.0001)	(0.0001)
AOT40	-0.004***	-0.004***	-0.004***	-0.004***	-0.004***	-0.004***
	(0.001)	(0.001)	(0.001)	(0.001)	(0.001)	(0.001)
Tmax	-0.083***	-0.082***	-0.083***	-0.083***	-0.082***	-0.083***
	(0.004)	(0.004)	(0.004)	(0.004)	(0.004)	(0.004)
SPEI	0.087***	0.089***	0.087***	0.087***	0.088***	0.087***
	(0.004)	(0.004)	(0.004)	(0.004)	(0.004)	(0.004)
RH		0.002**				-0.003
		(0.001)				(0.002)
Wind			0.008			0.014
			(0.009)			(0.009)
Solar				-0.00004		0.001*
				(0.0003)		(0.0004)
Evp					-0.155***	-0.405***
					(0.058)	(0.129)
County FE	Yes	Yes	Yes	Yes	Yes	Yes
Linear time	Yes	Yes	Yes	Yes	Yes	Yes
Quadratic trend	Yes	Yes	Yes	Yes	Yes	Yes
Observations	8,868	8,868	8,868	8,868	8,868	8,868
Adjusted R^2	0.435	0.436	0.435	0.435	0.436	0.436

Note: This table only presents regression results with AOT40. Yield, Harv, and GDD are in log format. Numbers in parenthesis are standard errors clustered at the county level. *p<0.1; **p<0.05; ***p<0.01.

Table A17. Robustness checks with secondary climatic variables for spring wheat

	Yield					
	Baseline	Relative humidity	Wind speed	Solar radiation	Potential evaporation	Full variables
	(1)	(2)	(3)	(4)	(5)	(6)
Harv	0.055***	0.052***	0.054***	0.056***	0.055***	0.052***
	(0.017)	(0.017)	(0.018)	(0.017)	(0.018)	(0.018)
FDD	0.0005*	0.0003	0.0004*	0.0003	0.0003	0.0002
	(0.0002)	(0.0003)	(0.0002)	(0.0003)	(0.0003)	(0.0003)
GDD	8.500***	7.084***	8.818***	8.457***	6.934***	8.250***
	(2.388)	(2.466)	(2.381)	(2.526)	(2.516)	(2.543)
GDD^2	-0.589***	-0.484***	-0.612***	-0.586***	-0.469**	-0.572***
	(0.177)	(0.181)	(0.176)	(0.187)	(0.185)	(0.188)
Prec	0.087***	0.070***	0.087***	0.083***	0.078***	0.069***
	(0.014)	(0.013)	(0.014)	(0.014)	(0.013)	(0.014)
Prec^2	-0.002***	-0.002***	-0.002***	-0.002***	-0.002***	-0.002***
	(0.0004)	(0.0003)	(0.0004)	(0.0004)	(0.0004)	(0.0003)
AOT40	-0.012***	-0.010***	-0.012***	-0.012***	-0.012***	-0.009**
	(0.004)	(0.004)	(0.004)	(0.004)	(0.004)	(0.004)
Tmax	-0.085***	-0.080***	-0.088***	-0.068***	-0.080***	-0.073***
	(0.020)	(0.020)	(0.021)	(0.021)	(0.021)	(0.021)
SPEI	-0.073***	-0.067***	-0.072***	-0.062**	-0.069***	-0.058**
	(0.024)	(0.025)	(0.024)	(0.024)	(0.024)	(0.025)
RH		0.012***				0.014**
		(0.004)				(0.007)
Wind			0.037			0.052
			(0.038)			(0.038)
Solar				-0.005***		-0.004**
				(0.002)		(0.002)
Evp					-0.612**	0.397
					(0.283)	(0.493)
County FE	Yes	Yes	Yes	Yes	Yes	Yes
Linear trend	Yes	Yes	Yes	Yes	Yes	Yes
Quadratic trend	Yes	Yes	Yes	Yes	Yes	Yes
Observations	812	812	812	812	812	812
Adjusted R^2	0.210	0.222	0.210	0.220	0.217	0.226

Note: This table only presents regression results with AOT40. Yield, Harv, and GDD are in log format. Numbers in parenthesis are standard errors clustered at the county level. *p<0.1; **p<0.05; ***p<0.01.

Table A18. Robustness checks with secondary climatic variables for winter wheat

	Yield					
	Baseline	Relative humidity	Wind speed	Solar radiation	Potential evaporation	Full variables
	(1)	(2)	(3)	(4)	(5)	(6)
Harv	0.064***	0.065***	0.063***	0.065***	0.063***	0.066***
	(0.007)	(0.007)	(0.007)	(0.007)	(0.007)	(0.007)
FDD	0.00000	0.00002	0.00000	-0.00001	0.00001	-0.00003
	(0.00002)	(0.00002)	(0.00002)	(0.00002)	(0.00002)	(0.00002)
GDD	13.528***	14.486***	13.238***	13.765***	14.045***	12.655***
	(1.667)	(1.636)	(1.677)	(1.652)	(1.634)	(1.618)
GDD^2	-0.824***	-0.884***	-0.806***	-0.841***	-0.857***	-0.770***
	(0.105)	(0.103)	(0.106)	(0.104)	(0.103)	(0.102)
Prec	0.005	0.007**	0.005	0.004	0.006*	0.002
	(0.003)	(0.003)	(0.003)	(0.003)	(0.003)	(0.003)
Prec^2	-0.0002***	-0.0002***	-0.0002***	-0.0002***	-0.0002***	-0.0001***
	(0.00004)	(0.00004)	(0.00004)	(0.00004)	(0.00004)	(0.00004)
AOT40	0.003***	0.001	0.003***	-0.0001	0.002***	-0.001
	(0.001)	(0.001)	(0.001)	(0.001)	(0.001)	(0.001)
Tmax	-0.025***	-0.029***	-0.026***	-0.039***	-0.029***	-0.036***
	(0.003)	(0.003)	(0.003)	(0.003)	(0.003)	(0.003)
SPEI	-0.010**	-0.006	-0.011**	0.002	-0.008*	-0.0001
	(0.004)	(0.004)	(0.004)	(0.004)	(0.004)	(0.004)
RH		-0.009***				-0.008***
		(0.002)				(0.002)
Wind			0.020			0.037***
			(0.013)			(0.013)
Solar				0.007***		0.008***
				(0.0004)		(0.001)
Evp					0.346***	-0.954***
					(0.128)	(0.184)
County FE	Yes	Yes	Yes	Yes	Yes	Yes
Linear time	Yes	Yes	Yes	Yes	Yes	Yes
Quadratic trend	Yes	Yes	Yes	Yes	Yes	Yes
Observations	5,504	5,504	5,504	5,504	5,504	5,504
Adjusted R^2	0.285	0.292	0.285	0.312	0.287	0.318

Note: This table only presents regression results with AOT40. Yield, Harv, and GDD are in log format. Numbers in parenthesis are standard errors clustered at the county level. *p<0.1; **p<0.05; ***p<0.01.

Table A19. Robustness checks with time fixed effects

	Yield			
	Corn	Soybean	Spring wheat	Winter wheat
	(1)	(2)	(3)	(4)
Harv	0.059***	0.005	0.030	0.055***
	(0.010)	(0.005)	(0.024)	(0.007)
FDD	0.0003***	0.0003***	0.001*	-0.00003
	(0.0001)	(0.0001)	(0.0003)	(0.00003)
GDD	10.897***	9.263***	9.056***	11.531***
	(0.927)	(0.960)	(2.969)	(2.141)
GDD^2	-0.685***	-0.545***	-0.680***	-0.679***
	(0.065)	(0.069)	(0.231)	(0.139)
Prec	0.015***	0.021***	0.063***	0.011***
	(0.003)	(0.003)	(0.014)	(0.003)
Prec^2	-0.0003***	-0.0004***	-0.002***	-0.0002***
	(0.0001)	(0.0001)	(0.0004)	(0.00004)
AOT40	-0.006***	-0.003***	-0.011***	0.0003
	(0.001)	(0.001)	(0.004)	(0.001)
Tmax	-0.136***	-0.122***	-0.031	-0.013***
	(0.006)	(0.007)	(0.034)	(0.004)
SPEI	0.034***	0.076***	-0.013	-0.006
	(0.005)	(0.005)	(0.027)	(0.005)
County fixed effect	Yes	Yes	Yes	Yes
Year fixed effect	Yes	Yes	Yes	Yes
Observations	11,801	8,868	812	5,504
Adjusted R^2	0.222	0.250	-0.049	0.061

Note: This table only presents regression results with AOT40. Yield, Harv, and GDD are in log format. Numbers in parenthesis are standard errors clustered at the county level. *p<0.1; **p<0.05; ***p<0.01.

Table A20. Robustness checks with fertilizer application and power consumptions for corn

	Yield						
	Baseline	Total power	Residential power	Commercial power	Industrial power	Fertilizer application	Power plus fertilizer
	(1)	(2)	(3)	(4)	(5)	(6)	(7)
Harv	0.06***	0.04***	0.05***	0.05***	0.04***	0.01	0.01
	(0.01)	(0.01)	(0.01)	(0.01)	(0.01)	(0.02)	(0.02)
FDD	0.0003***	0.0003***	0.0003***	0.0003***	0.0003***	0.0005***	0.0005***
	(0.0001)	(0.0001)	(0.0001)	(0.0001)	(0.0001)	(0.0001)	(0.0001)
GDD	13.50***	15.03***	15.19***	14.97***	14.91***	17.19***	17.12***
	(0.96)	(0.97)	(0.97)	(0.97)	(0.97)	(2.05)	(2.05)
GDD^2	-0.89***	-1.00***	-1.01***	-0.99***	-0.99***	-1.15***	-1.15***
	(0.07)	(0.07)	(0.07)	(0.07)	(0.07)	(0.14)	(0.14)
Prec	0.01***	0.01***	0.01***	0.01***	0.01***	0.01***	0.01***
	(0.003)	(0.003)	(0.003)	(0.003)	(0.003)	(0.004)	(0.004)
Prec^2	-0.0002***	-0.0003***	-0.0003***	-0.0003***	-0.0003***	-0.0003***	-0.0003***
	(0.0001)	(0.0001)	(0.0001)	(0.0001)	(0.0001)	(0.0001)	(0.0001)
AOT40	-0.01***	-0.01***	-0.01***	-0.01***	-0.01***	-0.01***	-0.01***
	(0.001)	(0.001)	(0.001)	(0.001)	(0.001)	(0.002)	(0.002)
Tmax	-0.11***	-0.10***	-0.10***	-0.10***	-0.10***	-0.09***	-0.09***
	(0.004)	(0.01)	(0.01)	(0.01)	(0.01)	(0.01)	(0.01)
SPEI	0.06***	0.05***	0.05***	0.05***	0.05***	0.06***	0.06***
	(0.01)	(0.01)	(0.01)	(0.01)	(0.01)	(0.01)	(0.01)
Total power		0.10***					0.13
		(0.03)					(0.11)
Residential power			0.14***				
			(0.04)				
Commercial power				0.05***			
				(0.01)			
Industrial power					0.03***		
					(0.01)		
Fertilizer						0.01	0.02
						(0.04)	(0.04)
County fixed effect	Yes	Yes	Yes	Yes	Yes	Yes	Yes
Linear time trend	Yes	Yes	Yes	Yes	Yes	Yes	Yes
Quadratic time trend	Yes	Yes	Yes	Yes	Yes	Yes	Yes
Observations	11,801	9,195	9,195	9,195	9,195	2,056	2,056
Adjusted R^2	0.47	0.40	0.40	0.40	0.40	0.38	0.38

Note: This table only presents regression results with AOT40. Yield, Harv, GDD, power consumption, and fertilizer application are in log format. Numbers in parenthesis are standard errors clustered at the county level. *p<0.1; **p<0.05; ***p<0.01.

Table A21. Robustness checks with fertilizer application and power consumptions for soybeans

	Yield						
	Baseline	Total power	Residential power	Commercial power	Industrial power	Fertilizer application	Power plus fertilizer
	(1)	(2)	(3)	(4)	(5)	(6)	(7)
Harv	0.002	0.01*	0.01*	0.01*	0.01*	0.06	0.06
	(0.005)	(0.01)	(0.01)	(0.01)	(0.01)	(0.04)	(0.04)
FDD	0.0003***	0.0003***	0.0003***	0.0003***	0.0003***	0.0003**	0.0003**
	(0.0000)	(0.0001)	(0.0001)	(0.0001)	(0.0001)	(0.0001)	(0.0001)
GDD	11.03***	12.10***	12.11***	12.06***	12.09***	12.94***	12.95***
	(0.88)	(0.97)	(0.98)	(0.97)	(0.97)	(1.90)	(1.90)
GDD^2	-0.69***	-0.77***	-0.77***	-0.77***	-0.77***	-0.81***	-0.81***
	(0.06)	(0.07)	(0.07)	(0.07)	(0.07)	(0.13)	(0.13)
Prec	0.02***	0.02***	0.02***	0.02***	0.02***	0.01*	0.01*
	(0.003)	(0.003)	(0.003)	(0.003)	(0.003)	(0.01)	(0.01)
Prec^2	-0.0004***	-0.0003***	-0.0003***	-0.0003***	-0.0003***	-0.0002**	-0.0002**
	(0.0001)	(0.0001)	(0.0001)	(0.0001)	(0.0001)	(0.0001)	(0.0001)
AOT40	-0.004***	-0.006***	-0.006***	-0.006***	-0.006***	0.001	0.001
	(0.001)	(0.001)	(0.001)	(0.001)	(0.001)	(0.002)	(0.002)
Tmax	-0.08***	-0.07***	-0.07***	-0.07***	-0.07***	-0.11***	-0.11***
	(0.004)	(0.005)	(0.005)	(0.005)	(0.005)	(0.01)	(0.01)
SPEI	0.09***	0.09***	0.09***	0.09***	0.09***	0.09***	0.09***
	(0.004)	(0.005)	(0.005)	(0.005)	(0.005)	(0.01)	(0.01)
Total power		-0.004					-0.03
		(0.03)					(0.12)
Residential power			0.002				
			(0.03)				
Commercial power				-0.01			
				(0.01)			
Industrial power					0.01		
					(0.01)		
Fertilizer						0.03	0.03
						(0.04)	(0.04)
County fixed effect	Yes	Yes	Yes	Yes	Yes	Yes	Yes
Linear time trend	Yes	Yes	Yes	Yes	Yes	Yes	Yes
Quadratic time trend	Yes	Yes	Yes	Yes	Yes	Yes	Yes
Observations	8,868	6,978	6,978	6,978	6,978	1,664	1,664
Adjusted R^2	0.44	0.36	0.36	0.36	0.36	0.35	0.35

Note: This table only presents regression results with AOT40. Yield, Harv, GDD, power consumption, and fertilizer application are in log format. Numbers in parenthesis are standard errors clustered at the county level. *p<0.1; **p<0.05; ***p<0.01.

Table A22. Robustness checks with fertilizer application and power consumptions for spring wheat

	Yield						
	Baseline	Total power	Residential power	Commercial power	Industrial power	Fertilizer application	Power plus fertilizer
	(1)	(2)	(3)	(4)	(5)	(6)	(7)
Harv	0.06***	0.07*	0.07*	0.07**	0.07*	0.07	0.05
	(0.02)	(0.04)	(0.04)	(0.04)	(0.04)	(0.11)	(0.11)
FDD	0.0005*	-0.0001	-0.0001	-0.0001	-0.0001	0.0001	0.0000
	(0.0002)	(0.0004)	(0.0004)	(0.0004)	(0.0004)	(0.001)	(0.001)
GDD	8.50***	-0.08	-0.03	-0.02	-0.10	2.16	1.40
	(2.39)	(3.68)	(3.68)	(3.66)	(3.68)	(10.24)	(10.15)
GDD^2	-0.59***	0.02	0.01	0.01	0.02	-0.12	-0.06
	(0.18)	(0.27)	(0.27)	(0.27)	(0.27)	(0.79)	(0.79)
Prec	0.09***	0.06***	0.06***	0.06***	0.06***	0.10**	0.10***
	(0.01)	(0.02)	(0.02)	(0.02)	(0.02)	(0.04)	(0.03)
Prec^2	-0.002***	-0.002***	-0.002***	-0.002***	-0.002***	-0.003**	-0.003**
	(0.0004)	(0.0004)	(0.0004)	(0.0004)	(0.0004)	(0.001)	(0.001)
AOT40	-0.01***	-0.01*	-0.01*	-0.01*	-0.01*	0.004	0.002
	(0.004)	(0.01)	(0.01)	(0.01)	(0.01)	(0.01)	(0.01)
Tmax	-0.09***	-0.07**	-0.07**	-0.07**	-0.07**	-0.09	-0.08
	(0.02)	(0.03)	(0.03)	(0.03)	(0.03)	(0.09)	(0.09)
SPEI	-0.07***	-0.08***	-0.08**	-0.08***	-0.08**	-0.07	-0.07
	(0.02)	(0.03)	(0.03)	(0.03)	(0.03)	(0.05)	(0.04)
Total power		0.07					-0.89
		(0.12)					(1.01)
Residential power			0.06				
			(0.16)				
Commercial power				0.17			
				(0.11)			
Industrial power					0.005		
					(0.07)		
Fertilizer						-0.43*	-0.49*
						(0.23)	(0.25)
County fixed effect	Yes	Yes	Yes	Yes	Yes	Yes	Yes
Linear time trend	Yes	Yes	Yes	Yes	Yes	Yes	Yes
Quadratic time trend	Yes	Yes	Yes	Yes	Yes	Yes	Yes
Observations	812	502	502	502	502	69	69
Adjusted R^2	0.21	0.03	0.03	0.03	0.03	-0.11	-0.11

Note: This table only presents regression results with AOT40. Yield, Harv, GDD, power consumption, and fertilizer application are in log format. Numbers in parenthesis are standard errors clustered at the county level. *p<0.1; **p<0.05; ***p<0.01.

Table A23. Robustness checks with fertilizer application and power consumptions for winter wheat

	Yield						
	Baseline	Total power	Residential power	Commercial power	Industrial power	Fertilizer application	Power plus fertilizer
	(1)	(2)	(3)	(4)	(5)	(6)	(7)
Harv	0.06***	0.06***	0.06***	0.06***	0.06***	0.11***	0.11***
	(0.01)	(0.01)	(0.01)	(0.01)	(0.01)	(0.02)	(0.02)
FDD	0.0000	0.0000	0.0000	0.0000	0.0000	-0.0001*	-0.0001*
	(0.0000)	(0.0000)	(0.0000)	(0.0000)	(0.0000)	(0.0000)	(0.0000)
GDD	13.53***	11.10***	11.35***	10.84***	11.21***	7.99	8.99
	(1.67)	(1.81)	(1.85)	(1.80)	(1.78)	(5.76)	(5.84)
GDD^2	-0.82***	-0.67***	-0.69***	-0.66***	-0.68***	-0.47	-0.53
	(0.11)	(0.11)	(0.12)	(0.11)	(0.11)	(0.36)	(0.37)
Prec	0.01	0.003	0.003	0.003	0.003	-0.01*	-0.01*
	(0.003)	(0.003)	(0.003)	(0.003)	(0.003)	(0.01)	(0.01)
Prec^2	-0.0002***	-0.0002***	-0.0002***	-0.0002***	-0.0002***	0.0000	0.0000
	(0.0000)	(0.0000)	(0.0000)	(0.0000)	(0.0000)	(0.0001)	(0.0001)
AOT40	0.003***	0.004***	0.004***	0.004***	0.004***	0.001	0.002
	(0.001)	(0.001)	(0.001)	(0.001)	(0.001)	(0.002)	(0.002)
Tmax	-0.03***	-0.02***	-0.02***	-0.02***	-0.02***	-0.03***	-0.03***
	(0.003)	(0.003)	(0.003)	(0.003)	(0.003)	(0.01)	(0.01)
SPEI	-0.01**	-0.01***	-0.01***	-0.01***	-0.01***	0.01	0.004
	(0.004)	(0.004)	(0.004)	(0.004)	(0.004)	(0.01)	(0.01)
Total power		-0.09**					-0.25**
		(0.04)					(0.11)
Residential power			-0.17***				
			(0.05)				
Commercial power				-0.06**			
				(0.02)			
Industrial power					0.01		
					(0.02)		
Fertilizer						-0.16***	-0.18***
						(0.05)	(0.04)
County fixed effect	Yes	Yes	Yes	Yes	Yes	Yes	Yes
Linear time trend	Yes	Yes	Yes	Yes	Yes	Yes	Yes
Quadratic time trend	Yes	Yes	Yes	Yes	Yes	Yes	Yes
Observations	5,504	4,976	4,976	4,976	4,976	1,010	1,010
Adjusted R^2	0.28	0.28	0.29	0.28	0.28	0.23	0.23

Note: This table only presents regression results with AOT40. Yield, Harv, GDD, power consumption, and fertilizer application are in log format. Numbers in parenthesis are standard errors clustered at the county level. *p<0.1; **p<0.05; ***p<0.01.

Table A24. Regression of AOT40 on a set of climate variables for those spring crops

	Log (AOT40)		
	(1)	(2)	(3)
FDD		-0.0003***	-0.0003
		(0.0001)	(0.0002)
GDD		-0.001***	-0.001***
		(0.0001)	(0.0001)
Prec		-0.015***	-0.015***
		(0.001)	(0.002)
Tmax	0.210***	0.232***	0.232***
	(0.005)	(0.008)	(0.014)
County FE	Yes	Yes	Yes
Year FE	Yes	Yes	Yes
Observations	22996	22996	22996
Adjusted R^2	0.13	0.15	0.15

Note: County FE and Year FE represent county fixed effects and year fixed effects, respectively. Numbers in parenthesis are standard errors. Standard errors in columns (1) and (2) are clustered at county-level, whereas at state-level in column (3) to address potential spatial correlations. *p<0.1; **p<0.05; ***p<0.01.

APPENDIX B

ARE CLIMATE CHANGE DAMAGES ON WINTER WHEAT YIELDS OVERSTATED? EVIDENCE FROM CHINA

A suite of robustness checks

In addition to the cross-validations in the main text, we also perform robustness checks examining to what extent our results are robust to different settings.

To examine whether our results are sensitive to the selection of growing period, we run regressions with Sep-May (Figure B2) and Sep-June (Figure B3), respectively. It should be noted that the degree-day variables in those regressions are constructed using the temperature thresholds estimated correspondingly for Sep-May and Sep-June. The thresholds are shown in Table B1 and are largely consistent with that for Oct-May.

The results are quite consistent with our baseline estimates with Oct-May. One exception is that in the regressions with Sep-June, we observe statistically significant negative effects of temperatures over 30 ºC in the spring. This could possibly because we have more temperatures over 30 ºC due to the inclusion of June. It leads to a concern of climate change damages in the future as we are expected to experience more heat waves (Hong et al. 2019). On the other hand, given winter wheat is usually harvested in June, we speculate that these negative effects could be attributed to the impacts of heat on labor productivity (Graff Zivin and Neidell 2014; Kjellstrom et al. 2009). This speculation is further supported by the fact that farm operations in China are still labor-intensive. A recent study in China shows that a 1 ºC increase in the mean temperature will reduce an average rural resident's time allocated to farm work by 7% (Huang et al. 2020).

In the baseline panel model, we jointly include variables of fall, winter, and spring. We also want to know whether the seasonal responses change if we run the model individually with each season. The results are shown in Table B4, which is consistent with our baseline estimates.

To test the robustness of our threshold setup (-5 and 8 ºC) in the winter season, we run regressions with winter degree-day variables derived from an alternative setup with only one temperature threshold (estimated at 8 ºC). In this setup, we have three degree-day variables for the winter season, namely freezing degree-day (temperature below 0 ºC), medium degree-day (temperatures between 0 ºC and 8 ºC), and high degree-day (temperatures above 8 ºC). The results are shown in Figure B4 and are consistent with our baseline estimates.

To address the sudden yield jump observed in 1989-1990 (see Figure 8 in the main text), we run the regression with data restricted to 1990-2015. The results are shown in Table B3 (column 1) and are rather consistent with that derived from the full sample, except that fewer damages are detected with heat and freezing days in the former regression possibly due to adaptations overtime.

We also expand our study region to have wider geographic coverage. In this case, we use data covering the entirety of seven provinces and municipalities including Hebei, Beijing, Tianjin, Henan, Shandong, Anhui, and Jiangsu (expanding to 11893 observations as opposed to 8867). The results are shown in Table B3 (column 2) and again are consistent with our baseline estimate. Nonetheless, as we discussed previously, our primary study region is narrowed down to address the concerns about the confounding effects of irrigation and differences in the growing period.

Finally, we also perform statistical inference using pair bootstrapping with replacement to address the uncertainties associated with the baseline estimates. Pseudo bootstrapping samples are randomly drawn from the original sample with replacement. The regression coefficients are estimated with the baseline model as above over each bootstrapping sample. This is repeated by

1000 times to establish distributions of coefficients. Standard errors are then constructed from those distributions. The resultant confidence intervals are provided in Table B5 and it turns out that the confidence intervals using standard errors clustered at the county-level largely overlap those constructed from bootstrapping.

Future yield projection results with SSP scenarios

To examine whether it is because of the uniform warming scenarios that cause the overestimation of climate change damages, we also perform yield projections with SSPs scenarios using climate data from the WorldClim database (Fick and Hijmans 2017). We downloaded historical monthly temperature data (1970-2000) and future temperature projection data (2041-2060) derived from the IPSL-CM6A-LR climate model at a spatial resolution of 4.6 km * 4.6 km. The gridded data are converted to county-level by weighted-averaging over grid cells that cover each county with the overlapped areas acting as weights. Following that, changes in monthly mean temperature (2041-2060 relative to 1970-2000) are calculated and applied to the historical series of hourly temperatures that we use above, and then the degree-day variables are recalculated. Finally, changes in yield are estimated under a variety of SSPs scenarios (SSP126, SSP 245, SSP 370, and SSP 585).

It should be noted that, ideally, we should measure the temperature changes in 2041-2060 relative to 1981-2015. Unfortunately, the database does not provide the model output of 1981-2015. Also note that one cannot directly compare the output of climate models with historical observations (Auffhammer et al. 2013). Nonetheless, we average the model output of 1970-2000 and the output of 2021-2040 (under the SSP126) to represent the temperatures of 1981-2015. Using these as base temperatures, we redo the projections.

The results are shown in Figure B5 and B6. Projections with different base periods are quite consistent. The warming damages are much larger and even of a different sign if the effects of freezing days are omitted. Moreover, unlike projections under uniform warming, the results under all of the SSP scenarios suggest region-wide yield gains. The difference in projections between the SSP-based and uniform temperature increase scenarios could be because climate change-induced temperature increases are not uniform across seasons, i.e., we may expect more evident temperature increases in the winter and spring seasons. Spatial variations would also be expected as well.

Supplementary tables

Table B1. Estimated temperature thresholds for alternative growing periods

September to May	
Season	Lower and upper thresholds (in ºC)
Fall (Sep-Nov)	17 and 24
Winter (Dec-Feb)	-5 and 8
Spring (March-May)	25 and 30
September to June	
Season	Lower and upper thresholds (in ºC)
Fall (Sep-Nov)	18 and 23
Winter (Dec-Feb)	-5 and 8
Spring (March-June)	25 and 30

Table B2. Summary statistics of key variables

Statistic	Min	Max	Mean	St. Dev.
Panel one: Summary statistics of yield and precipitation variables				
Yield (in tons/ha)	0.01	9.5	4.7	1.7
Prec_fall (in mm)	0.002	343.4	62.0	47.9
Prec_winter (in mm)	0.002	321.5	43.5	37.2
Prec_spring (in mm)	9.0	483.3	124.3	66.2
Panel two: Degree day variables using hourly temperatures (in 10 degree*days)				
Frez_fall	0	8.6	0.4	0.7
DDlow_fall	23.3	88.6	66.7	8.1
DDmed_fall	0	12.4	4.6	1.8
DDhigh_fall	0	2.5	0.4	0.5
DDlow_winter	0	23.1	2.1	2.4
DDmed_winter	20.9	45.8	32.2	3.0
DDhigh_winter	0.001	12.4	2.7	1.8
Frez_spring	0	7.9	0.3	0.5
DDlow_spring	63.8	159.1	131.2	13.0
DDmed_spring	0	5.7	2.2	1.0
DDhigh_spring	0	2.2	0.3	0.3
Panel three: Degree days variables using daily temperatures (in 10 degree*days)				
Frez_fall	0	6.7	0.2	0.5
DDlow_fall	16.0	74.8	49.9	8.2
DDmed_fall	0	13.2	2.9	2.2
DDhigh_fall	0	0.9	0.01	0.1
DDlow_winter	0	16.2	0.6	1.1
DDmed_winter	9	37.6	23.2	4.4
DDhigh_winter	0	7.3	0.9	1.1
Frez_spring	0	6.7	0.1	0.3
DDlow_spring	62.2	156.8	127.4	10.8
DDmed_spring	0	3.2	0.4	0.5
DDhigh_spring	0	0.35	0.002	0.02

Note: As we can see from the table, degree-day variables constructed from daily temperatures tend to be smaller and the differences are more evident for variables that represent heat and freezing. For instance, the maximum and mean of *DDhigh_fall* calculated from hourly temperatures are 2.5 and 0.5 (in the unit of 10 degree-days) respectively, whereas they are as low as 0.9 and 0.01 if calculated from daily temperatures. Furthermore, the variations of degree-day variables calculated from hourly temperatures are greater than those from daily temperatures.

Table B3. Estimated coefficients from various versions of regressions

	Winter wheat yields		
	1990-2015	Full NCP	Baseline estimates
	(1)	(2)	(3)
Frez_fall	-0.001 (0.005)	0.004 (0.007)	-0.001 (0.008)
DDlow_fall	-0.002** (0.001)	-0.0002 (0.001)	-0.002 (0.001)
DDmed_fall	0.011*** (0.004)	0.015** (0.006)	0.022*** (0.007)
DDhigh_fall	-0.022* (0.012)	-0.103*** (0.019)	-0.114*** (0.021)
DDlow_winter	0.005 (0.003)	-0.009*** (0.003)	-0.008 (0.006)
DDmed_winter	0.005*** (0.002)	0.013*** (0.003)	0.017*** (0.003)
DDhigh_winter	-0.005 (0.003)	-0.014*** (0.005)	-0.019*** (0.006)
Frez_spring	-0.046*** (0.010)	-0.116*** (0.014)	-0.113*** (0.019)
DDlow_spring	-0.0003 (0.001)	-0.007*** (0.001)	-0.006*** (0.001)
DDmed_spring	0.024*** (0.006)	0.026*** (0.008)	0.037*** (0.010)
DDhigh_spring	-0.076*** (0.013)	0.007 (0.017)	-0.015 (0.020)
Prec_fall	0.049*** (0.016)	0.057*** (0.020)	0.070*** (0.024)
Prec_fall^2	-0.012 (0.007)	-0.022** (0.009)	-0.026** (0.011)
Prec_winter	-0.031 (0.021)	0.003 (0.027)	0.004 (0.031)
Prec_winter^2	-0.010 (0.010)	-0.020 (0.012)	-0.022 (0.016)
Prec_spring	0.110*** (0.013)	0.117*** (0.017)	0.114*** (0.020)
Prec_spring^2	-0.037*** (0.004)	-0.031*** (0.005)	-0.030*** (0.006)
County fixed effect	Yes	Yes	Yes
Linear time trend	Yes	Yes	Yes
Quadratic time trend	Yes	Yes	Yes
Observations	7,433	11,893	8,867
Adjusted R^2	0.288	0.526	0.527

Note: Precipitations in the table are in 100 mm. Column (1) indicates the regression results with data restricted to 1990-2015. Column (2) presents the results with full NCP coverage, i.e. the entirety of seven provinces and municipalities including Hebei, Beijing, Tianjin, Henan, Shandong, Anhui, and Jiangsu. Column (3) shows the estimates from the baseline panel model as in equation (1) in the main text. Standard errors are clustered at the county-level and are shown in the parentheses.

Table B4 Regression coefficients with the individual season and all seasons, respectively

	Winter wheat yields			
	Only fall	Only winter	Only spring	Full season
	(1)	(2)	(3)	(4)
Frez_fall	-0.015* (0.008)			-0.001 (0.008)
DDlow_fall	-0.004*** (0.001)			-0.002 (0.001)
DDmed_fall	0.034*** (0.005)			0.022*** (0.007)
DDhigh_fall	-0.125*** (0.017)			-0.114*** (0.021)
DDlow_winter		-0.010* (0.005)		-0.008 (0.006)
DDmed_winter		0.008*** (0.003)		0.017*** (0.003)
DDhigh_winter		-0.008 (0.005)		-0.019*** (0.006)
Frez_spring			-0.119*** (0.021)	-0.113*** (0.019)
DDlow_spring			-0.006*** (0.001)	-0.006*** (0.001)
DDmed_spring			0.047*** (0.008)	0.037*** (0.010)
DDhigh_spring			-0.039** (0.016)	-0.015 (0.020)
County fixed effect	Yes	Yes	Yes	Yes
Linear time trend	Yes	Yes	Yes	Yes
Quadratic time trend	Yes	Yes	Yes	Yes
Observations	8,867	8,867	8,867	8,867
Adjusted R^2	0.518	0.515	0.521	0.527

Note: Columns (1) – (4) corresponds to separate regressions for fall, winter, spring, and all seasons, respectively. Standard errors are clustered at the county-level and are shown in the parentheses.

Table B5 Confidence intervals constructed from clustering and bootstrapping, respectively

	Winter wheat yields	
	Clustered at county-level	Bootstrapping
	(1)	(2)
Frez_fall	-0.001 (-0.017, 0.014)	-0.001 (-0.017, 0.014)
DDlow_fall	-0.002 (-0.004, 0.0004)	-0.002 (-0.005, 0.0004)
DDmed_fall	0.022*** (0.008, 0.036)	0.022*** (0.008, 0.036)
DDhigh_fall	-0.114*** (-0.155, -0.073)	-0.114*** (-0.155, -0.074)
DDlow_winter	-0.008 (-0.019, 0.003)	-0.008 (-0.019, 0.003)
DDmed_winter	0.017*** (0.010, 0.023)	0.017*** (0.010, 0.023)
DDhigh_winter	-0.019*** (-0.030, -0.007)	-0.019*** (-0.030, -0.008)
Frez_spring	-0.113*** (-0.151, -0.075)	-0.113*** (-0.153, -0.073)
DDlow_spring	-0.006*** (-0.009, -0.004)	-0.006*** (-0.009, -0.004)
DDmed_spring	0.037*** (0.018, 0.056)	0.037*** (0.018, 0.056)
DDhigh_spring	-0.015 (-0.055, 0.025)	-0.015 (-0.053, 0.024)
County fixed effect	Yes	Yes
Linear time trend	Yes	Yes
Quadratic time trend	Yes	Yes
Observations	8,867	8,867
Adjusted R^2	0.527	0.527

Note: Confidence intervals of 95% are shown in the parentheses. Column (1) indicates the confidence interval calculated using clustered standard errors whereas column (2) displays the confidence intervals constructed from the bootstrapping.

Supplementary figures

Figure B1. The study region

Note: This region (also known as the “Huang-Huai-Hai” plain) mainly covers the south part of Hebei, most of Henan, the entirety of Shandong, and the north part of Anhui and Jiangsu.

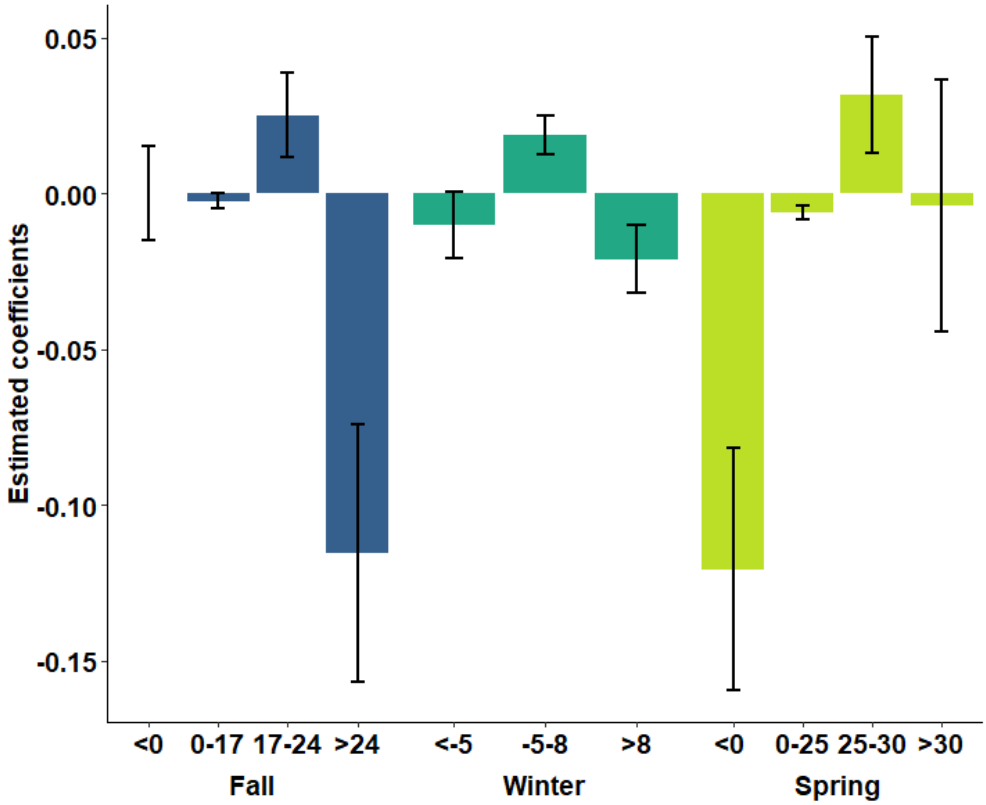

Figure B2 The robustness check with a growing season of Sep-May

Note: The x-axis indicates the degree-day variables constructed from the associated temperature thresholds. Bars show the estimated coefficients of the respective degree-day variables and the 95% confidence intervals using standard errors clustered at the county-level.

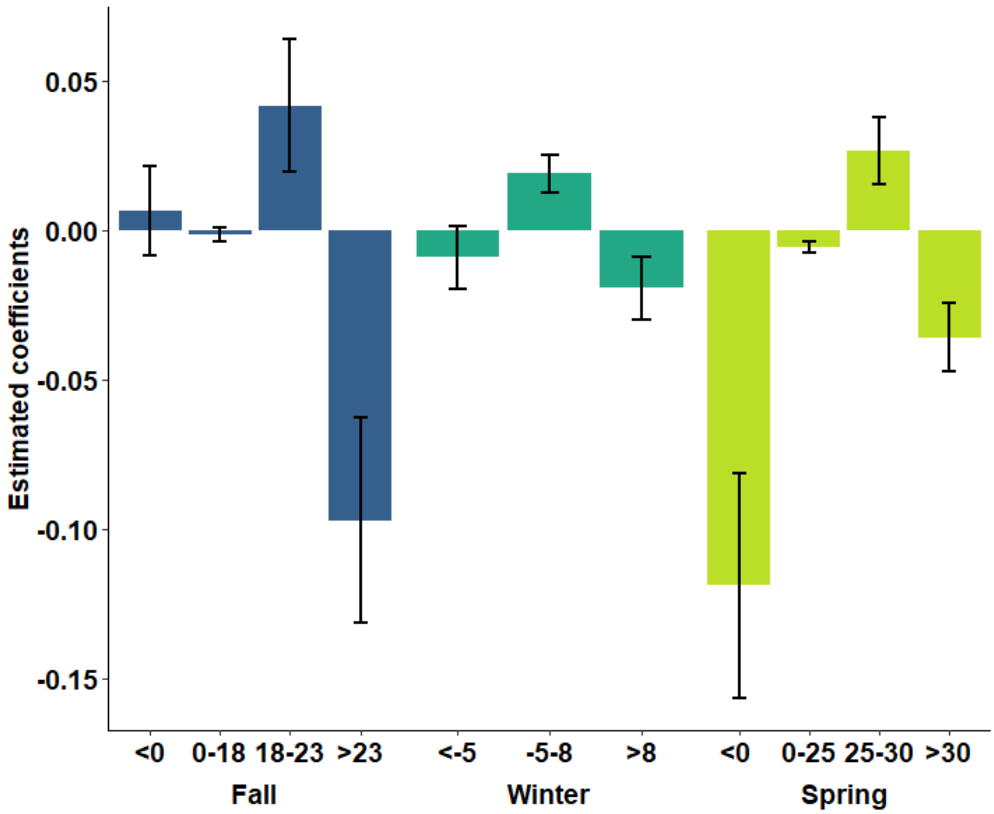

Figure B3 The robustness check with a growing season of Sep-June

Note: The x-axis indicates the degree-day variables constructed from the associated temperature thresholds. Bars show the estimated coefficients of the respective degree-day variables and the 95% confidence intervals using standard errors clustered at the county-level.

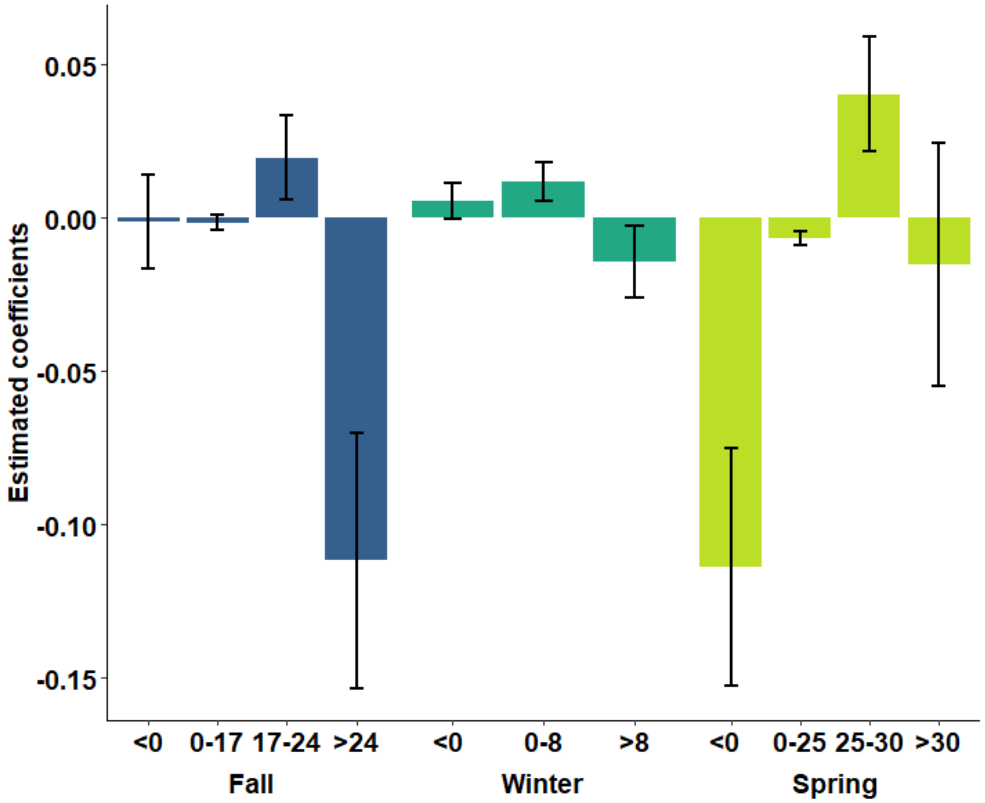

Figure B4 The robustness check with an alternative winter temperature threshold setup

Note: The x-axis indicates the degree day variables constructed from the associated temperature thresholds. Bars show the estimated coefficients of the respective degree day variables and the 95% confidence intervals using standard errors clustered at the county-level.

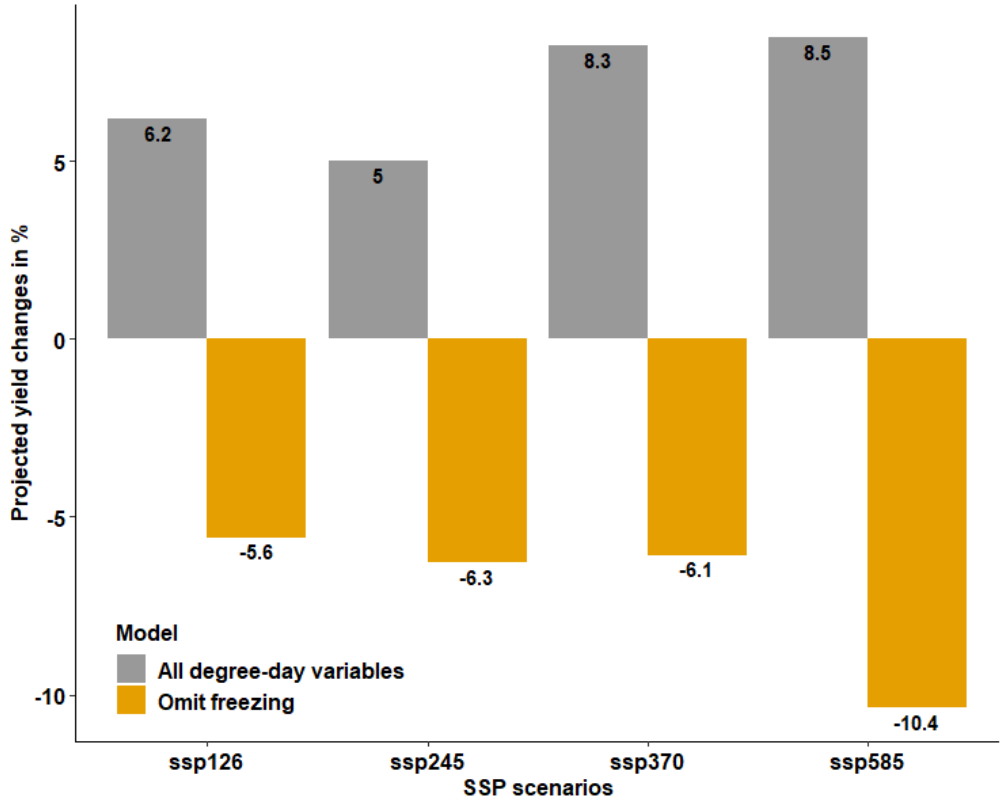

Figure B5 Projected yield consequences under SSP scenarios with the base period of 1970-2000

Note: "All degree-day variables" denotes the yield projections with all degree-day variables, whereas "Omit freezing" indicates the yield projection without the consideration of terms capturing freezing effects (Frez_fall, DDlow_winter, and Frez_spring).

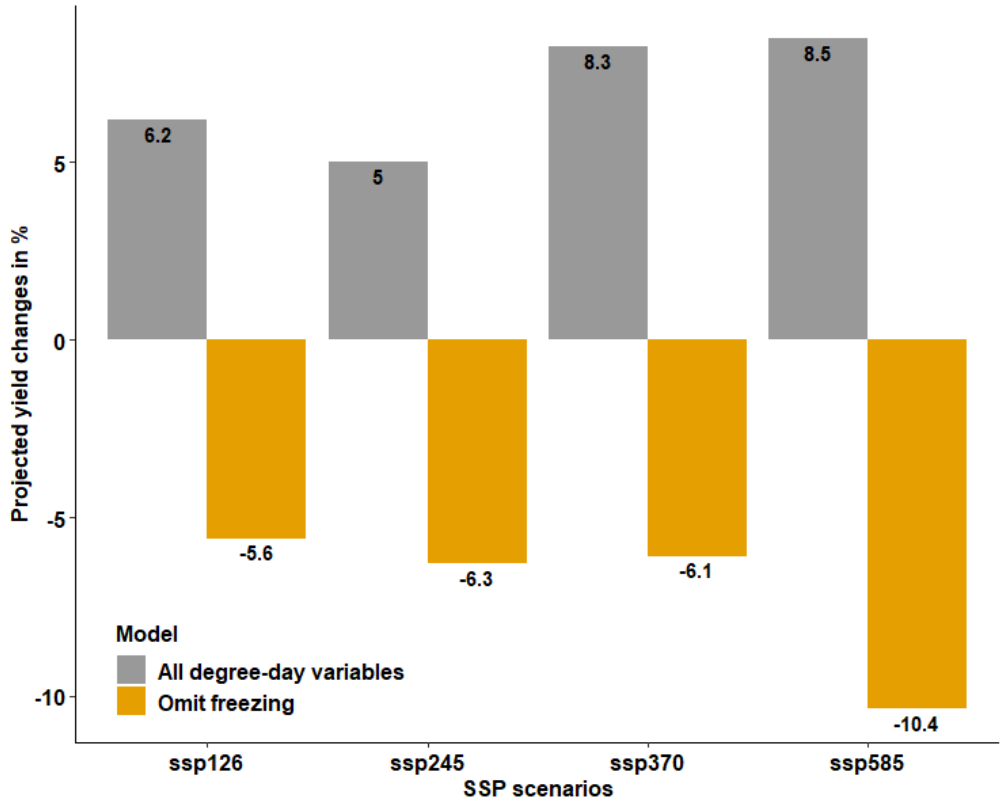

Figure B6 Projected yield consequences under SSP scenarios with the base period of 1981-2015

Note: "All degree-day variables" denotes the yield projections with all degree-day variables, whereas "Omit freezing" indicates the yield projection without the consideration of terms capturing freezing effects (Frez_fall, DDlow_winter, and Frez_spring).